Protein Engineering Studies on Phosphoglycerate Mutase from *Saccharomyces cerevisiae*

Thesis presented for the degree of Doctor of Philosophy
University of Edinburgh
1999

I declare that the work contained in this thesis has been carried out by me unless otherwise acknowledged, and that none of the work has been submitted for any other degree.

Rebecca Walter

Abstract

The glycolytic enzyme phosphoglycerate mutase from *Saccharomyces cerevisiae* catalyzes the interconversion of 2- and 3-phosphoglycerate via a Ping-Pong mechanism involving a phosphorylated histidine residue. It also shows a low level of phosphatase activity which is thought to be a result of the non-productive transfer of a phospho group to water.

The C-terminal 14 residues are not seen in the electron density map and are thought to constitute a flexible tail, which has been suggested to be involved in catalysis by closing over the active site and excluding water. Attempts to construct a mutant lacking the tail region were unsuccessful, but limited proteolysis of the wild type enzyme show the importance of the tail in the mutase reaction. The phosphatase activity is unaffected. Further evidence for the involvement of the tail comes from studies using a range of inhibitors which have been modelled in the active site. These provide protection from proteolysis similar to that provided by the substrate 2,3-bisphosphoglycerate. The other substrate, 3-phosphoglycerate, does not provide this protection.

The two C-terminal residues are both lysines, and it has been suggested that they are involved in catalysis. Three mutants in which one or both lysines are replaced by glycine have been characterized (K246G, K245G and K245G/K246G). The K246G mutant has kinetic properties almost identical to the wild type. When the lysine 245 residue is replaced, there are some differences in the kinetic parameters of the resulting mutants which suggest changes in the binding of the substrate and/or release of the product, but it is unlikely that either lysine is involved in electrostatic interactions crucial to the catalytic mechanism.

Phosphoglycerate mutase also catalyzes a 2,3-bisphosphoglycerate synthase activity, although at a much lower level than the mutase activity, and the yeast enzyme is closely related to the bisphosphoglycerate synthase enzyme present in red blood cells. This enzyme catalyzes the same three reactions as the yeast mutase, but the synthase activity is much higher in the erythrocyte enzyme. Comparison of the amino acid sequences of the two proteins show two significant differences in the active site region: residues 11 and 60 (S. cerevisiae numbering) are a serine and an alanine respectively in the yeast mutase, and a glycine and a serine in the erythrocyte synthase. Characterization of yeast mutase mutants with residues 11 and 60 replaced by the corresponding synthase residues (S11A and A60S) showed differences in the catalytic parameters and decreased mutase activity. However, circular dichroism shows that this could be due to structural differences rather than a change in functional groups in the active site.

Another active site residue implicated in the catalytic mechanism is glutamate 86. When this residue is replaced with a glutamine, there is a very significant decrease in mutase activity, and the K_M values for each of the substrates are increased significantly. It has been suggested that this residue is involved in a catalytic triad in the related enzyme 6-phosphofructo-2-kinase/ fructose-2,6-bisphosphatase. These results support a similar role for the residue in the mutase activity of the *S. cerevisiae* phosphoglycerate mutase.

Contents

Acknowledgements

Without the help of the people below, the work contained in this thesis could not have been carried out, and I would therefore like to thank:

Dr Linda Gilmore for her enthusiastic supervision.

Dr Jacqueline Nairn for her advice and support, and for the gift of a sample of partially purified *S. pombe* phosphoglycerate mutase.

Dr Malcolm White for the preparation of the mutant *S. cerevisiae* phosphoglycerate mutase genes and the phosphoglycerate mutase-deficient strain of yeast, and for helpful initial discussions.

Dr Daniel Rigden for the inhibitor-enzyme complex modelling, help with the preparation of some of the figures contained in this thesis and many invaluable discussions.

Dr Nick Price and Dr Sharon Kelly for carrying out the c.d. measurements

Tino Krell and Jacqueline Nairn for performing the mass spectrometry analysis.

Dr Andrew Cronshaw, Douglas Lamont and Dr Daniel Rigden of the Welmet Protein Characterisation Facility for the protein sequencing.

Richard Collins, Simon Potter, Thales Rocha, Daniel Rigden, Jacqueline Nairn and everyone from 327 for friendship and support.

Eve Laird, Elizabeth Lovejoy, Kim Midwood and Sue Webber for preparing the E86Q mutant phosphoglycerate mutase gene.

Ann Brown for yeast advice and coffee and cakes.

My parents, whose consistent pride and support (moral and financial) have sustained me through all the endless student years.

Tim, for everything.

The financial support of the Biotechnology and Biological Sciences Research Council is acknowledged.

Abbreviations

ADP	adenosine diphosphate
ATP	adenosine triphosphate
B123	benzene 1,2,3-triphosphate
B124	benzene 1,2,4-triphosphate
B135	benzene 1,3,5-triphosphate
B1245	benzene 1,2,4,5-tetraphosphate
BHC	benzene hexacarboxylate
2,3-BPGA	2,3-bisphosphoglyceric acid
BPGAM	bisphosphoglycerate mutase
DMSO	dimethyl sulfoxide
DNA	deoxyribonucleic acid
DTT	dithiothreitol
Fru-2,6-BPase	fructose-2,6-bisphosphatase
IHP	inositol hexakisphosphate
NAD^+	nicotinamide adenine diphosphate (oxidized form)
NADH	nicotinamide adenine diphosphate (reduced form)
OD	optical density
2-PGA	2-phosphoglyceric acid
3-PGA	3-phosphoglyceric acid
PGAM	phosphoglycerate mutase
RPAP	rat prostatic acid phosphatase
SDS	sodium dodecyl sulphate
SDS-PAGE	sodium dodecyl sulphate polyacrylamide gel electrophoresis
WT	wild type

List of Figures

1. Introduction

3. The effect of limited proteolysis on phosphoglycerate mutase

4. The role of the C-terminal lysine residues

5. Inhibitor studies

6. The mutase/synthase relationship

7. The role of Glu86

List of Tables

1. Introduction

3. The effect of limited proteolysis on phosphoglycerate mutase

4. The role of the C-terminal lysine residues

5. Inhibitor studies

6. The mutase/synthase relationship

7. The role of Glu86

Chapter One

Introduction

1.1 Glycolysis.

Glycolysis is a central metabolic pathway, occurring in nearly all organisms, which provides both energy and metabolic intermediates for other pathways. The reactions of glycolysis are shown in figure 1.1. The reactions can occur in cells growing anaerobically as part of a fermentation, or in actively respiring cells, with the product pyruvate oxidized and entered into the citric acid cycle.

1.2 The phosphoglycerate mutases.

Phosphoglycerate mutase (PGAM) catalyzes the interconversion of 3- and 2-phosphoglycerate in the lower half of the glycolytic pathway. The enzyme was first discovered over 60 years ago (Meyerhof and Kiessling, 1935), and has subsequently been found to be almost ubiquitous, found in all organisms so far studied with the possible exception of some thermophilic archaea (De Rosa *et al.*, 1984, Budgen and Danson, 1986).

There are two main types of mutase - those which require small quantities of 2,3-bisphosphoglycerate for activity (termed cofactor-dependent mutases) and those which do not have this requirement (cofactor-independent). The two types show no significant sequence similarity and are therefore probably heterologous.

Vertebrates possess only cofactor-dependent, and higher plants only cofactor-independent mutases. In other groups of organisms the situation is less clear-cut. The mutases from the fungi *Saccharomyces cerevisiae* and *Schizosaccharomyces pombe* are cofactor-dependent (Carreras *et al.*, 1982, Price *et al.* 1985), whereas those from *Neurospora crassa* and *Aspergillus nidulans* (filamentous fungi) are cofactor-independent (Huang *et al.*, 1993, Johnson and Price, 1988). Both types can also be found in bacteria. Mutases from *Bacillus spp.* have been found to be cofactor-independent, although they are so far unique in also displaying an absolute requirement for Mn^{2+} (Singh and Setlow, 1979, Watanabe and Freese, 1979). It was thought until recently that all gram-negative bacteria had cofactor-dependent mutases, but a gene from *Pseudomonas syringae* has been shown to have considerable identity to various cofactor-independent mutases (Morris *et al.*, 1995).

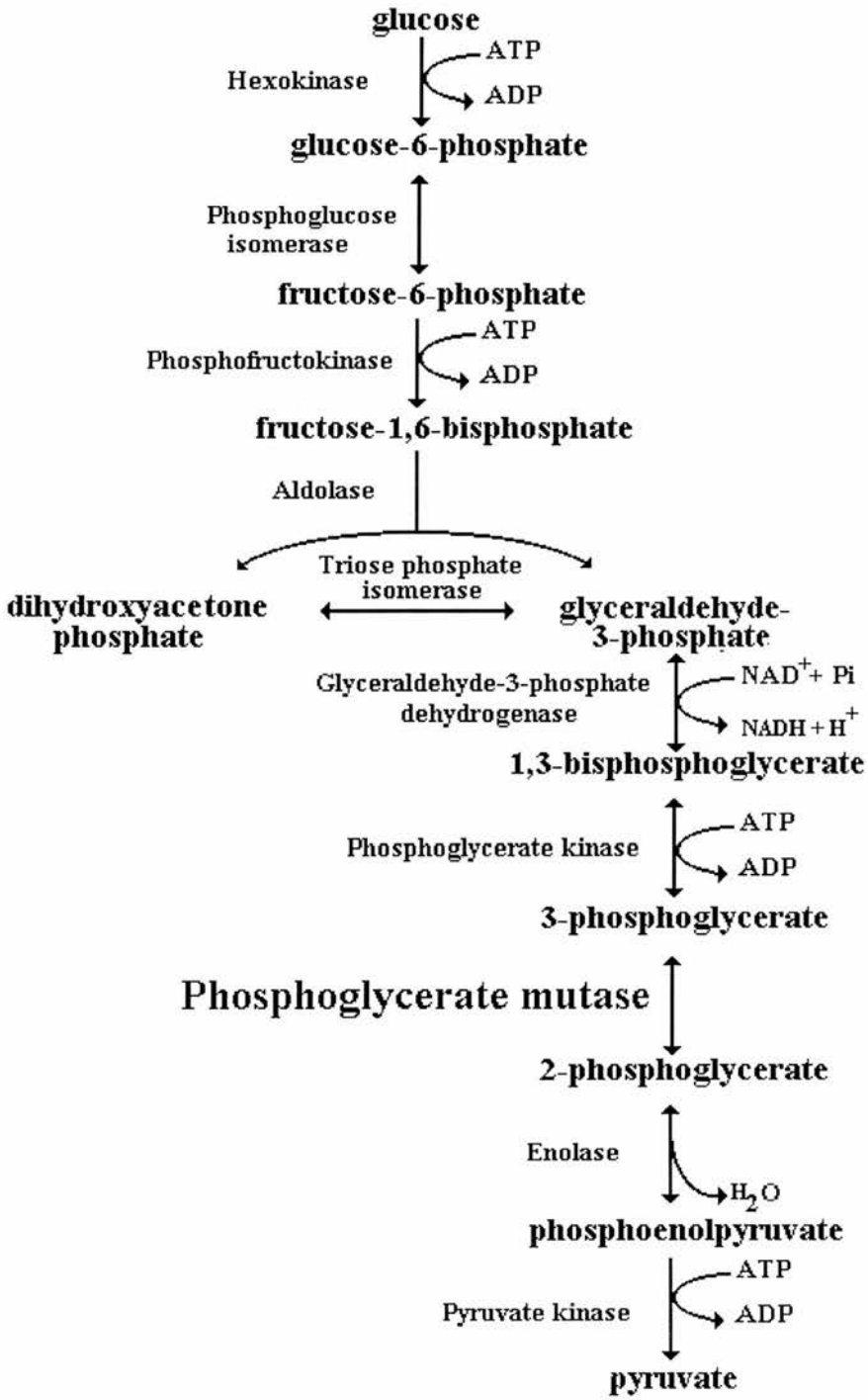

Figure 1.1

The reactions of glycolysis, highlighting the phosphoglycerate mutase reaction.

This complex distribution has been reviewed (Fothergill-Gilmore and Michels, 1993) and it is likely that both types of gene were present early in evolution, with animals losing the gene encoding the independent mutase before the radiation of vertebrates, and plants losing the dependent type gene around the time of the diversion of more complex forms from the primitive single cells (see section 1.6).

1.3 Cofactor-independent mutases

These mutases tend to be unstable and are consequently difficult to purify. This has limited the amount of data available. However, mutases from *Bacillus spp.* and more recently some higher plants (castor and maize) have been studied in some detail.

In the absence of added Mn^{2+}, *Bacillus* does not sporulate, and there is a build-up of 3-PGA. The block occurs at phosphoglycerate mutase (Singh and Setlow, 1979). The enzyme has been isolated from *B. subtilis* (Watanabe and Freese, 1979) and *B. megaterium* (Singh and Setlow, 1979). Both are monomer molecular weights of around 61,000 (*B. subtilis*) and 74,000 (*B. megaterium*), and show a specific requirement for Mn^{2+}. The activation is slow and temperature-dependent which suggests that a conformation change between active and inactive forms is involved. This interconversion is also pH-dependent (Kuhn *et al.*, 1993). Changes in pH and Mn^{2+} concentration occur during sporulation, when significant amounts of 3-phosphoglycerate are accumulated, and these probably regulate the mutase activity (Magill *et al.*, 1994).

The higher plant mutases are also monomers, with a molecular weight of around 60,000 (Botha and Dennis, 1986, Huang *et al.*, 1993). The first amino acid sequence to be reported was from maize, and it contained a cluster of residues that are highly conserved in the alkaline phosphatase family of enzymes (involved in metal ion binding). It was therefore suggested that the cofactor-independent enzymes might be members of this enzyme family (Grana *et al.* 1992). However, a subsequent comparison of the amino acid sequences of maize, castor and tobacco showed that this particular motif is not conserved (Huang *et al.* 1993). The cofactor-independent

mutase sequences show a high degree of similarity to each other and may therefore be homologous.

Higher plant mutases exist as both plastid and cytosolic isoenzymes, both of which are acid and heat labile, however the cytosolic form is more sensitive to pH. The catalytic mechanism must differ from that of the cofactor-dependent enzyme, because 2,3-BPGA has no effect on activity. However, there is evidence that it also proceeds via a phosphoenzyme intermediate (Breathnach and Knowles, 1977). Recently, three histidine residues have been shown to be essential for catalytic activity (Huang and Dennis, 1995). It is therefore possible that although the cofactor-dependent and -independent enzymes may be heterologous, they are functionally convergent (catalyzing the same reaction), and may also be mechanistically convergent both using histidines to mediate the transfer of protons and phospho groups.

1.4 Cofactor-dependent phosphoglycerate mutases

The glycolytic enzyme, which primarily catalyzes the interconversion of 3- and 2-PGA, is termed a monophosphoglycerate mutase. There is also a bisphosphoglycerate mutase (also known as bisphosphoglycerate synthase), found in mammalian red blood cells. The main function of this enzyme is to maintain levels of 2,3-BPGA, the effector molecule controlling the oxygen affinity of haemoglobin (see section 1.12).

1.5 Phosphoglycerate mutase isoenzymes

In mammals, there are two genes that encode monophosphoglycerate mutase (Fundele *et al.* 1981, Junien *et al.* 1982). B-type is expressed in brain and most other tissues except skeletal muscle. M-type is expressed in muscle (cardiac and skeletal). The gene products, the M and B subunits, have a molecular weight of around 30,000, and form dimers. The expression of M is developmentally regulated. In early foetal muscle, only B is expressed giving rise to the BB dimer, which is replaced during further development by MM through the MB heterodimer. The appearance of the M gene product correlates with the initiation of spontaneous cell contraction in rat

satellite cell cultures (Castella-Escola *et al.* 1990). Birds appear only to have the B form (Mezquita and Carreras 1981). M and B forms show a high level of sequence identity, but differ significantly in their basic and acidic amino acid content (Sakoda *et al.*, 1988). MM, MB and BB isoenzymes have very similar kinetic properties, but can be distinguished by electrophoretic mobility, thermal lability and sensitivity to sulphydryl group reagents (Mezquita *et al.*, 1981).

A third gene encodes bisphosphoglycerate mutase (E-type). It shows a high level of sequence identity with M, B and yeast mutases and is considered another isoenzyme. The E subunit has been shown to form heterodimers with M and B subunits *in vitro* (Pons *et al.* 1985, Prehu *et al.* 1988). The gene is expressed in erythropoeitic cells - foetal liver, spleen and reticulocytes. Trace levels of E mRNA have also been found in adult liver, which may indicate low level expression in non-erythroid cells (Joulin *et al.* 1989). The level of expression of the E-isoenzyme also changes during development. In developing red cells, there is a low level of expression of bisphosphoglycerate mutase, and a high level of expression of glycolytic enzymes. In mature erythrocytes however, there is a high level of BPGAM expression and low levels of pyruvate kinase (Sasaki *et al.*, 1982). This greatly increases the flux through the bypass from glycolysis that represents the synthesis and breakdown of 2,3-BPGA (the Rapoport-Luebering shunt, see section 1.7 and figure 1.3). In mature red cells this constitutes 15-25% of the overall flux through glycolysis, and leads to high (mM) levels of 2,3-BPGA, which is the most abundant phosphorylated metabolite in the red cells of most adult mammals. The levels of 2,3-BPGA rise linearly with rising levels of haemoglobin (foetal haemoglobin has a higher oxygen efficiency than adult haemoglobin and is much less sensitive to 2,3-BPGA).

1.6 Evolution of the phosphoglycerate mutase isoenzymes

The phosphoglycerate mutase isoenzymes probably evolved from a common ancestor by two separate gene duplication events, and their evolution can be studied by looking at their distribution. As described in section 1.4, the E isoenzyme (bisphosphoglycerate mutase) is responsible for maintaining the levels of

2,3-bisphosphoglycerate, an effector molecule for haemoglobin in mammals and amphibia. Inositol pentaphosphate and ATP are important effectors in birds, and the latter is also important in fish, amphibia and reptiles. Therefore in considering the position of the divergence of the E-isoenzyme, the distribution of haemoglobin effector molecules is relevant.

Fish and higher vertebrates have both M and B isoenzymes, but birds only have the B-type. Evidence for the B-type being the ancestral form comes from its wider distribution and from the presence in the human and mouse genomes of a large number of pseudogenes that are related to the B gene and not M (Sakoda *et al.*, 1988). As B is found in both mammals and birds, the divergence of the M and B types probably occurred before the radiation of the mammalian line (around 400 million years ago). Reptiles have both genes, so the M-type was probably lost from birds after divergence from reptiles (145 million years ago).

Looking at effector function distribution, the gene duplication giving rise to the E-type gene can be placed after the divergence of mammals and fish (400 million years ago) but before the divergence of mammals and amphibia (300 million years ago). The E isoenzyme is present in amphibia and higher vertebrates. This scheme is shown in figure 1.2 A (from Fothergill-Gilmore and Michels, 1993).

An alternative scheme is suggested by a comparison of the isoenzyme sequences. The M- and B-types are more similar to each other than either is to the E-type. If a constant rate of evolution is assumed, this would imply that the E isoenzyme diverged from a B/M ancestor and was subsequently lost from the fish and reptile/bird lines. The B and M isoenzymes then diverged before mammalian radiation (Sakoda *et al.*, 1988). This scheme is shown in figure 1.2.B.

Until more sequences are available, it is not possible to determine absolutely which scheme is correct, but Fothergill-Gilmore and Michels favour the first, as it requires the loss of an isoenzyme in only one line. It is possible that the rate of evolution of the E-gene is not constant, and that it underwent rapid change after gene duplication to give rise to the different primary structure and kinetic properties observ

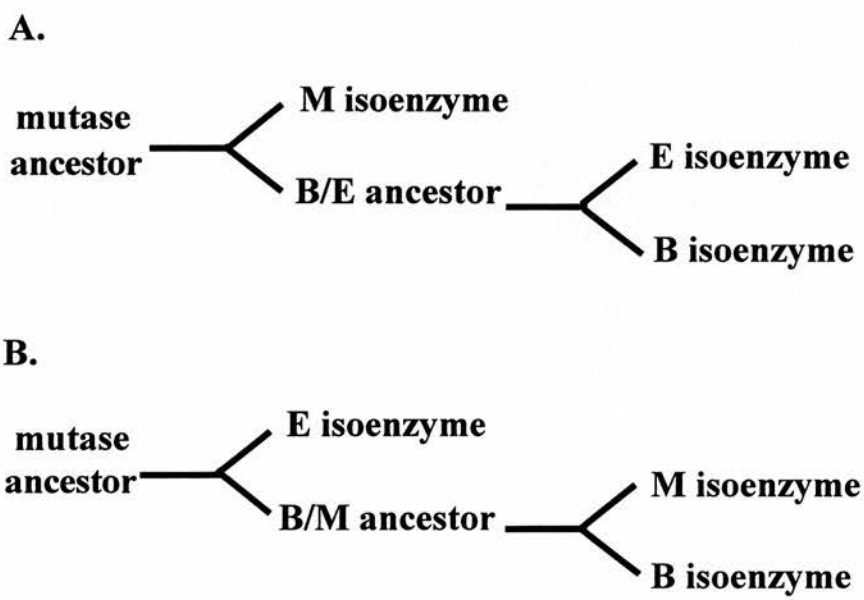

Figure 1.2
Possible schemes showing the evolution of the phosphoglycerate mutase isoenzymes.

1.7 The Reactions of Phosphoglycerate mutases

The reactions catalyzed by cofactor-dependent phosphoglycerate mutases are shown in figure 1.3. The monophosphoglycerate mutase reaction was first described by Meyerhof and Kiessling in 1935, and the bisphosphoglycerate mutase reaction by Rapoport and Luebering in 1950. The bisphosphoglycerate mutase activity is usually termed the synthase activity to avoid confusion with the glycolytic reaction.

It was originally supposed that the three activities were catalyzed by three different enzymes, but the attempts to purify both the monophosphoglycerate mutase from various sources and the bisphosphoglycerate synthase from erythrocytes resulted in the co-purification of the other activities (Rose, 1968, Sasaki *et al.*, 1971, Laforet *et al.*, 1974, Rosa *et al.,* 1975). Shortly after, it was shown that the three activities were indeed catalyzed by a single polypeptide, and at a common active site (Rosa *et al.,* 1973, Sasaki *et al.*, 1975, Ikura *et al.* 1976). The rate at which the three reactions are catalyzed differs significantly in mono- and bisphosphoglycerate mutases. The monophosphoglycerate mutases catalyze the mutase reaction at a rate some four orders of magnitude higher than the synthase and mutase reactions. Bisphosphoglycerate mutase (the E isoenzyme) from red blood cells catalyzes the synthase activity at a higher rate than either of the other two activities (Rose, 1980).

As monophosphoglycerate mutase is also present in erythrocytes, it is unlikely that the E-isoenzyme is important in glycolysis. The function of bisphosphoglycerate mutase is to maintain the high concentration of 2,3-BPGA found in erythrocytes, where it is an important regulator of haemoglobin oxygen affinity. The synthase and phosphatase activities of this enzyme constitute a bypass of the phosphoglycerate kinase step of glycolysis (known as the Rapoport-Luebering shunt) controlling the synthesis and breakdown of 2,3-BPGA.

The phosphatase activity of both mono- and bisphosphoglycerate mutases is very low, but is increased by anions, in particular the two carbon substrate analogue 2-phosphoglycollate (Rose and Liebowitz, 1970, Sasaki *et al.*, 1971, Rose and Dube, 1976). In erythrocytes, the rate of the phosphatase reaction is not thought to be dependent on the concentration of the substrate 2,3-BPGA, as this is always present

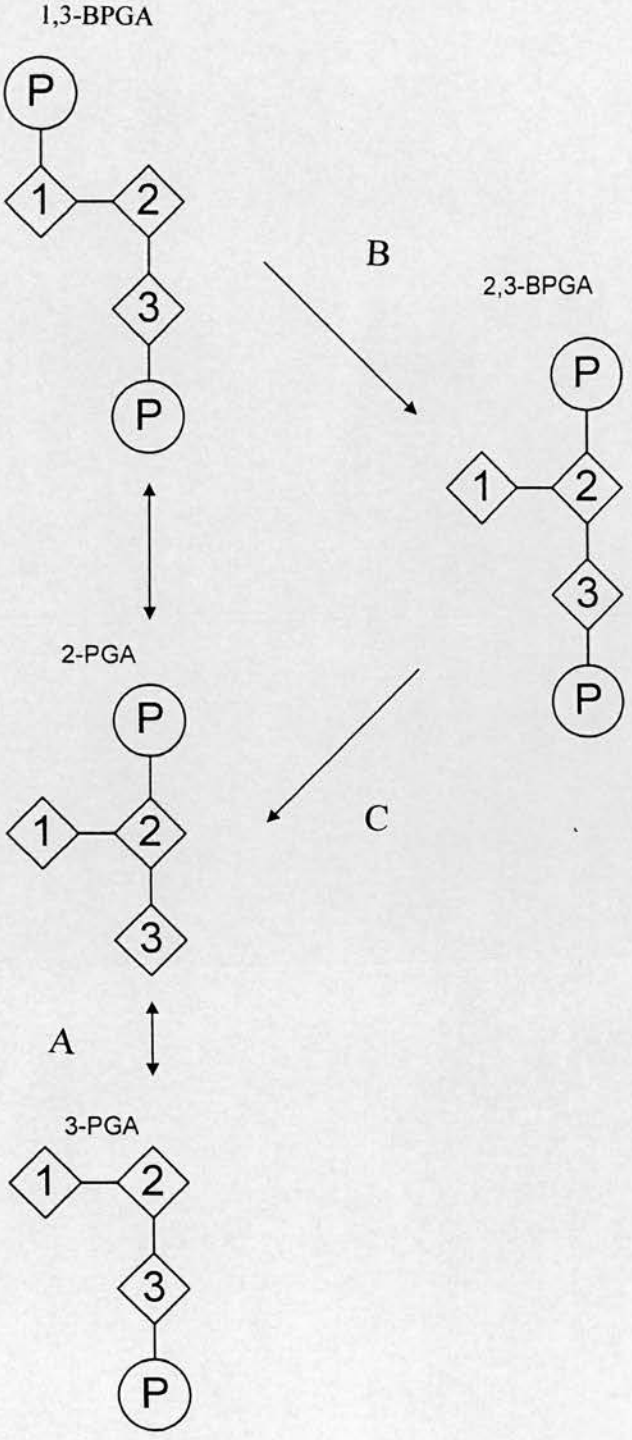

Figure 1.3

The reactions catalyzed by cofactor-dependent phosphoglycerate mutases.
A. The glycolytic mutase reaction.
B. The bisphosphoglycerate mutase reaction (known as the synthase reaction).
C. The bisphosphoglycerate synthase reaction.
The synthesis and breakdown of 2,3-BPGA constitute a bypass of glycolysis known as the Rapoport-Luebering shunt.

in saturation - the K_M for the substrate is in the micromolar range and the substrate is present in the millimolar range. The rate may therefore be at least partially dependent on the levels of activators present. Rose and Salon (1979) showed that 2-phosphoglycollate is present in normal red blood cells at levels sufficient to enhance the phosphatase activity of bisphosphoglycerate synthase. The cofactor-independent mutases only exhibit the glycolytic mutase reaction.

The table below shows catalytic constants for the reactions catalyzed by different phosphoglycerate mutases.

Reactions			k_{cat} (s^{-1})		
			MPGAM (dep)	**BPGAM**	**MPGAM (ind)**
3-PGA (2,3-BPGA)	2-PGA	cofactor-dependent mutase	1333	1.7	0
1,3-BPGA 2,3-BPGA		synthase	0.4	12.5	0
2,3-BPGA	PGA + P_i	phosphatase	2.78	2.57	0
3-PGA	2-PGA	cofactor-independent mutase	0	0	950

Table 1.1
Table showing the catalytic constants for the reactions catalyzed by the phosphoglycerate mutases. Abbreviations: MPGAM-ind, cofactor-independent phosphoglycerate mutase from wheatgerm (Leadley *et al.,* 1977); MPGAM-dep, cofactor-dependent phosphoglycerate mutase from chicken muscle (Rose, 1980); BPGAM, bisphosphoglycerate mutase from horse red cells (Rose, 1980). The k_{cat} for the phosphatase reaction is for the reaction activated by 2-phosphoglycollate.

1.8 Structure of the phosphoglycerate mutases.

1.8.1 Primary Structures.

Complete amino acid sequences are available for a number of cofactor-dependent phosphoglycerate mutases: *S. cerevisiae* (Fothergill and Harkins, 1982, White and Fothergill-Gilmore, 1988), *S. pombe* (Nairn *et al.*, 1994), *Streptomyces coelicolor* (White *et al.*, 1992), *Zymomonas mobilis* (Yomano *et al.*, 1993), the rat M and B isoenzymes (Castella-Escola *et al.*, 1989, Urena *et al.*, 1992), human M and B isoenzymes (Shankse *et al.*, 1987, Sakoda *et al.*, 1988), and the E isoenzyme from human, rabbit and mouse erythrocytes (Haggarty *et al.*, 1983, Joulin *et al.*, 1986, Yanagawa *et al.*, 1986, LeBoulch *et al.*, 1988). The sequences are shown aligned in figure 1.4, and sequence identities are given in table 1.2. The high level of identity shows that the phosphoglycerate mutases have the slow rate of evolution typical of glycolytic enzymes.

1.8.2 Tertiary structure

The crystal structure of only one phosphoglycerate mutase has been determined - that from *S. cerevisiae*. Until very recently, the only structure available was that determined by Winn *et al.* (1981). There are a number of problems with this structure. It is of relatively poor resolution (2.8 A), and is based on an amino acid sequence that has since been shown to have a number of errors (Fothergill and Harkins, 1982, White and Fothergill-Gilmore, 1988). However, this structure has formed the basis of protein engineering work on the yeast mutase, in particular the work contained in this thesis, and therefore it should be described in some detail.

The 2.8Å structure shows the enzyme as a homotetramer, arranged with almost exact 222 symmetry. The tetramer is shown in figure 1.5. Each subunit consists of a polypeptide chain folded into a single domain, consisting of a central core of β-strands surrounded by α-helices. The arrangement is similar to the nucleotide-binding domain of dehydrogenases (Ohlsson *et al.*, 1974). However, no nucleotide binding requirement has been demonstrated for PGAM, although these molecules can bind to PGAM. The active site was located by soaking crystals of

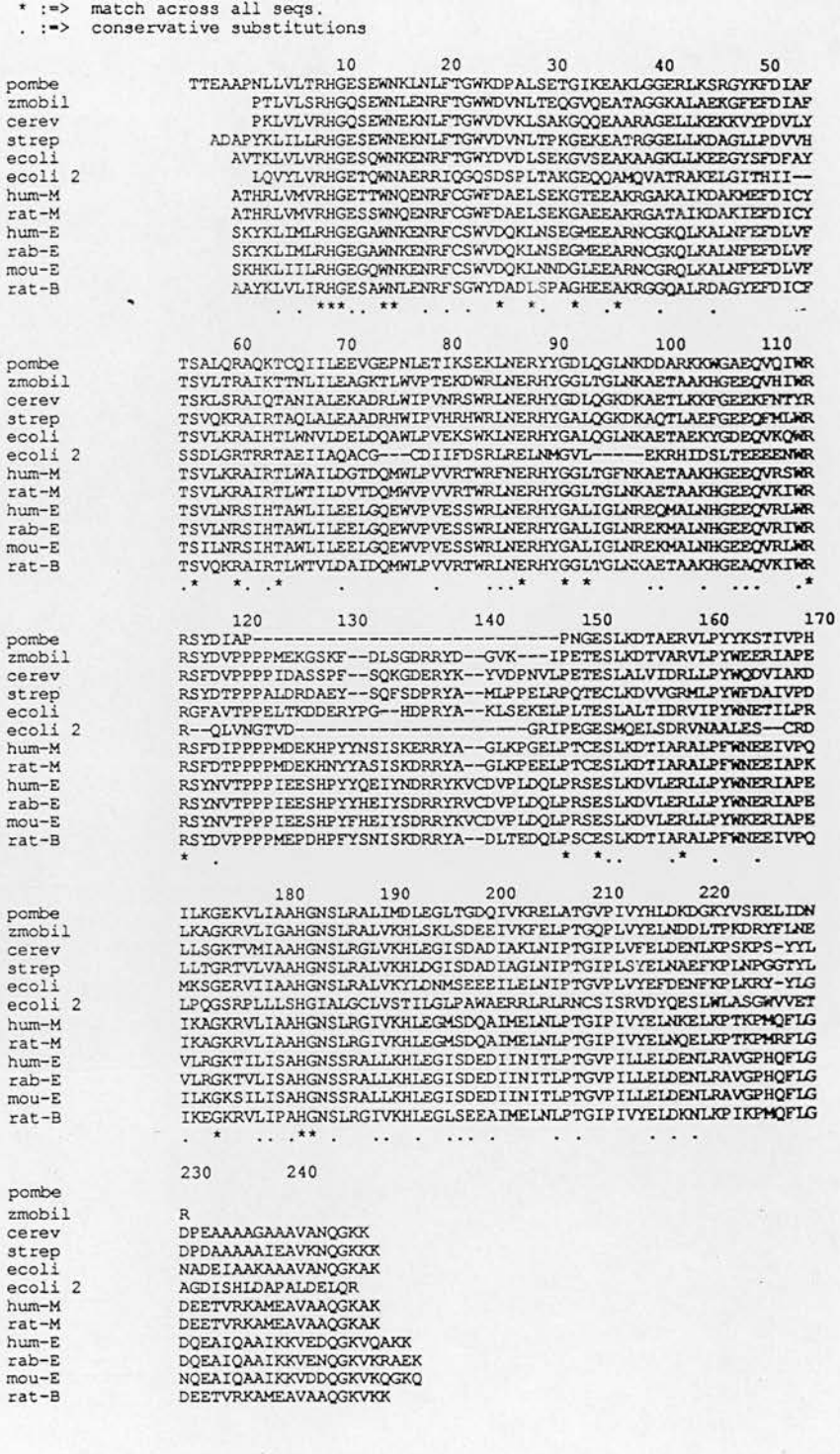

Figure 1.4

Alignment of the amino acid sequences of cofactor-dependent phosphoglycerate mutases.

Abbreviations: Abbreviations: *S.cerev, S. cerevisiae* PGAM (White and Fothergill-Gilmore, 1988); *S.pombe,* S. pombe PGAM (Nairn *et al.* 1994); *S.coel, Streptomyces coelicolor* PGAM (White *et al.*, 1992)*; Z.mob, Zymomonas mobilis* PGAM (Yomano *et al.*, 1993)*; Hum-M, human M-type PGAM (Shankse et al., 1987); Rat-M, rat M-type PGAM (Castella-Escola et al.*, 1989); Hum-B, human B-type (Sakoda *et al.*, 1988); rat-B, rat B-type (Urena *et al.* 1992); Hum-E, human E-type (Joulin *et al.*, 1986); Mouse-E, mouse E-type *(*LeBoulch *et al.*, 1988*)*

	S.cerev	*S.pombe*	*S.coel*	*Z.mob*	*E.coli*	*Hum-M*	*Rat-M*	*Hum-B*	*Rat-B*	*Hum-E*	*Mouse-E*
S.cerev	100	45	64	53	54	50	52	51	49	48	46
S.pombe		100	45	52	50	48	46	50	48	44	45
S.coel			100	51	50	51	52	52	52	48	45
Z.mob				100	54	58	59	59	58	51	51
E.coli					100	56	56	59	57	47	46
Hum-M						100	93	81	78	51	50
Rat-M							100	79	76	51	50
Hum-B								100	97	53	51
Rat-B									100	53	51
Hum-E										100	92
Mouse-E											100

Table 1.2

Summary of amino acid sequence alignment, showing % differences (only matched sequences included).
Abbreviations: *S.cerev*, *S. cerevisiae* PGAM (White and Fothergill-Gilmore, 1988); *S.pombe, S. pombe PGAM (Nairn et al. 1994)*; *S.coel, Streptomyces coelicolor (White et al., 1992); Z.mob, Zymomonas mobilis (Yomano et al., 1993); Hum-M,* human M-type PGAM (Shankse *et al.*, 1987); *Rat-M*, rat M-type PGAM (Castella-Escola *et al.*, 1989); *Hum-B*, human B-type (Sakoda *et al.*, 1988); *Rat-B*, rat B-type (Urena *et al.* 1992); *Hum-E*, human E-type (Joulin *et al.*, 1986); *Mouse-E*, mouse E-type (LeBoulch *et al.*, 1988).

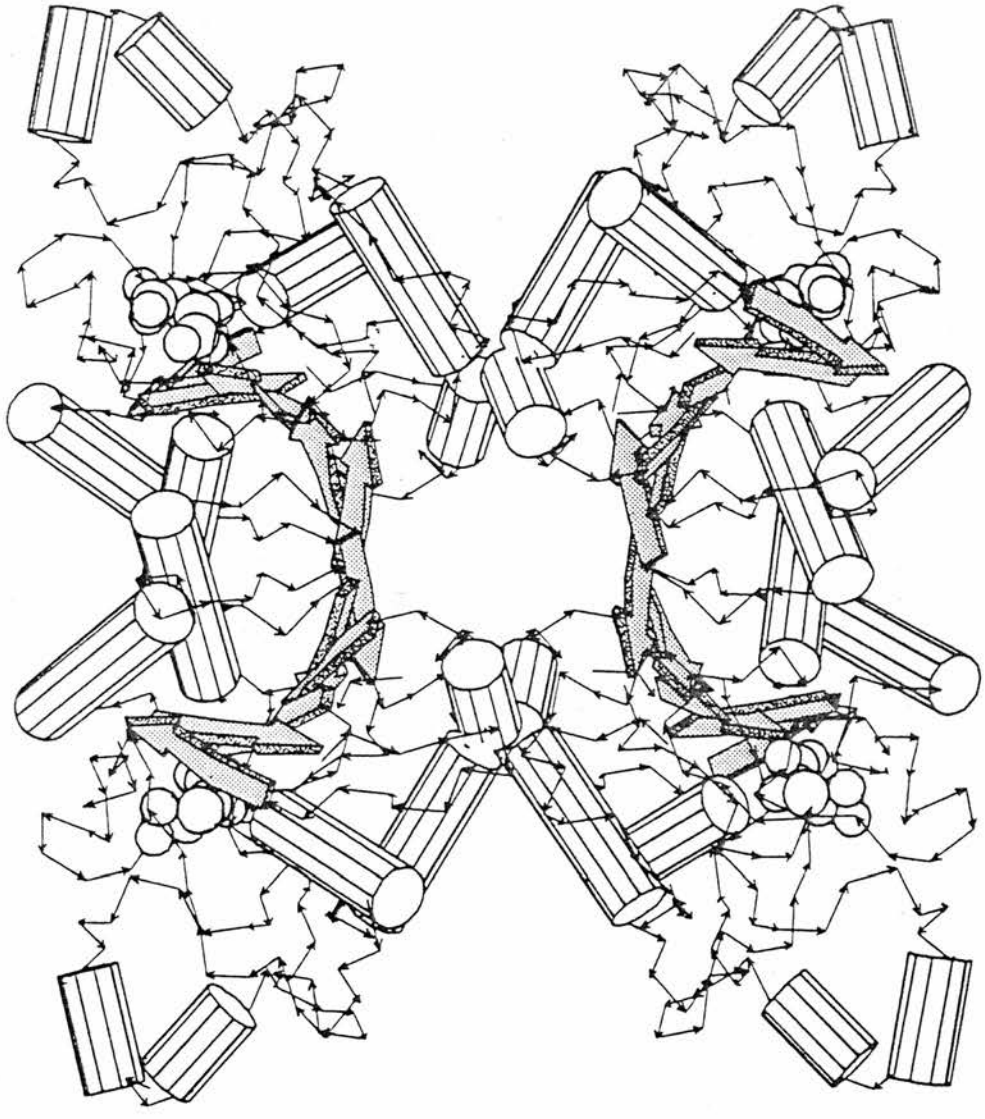

Figure 1.5
The *S. cerevisiae* PGAM tetramer (2.8A structure, Campbell *et al.*, 1974, Winn *et al.*, 1982).

PGAM in 3-PGA (Winn *et al.* 1981). The enzyme used in the study was not phosphorylated, and therefore was inactive as a mutase. However, 3-PGA acts as a competitive inhibitor with respect to 2,3-BPGA at high concentrations and confers protection against reagents known to modify the active site, so it is reasonable to assume that the monophosphoglycerate substrate can bind to the active site of the unphosphorylated enzyme. The results obtained by soaking the crystals in 3-PGA show that the active site lies at the bottom of a hollow formed by the residues of one subunit only. The four sites are well separated in the tetramer (figure 1.5) and appear to be freely accessible to the solvent.

A single subunit showing active site residues is shown in figure 1.6. The crystals were grown in ammonium sulphate, and in the crystal structure, sulphate ions occupy the positions in the active site presumed to be occupied in the ligated enzyme by the phospho groups of 2,3-BPGA. A second sulphate is thought to occupy the position of the non-transferred phospho group of the 2,3-bisphosphoglycerate substrate/cofactor. Figure 1.7 shows the active site with bound sulphate ions. Assuming the transferable phospho group binds in these positions, the oxygen atoms could form hydrogen bonds with the hydroxyl groups of Ser11 and Thr20. The hydroxyl on C2 of the monophosphoglycerate substrate could make a hydrogen bond with a main chain carbonyl oxygen. The phospho group on C2 of 2,3-BPGA in a similar position to sulphate 2 could interact with the positive charge associated with the dipole at the N-terminus of helix 7. The C1 carboxyl points towards the back of the active site, near to Arg59. As described in section 1.9, Pizer and Ballou (1959) showed a substrate requirement for this negatively charged group on C1, and this charge-charge interaction could help position the substrate for phospho transfer.

Two histidines are located in the active site and are arranged in a distinctive "clapping hands" formation, parallel and about 4A apart. His8 is close to the 3-PGA phospho group, and His181 is close to the hydroxyl on C2. The active site pocket is lined by several positively charged side chains, particularly of arginine, as would be expected where the substrates are negatively charged.

A new, higher resolution (2.3 Å) structure has recently been determined (Rigden *et al.*, 1997). This shows some important differences to the earlier structure.

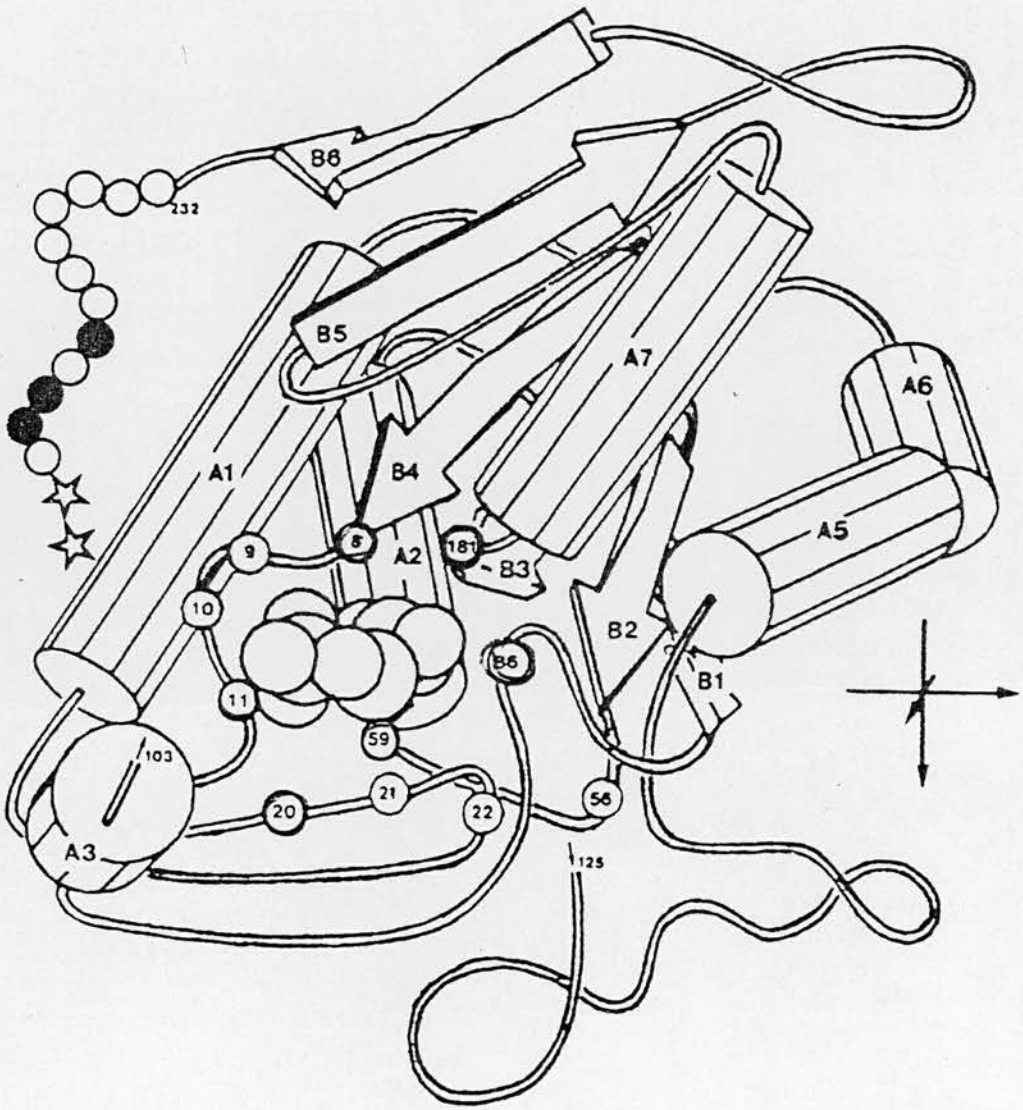

Figure 1.6

A single subunit of *S. cerevisiae* PGAM, showing active site residues mentioned in the text (2.8A structure, Campbell *et al.*, 1974). The substrate is shown in the active site, which was located by soaking crystals in a solution of 3-PGA (Winn *et al.*, 1982). No electron density was observed after residue 232. Residues 233-246 are represented by symbols. Lysines are shown as stars, small uncharged residues as open circles and polar residues as closed circles.

Figure 1.7
The active site of *S. cerevisiae* PGAM, showing key residues and the two bound sulphate groups (2.8Å structure, Campbell *et al.*, 1974, Winn *et al.*, 1982).

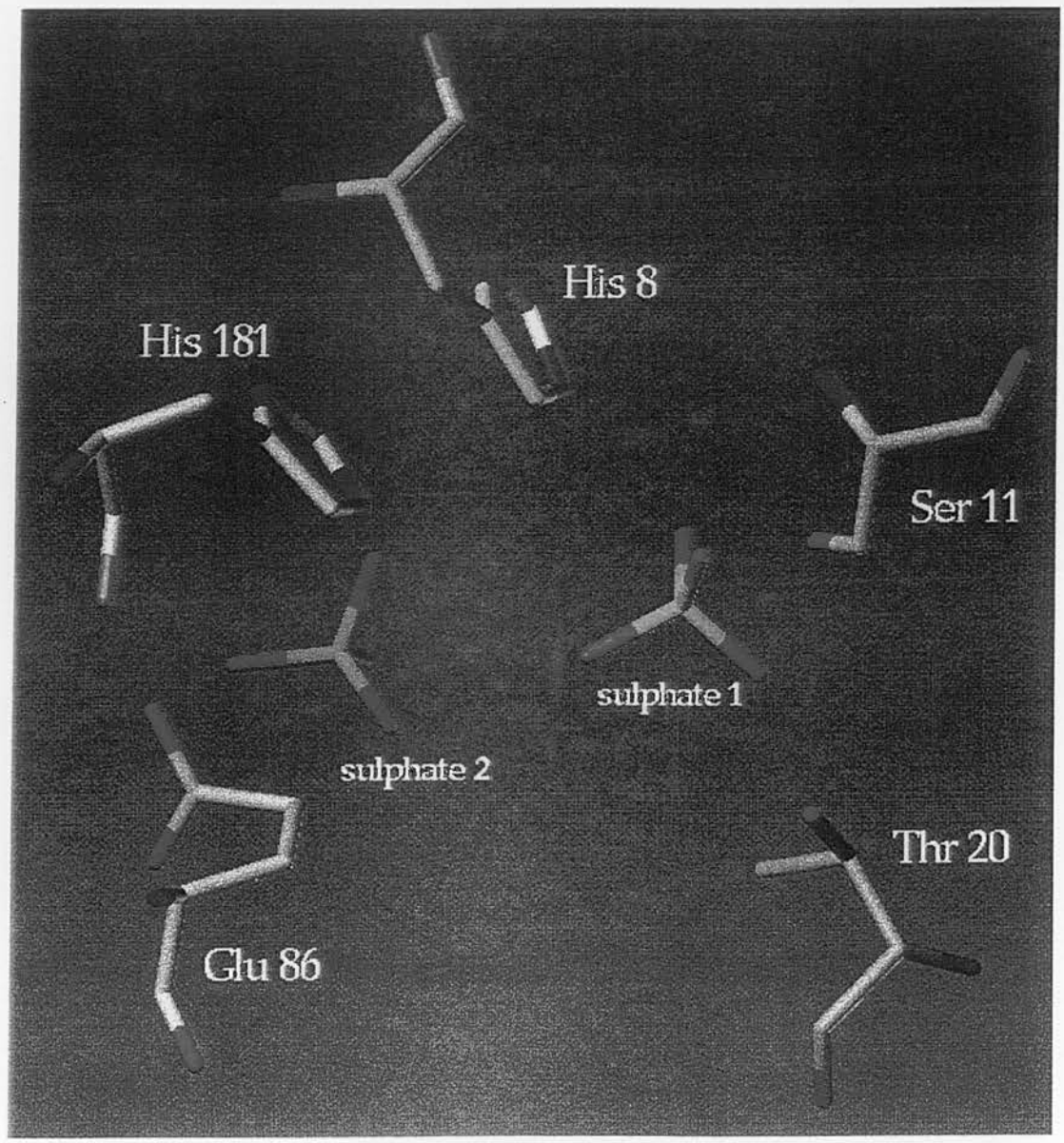
His 8
His 181
Ser 11
sulphate 1
sulphate 2
Thr 20
Glu 86

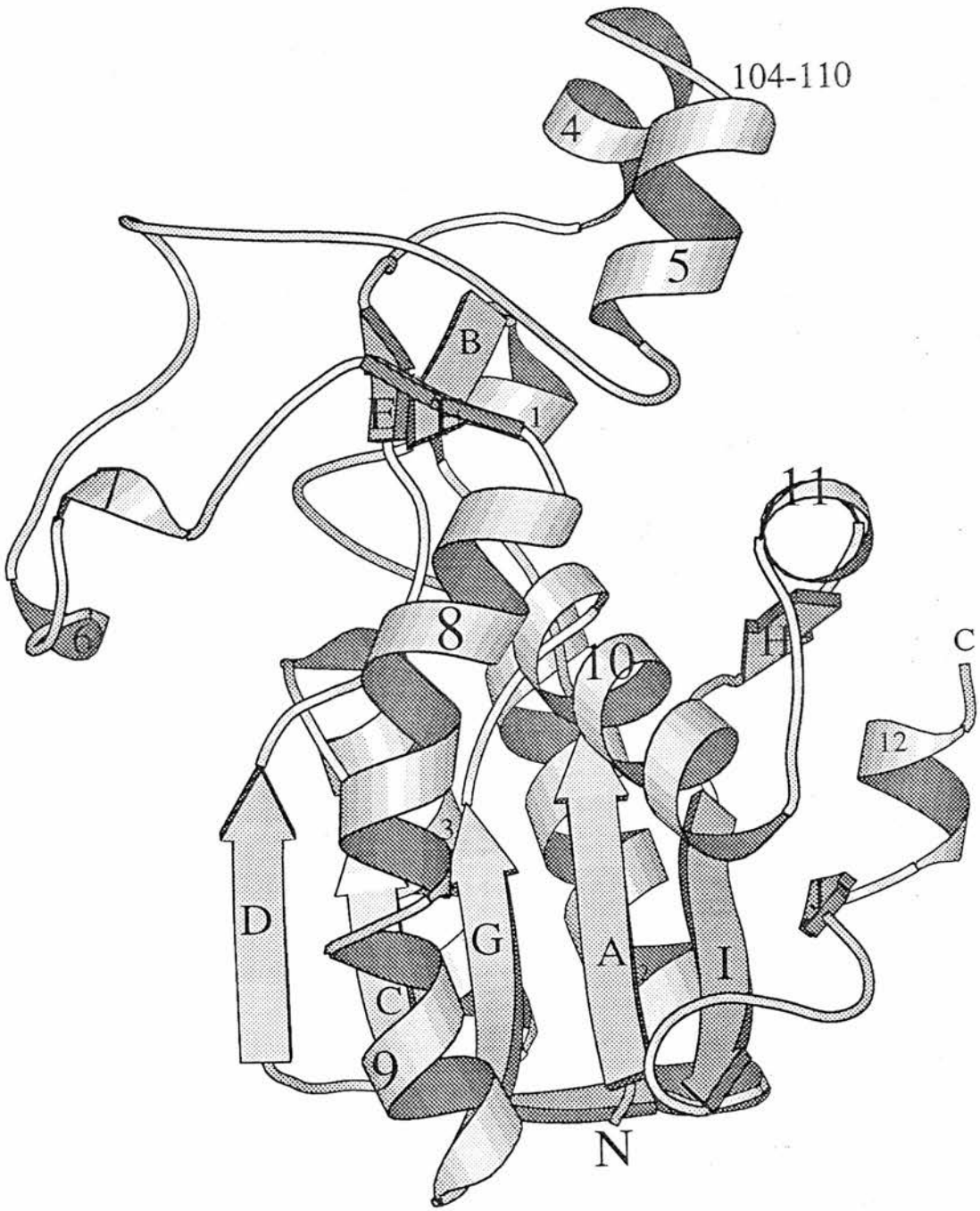

Figure 1.8
Ribbon diagram of a single subunit of *S. cerevisiae* PGAM, with alpha helices labelled 1-12 and beta strands A-K (2.3Å structure, Rigden *et al.*, 1997).

Each subunit is made up of two domains; in addition to the large domain with the nucleotide binding fold which was identified in the previous structure, there is another smaller domain in a region which was previously considered to have little secondary structure. It is made up of short β-strands and α-helices. Figure 1.8 shows a single subunit showing the two domains. The two active site histidines are found at the ends of strands A and G. The catalytic site is situated at the bottom of a deep cleft, 7A deep and with a minimum diameter of 7Å (the cleft is narrower and deeper than in the 2.8Å structure). This diameter could be increased by movements of the side chains of the many lysine and arginine residues in the cleft. The two histidines (His8 and His181) are shown not to be in the "clapping hands" conformation, but in an orientation closer to that seen in two other histidine phosphatase enzymes, rat prostatic acid phosphatase (RPAP) and fructose-2,6-bisphosphatase (see Section 1.13). They are very close together, 3.2Å compared with 4.7Å in RPAP and 4.2Å in fructose-2,6-bisphosphatase, but this may be because the mutase was crystallized with no salt or other ligand in the active site, unlike the other enzymes.

Another key difference between the two structures is the orientation of Glu15. In the 2.8Å structure this was shown to point into the active site, and it was suggested that the carboxyl side chain may act as a proton withdrawing group from the hydroxyl on C2 of the substrate. The new structure shows that Glu15 in fact faces away from the active site and therefore any role in catalysis is unlikely.

The positions of key active site residues is shown in figure 1.9. Arg59 is still situated near the two histidines, and its position is compatible with the role previously suggested - interacting with the carboxyl group of the substrate. Arg7 could also be involved in ligand binding. The hydroxyl group of Ser55 is likely to contribute to the orientation of the His181 side chain by hydrogen bonding to atom NE2. His181 and Arg59 are within hydrogen bonding distance of His8, which suggests that this residue is unprotonated (see figure 1.10). This is required for the suggested mechanism (section 1.10).

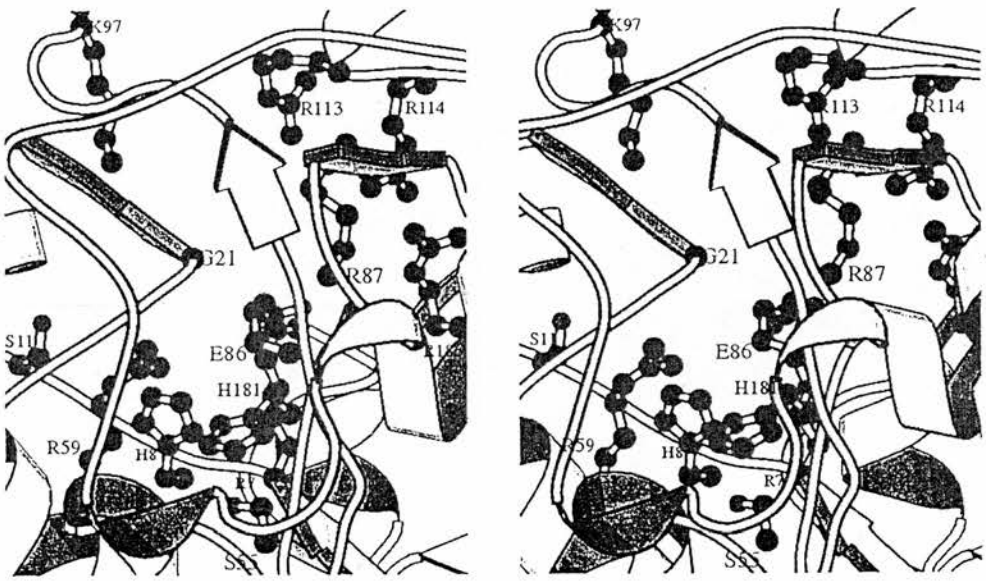

Figure 1.9

Stereo diagram of the active site of *S. cerevisiae* PGAM, showing the catalytic histidines and other residues mentioned in the text (2.3Å structure, Rigden *et al.*, 1997).

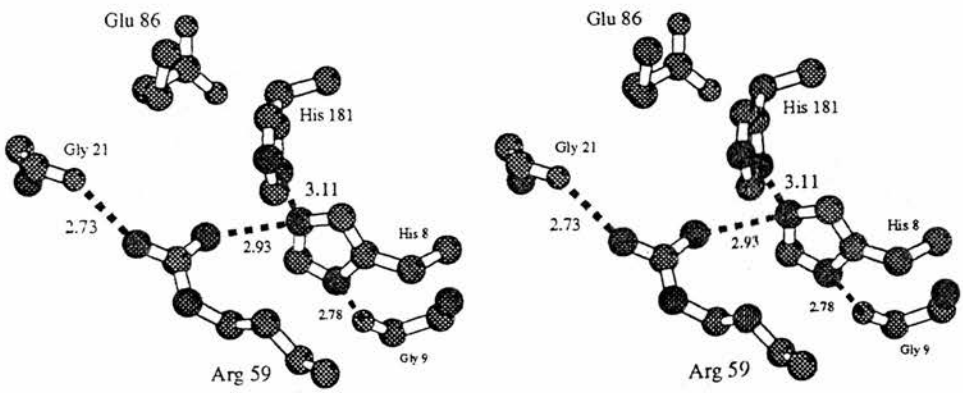

Figure 1.10
Stereo diagram of the H-bonding network around His8. H-bonds are represented by dotted lines and their lengths in Å are given.

1.8.3 Quaternary Structure

The cofactor-dependent phosphoglycerate mutases are unusual in that the most active form of the enzyme can be found in a variety of oligomeric structures depending on the organism from which it is isolated. For example, the mutases from *Saccharomyces cerevisiae*, *Penicillium janthinellum* and *Fasciola hepatica* are tetramers (Edelhoch *et al.*, 1957, Willets, 1980, Shulman and Valentino 1982), the vertebrate and bacterial *(Zymomonas mobilis* and *Escherichia coli)* enzymes are dimers (Cowgill and Pizer, 1956, Pawluk *et al.* 1986, D'Alessio and Josse, 1971), and the enzymes from *Schizosaccharomyces pombe* and *Pseudomonas* AM1 are monomers (Price *et al.* 1985, Hill and Attwood, 1976). PGAM is the only glycolytic enzyme that displays this range of fully active oligomeric forms. Hexokinase, phosphofructokinase and pyruvate kinase are found in different forms, but these display different activities and are probably the result of a control mechanism. PGAM shows no cooperativity between subunits.

The 2.8Å structure of the *S.cerevisiae* tetramer (figure 1.5) has two main sets of intersubunit contacts. The most extensive is termed CR (contact region) 1/2 and involves residues in β strand I, helix 2 and in the connecting loop, i.e. the 25 residues from Leu57 to Ser81. The side chains of the residues of the connecting loop (Leu74 to Val78) are thought to fill a hydrophobic pocket formed by the adjacent subunit, stabilizing the CR1/2 intersubunit contacts in the tetramer. These are essentially conserved in all the tetrameric and dimeric PGAMs (see figure 1.4) but in the *S.pombe* enzyme there are some radical substitutions, Trp75 to Asn, and Pro77 to Glu (*S.cerevisiae* numbering). These substitutions would be likely to weaken the interactions across the interface (Nairn *et al.* 1995).

The second set of contacts is termed CR5. In the *S.cerevisiae* structure, this set involves interactions between the side chains of residues in the loop preceding helix 5 (Tyr139 to Val144), which fit between side chains in helix 6 and the loop region between strands 5 and 6 of the symmetry-related subunit. In the *S.pombe* enzyme, there is a deletion of residues 122-146, consistent with its monomeric structure. The loop section (139-144) varies in sequence and length in the dimeric

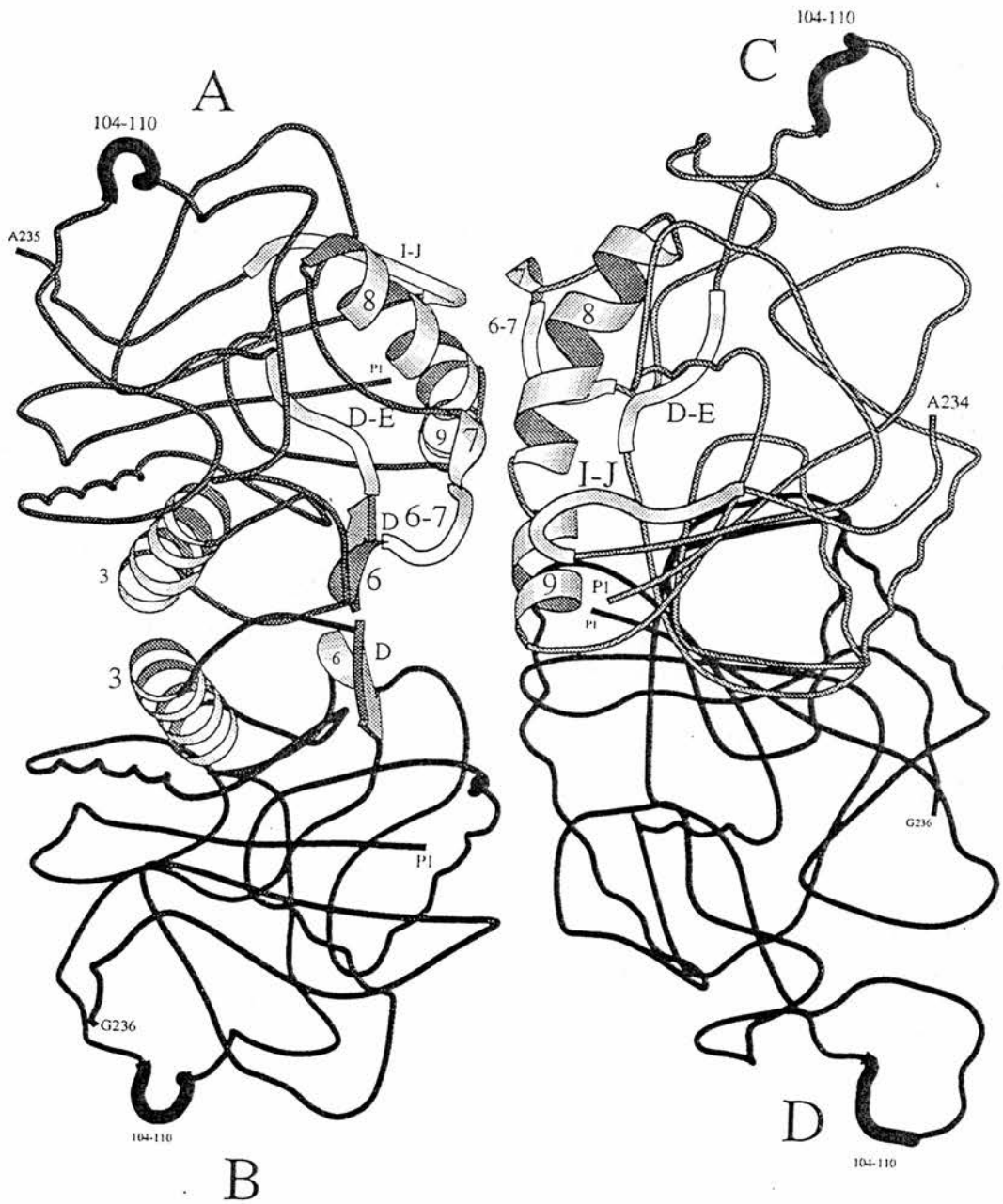

Figure 1.11

The *S. cerevisiae* PGAM tetramer (2.3Å structure, Rigden *et al.*, 1997).The subunits are labelled A-D. The ribbons represent the secondary structure involved in subunit contacts.

enzymes (figure 1.4) and this could explain the weakening of the CR5 contacts, giving rise to the dimers.

However, the new structure (Rigden *et al.* 1997) shows that, rather than one interface being more extensive than the other, the interfaces in fact bury similar amounts of solvent-accessible area and there are similar numbers of atomic contacts at each. The tetramer is shown in figure 1.11. At the A-B interface, most of the contacts involve helix 3 and strand D. Glu135 and Arg136 from helix 6 also form contacts. At the A-C interface, contacts are formed by a number of different regions of the protein. Among the larger contributors are Arg83, residues 163-164 from the end of helix 8 and residues 138-144. This last region is included in the deletion seen in the *S. pombe* mutase. Another residue at this interface is Lys168, which is a proline in the dimeric mutases. Site-directed mutagenesis of the lysine to a proline destabilizes the tetramer (White *et al.*, 1993b), therefore it is probable that the A-C interface is only present in the tetrameric forms. The *S. pombe* enzyme has a number of differences at both interfaces, explaining its monomeric form.

1.8.4 The C-terminal tail.

In the 2.8Å structure, the last 14 amino acids are not defined, as they were not seen in the electron density map, and were therefore thought to constitute a flexible tail region. The side chains of these residues tend to be small and uncharged, which would permit this flexibility.

-^{233}A A A G A A A V A N Q G K K^{246}

In the new structure, the tail adopts a helical conformation from residue 230 to 234. This short helix (helix 12) can be seen in figure 1.8. The helix makes no contacts with the rest of the enzyme, which supports the idea that this tail region is flexible. No structure could be defined after residue 236.

Early attempts to purify the enzyme from yeast gave a mixture of enzyme forms with differing electrophoretic mobilities. The component with the lowest

electrophoretic mobility had the highest specific activity and *vice versa*. The endogenous protease was partially purified and shown to cause the loss of nine or ten residues per subunit of PGAM (Sasaki *et al.*, 1966). Comparison of the amino acid composition of the native and modified enzyme showed that they were similar, but that the proteolyzed protein contained less alanine, lysine, glycine, valine, aspartic acid and glutamic acid. The difference between the two corresponded closely to the number of residues liberated during modification. Alanine, glycine, lysine and valine are all found at the C-terminus of the protein (the tail region). Removal of these residues did not alter the optical rotary dispersion pattern of the enzyme, and although the mutase activity was severely affected, the 2,3-BPGA phosphatase activity was unchanged. These results indicate that the residues of the C-terminal tail are important for mutase activity. Further evidence for the importance of this region comes from site-directed mutagenesis studies on human bisphosphoglycerate mutase (Garel *et al.* 1989). These showed that the deletion of a minimum of seven residues at the C-terminus removed all activity from the enzyme (synthase, mutase and phosphatase). Deletion of the two C-terminal lysines alone removed 38% of the synthase activity.

In figure 1.8, it can be seen that the tail could adopt a position over the entrance to the active site. An interesting feature of the tail is the pair of lysine residues at the C-terminus, at least one of which is conserved in all the PGAM sequences so far determined, with the exception of the *S.pombe* and *Z.mobilis* enzymes which lack the region corresponding to the tail (see figure 1.4).

Fothergill-Gilmore and Watson (1989) have suggested three possible roles for the tail. Firstly, that it physically excludes water from the active site, preventing the transfer of a phospho group to water instead of to the monophosphoglycerate substrate. Secondly, that it provides a third phospho ligand for the substrates, intermediate and transition state (see section 1.8.2). Thirdly, that it helps to retain the bisphosphoglycerate cofactor-intermediate in the active site during the reaction sequence (see section 1.10) by charge stabilization.

1.9 Ligand Binding

1.9.1 K_M values

The different substrates in the reactions catalyzed by the cofactor-dependent phosphoglycerate mutases have significantly different K_M values. The actual values of course vary between species, but the overall relationship between them is fairly constant. Representative values are given in table 1.3.

		K_M (μM)	
Reaction	**Substrate**	**MPGAM**	**BPGAM**
mutase	2,3-BPGA	0.7	
	3-PGA	170	
	2-PGA	15	
synthase	1,3-BPGA		0.4
	3-PGA		0.5
phosphatase	2,3-BPGA	0.05	2.5

Table 1.3
The K_M values of substrates involved in the reactions catalyzed by cofactor-dependent phosphoglycerate mutases, taken from Rose, 1980. Abbreviations: MPGAM, monophosphoglycerate mutase from chicken muscle; BPGAM, bisphosphoglycerate mutase from horse red cells.

These values are significantly influenced by ionic strength. In the presence of 400mM KCl, the K_M values are increased 10-fold (Grisolia and Cleland, 1968). Modelling studies using the 2.8Å structure (see section 1.8.2) show that the differences could be explained by the extra phospho group of 2,3-BPGA. The monophosphoglycerates would form the same number and type of specific interactions. The lower K_M for 2-PGA may be due to better hydrophobic contacts (Fothergill-Gilmore and Watson, 1989). The second phospho group of 2,3-BPGA would allow additional charge interactions to be formed in active site, which has a

high overall positive charge. The increased $K_M^{2,3\text{-BPGA}}$ for bisphosphoglycerate mutase is probably due to the lack of a specific phospho ligand, Ser11 (see section 1.13).

1.9.2 Substrate specificity

Pizer and Ballou (1959) tested the ability of a wide range of substrate analogues to act as phospho donors and/or acceptors in the mutase reaction. Their experiments defined a number of structural requirements needed for compounds to participate.

Firstly, carbon 1 (C1) must carry a negative charge. A sulphonic acid group can substitute for the carboxyl group, but not an aldehyde or a methyl ester. Carbon 2 (C2) is asymmetric. In the natural substrate, the hydroxyl group is in the D-configuration. The L-isomer can accept a phospho group, but at a considerably reduced rate. When the hydrogen on C2 is replaced with a methyl group, there is no phospho transfer, probably due to steric hindrance by the larger group. Carbon 3 (C3) can carry a methyl group in place of a hydrogen, but only when the hydroxyl groups on C2 and C3 are in the D-*erythro* configuration. When the hydroxyl group is replaced with an amino group, as in serine phosphate, there is no phospho transfer.

In summary, acceptor molecules are required to have three groups: a carboxyl or charged equivalent, a phospho group and a hydroxyl. Donor specificity was tested by assaying ability to activate the enzyme. Only diphosphates of phosphoglycerate and D-erythro-hydroxybutyric acid were active. ATP, ADP, CTP, UTP and creatine phosphate all showed no donor activity.

1.10 Enzyme Mechanism

Sutherland *et al.* (1949) used ^{32}P radiolabelled 3-PGA in the mutase reaction and showed that the label becomes distributed amongst the three ligands, 3-PGA, 2-PGA and 2,3-BPGA. This suggests that the 2,3-BPGA must bind to the active site and be formed by the phosphorylation of the monophosphoglycerate. Ionic strength affects the pattern of labelling (Cascales and Grisolia, 1966). In low salt concentrations, 2-PGA is preferentially labelled, whereas at higher concentrations

(~0.5M), 2,3-BPGA is favoured. Higher salt concentrations presumably promote the dissociation of the BPGA intermediate.

Early attempts to determine the mechanism of the enzyme gave conflicting results. Grisolia and Cleland (1968) suggested a ping-pong mechanism with a phosphoenzyme intermediate, but Chiba *et al.* (1970) proposed a sequential mechanism, with the direct transfer of a phospho group from 2,3-BPGA to a monophosphoglycerate. Britton and his co-workers developed an induced transport test based on flux kinetics to confirm that the mutase reaction proceeded via an intermolecular ping-pong mechanism involving a phosphoenzyme (Britton *et al.*, 1972, Britton and Clarke, 1972). The reaction kinetics suggest that there is only one phosphorylation site, as the rate of isomerization of phosphoenzyme intermediates would be not less than $4x10^6$ sec^{-1}, which is unrealistically rapid (Britton and Clarke, 1982). Therefore the monophosphoglycerates must bind so either C2 or C3 can be phosphorylated, and 2,3-BPGA so that either phospho group can be transferred, i.e. the substrate can bind in two different orientations, or can bind in a position where C2 and C3 are both close to the phosphorylation site.

In the enzyme phosphoglucomutase, which also has a phosphoenzyme intermediate involved in its mechanism, the residue which is phosphorlyated is the serine. The pH profile for isotope exchange with PGAM suggests the involvement of a histidine site in the mechanism (Cascales and Grisolia, 1966). Rose (1970) showed that the phosphoenzyme bond is acid labile and alkaline stable, which strongly suggests a phosphohistidine. Subsequently the sequences of active site peptides containing a phosphohistidine have been identified, and show that His8 (yeast numbering) is the phosphorylation site (Han and Rose, 1979, Haggarty and Fothergill, 1980, Hass *et al.*, 1980, Fothergill and Harkins, 1982).

A mode of action for the cofactor-dependent phosphoglycerate mutases has been suggested by Fothergill-Gilmore and Watson (1989). Firstly, a 2,3-BPGA molecule binds in the active site of the unligated enzyme in one of two orientations. One position is with the phospho group on C2 near to His8, also near enough to form hydrogen bonds with Ser11 and Thr20. They also suggest that a third phospho ligand is provided by the C-terminal lysines (Section 1.8.4). The phospho group on C3

interacts with the positive charge on the dipole at the N-terminus of helix 7. The other position has these two phospho groups reversed. The carboxyl group is in a position to form a salt bridge with Arg59. Phospho transfer from BPGA to His-8 then occurs, and a proton is provided by His181. This role for the second active site histidine was suggested by Rose (1980) and is supported by mutagenesis studies in which this residue is replaced by an alanine, with an associated decrease of catalytic efficiency (White and Fothergill-Gilmore, 1992). The resulting monophosphoglyerate is then released leaving the phosphoenzyme.

Either a 3-PGA molecule (in glycolysis) or 2-PGA (gluconeogenesis) binds to the active site, and the phospho group on His8 is transferred to the carbon atom carrying the hydroxyl group, forming a 2,3-BPGA intermediate. This molecule must then reorientate itself in the active site, so the phospho group that has *not* just been transferred is now adjacent to His8. Another phospho transfer occurs, and the monophosphoglyerate product is released leaving the phosphoenzyme ready for another round of catalysis.

The half life of the phosphoenzyme has been measured at 1-2 minutes (Britton *et al.* 1972*a*), and so the observed low level of phosphatase activity could be due to the hydrolysis of the phosphoenzyme.

1.11 Inhibitors

1.11.1 Substrates and substrate analogues

In a multifunctional enzyme which catalyzes more than one reaction, the substrate of one of the reactions is likely to act as a competitive inhibitor of another. As expected, 3-PGA, 2-PGA, 2,3-BPGA and 1,3-BPGA all act as competitive inhibitors at certain concentrations (Rose, 1980). Another important group of inhibitors are substrate analogues. The phosphonomethyl analogues of 3-PGA and 2,3-BPGA act as competitive inhibitors, with K_i values of 1.3mM and 0.8mM respectively. These molecules have the bridge oxygen replaced with a methylene group, and cannot transfer a phospho group, but are thought to bind to the active site in the same orientation as the substrates.

1.11.2 Anions

The natural substrates are all negatively charged, and the active site has a large overall positive electrostatic potential (Warwicker, 1986, Rigden *et al.*, 1997), and anions have been found to act as potent inhibitors. As has already been described, salts have a significant effect on the enzyme activities (Cascales and Grisolia, 1966). These include sulphate, phosphate and chloride. Among the most effective inhibitors are a number of polycarboxylates and polyphosphates, which have K_i values in the micromolar range. These are competitive with 2,3-BPGA and not with the monophosphoglycerate substrate analogue 2-phosphoglycollate, and therefore presumably bind to the non-phosphorylated enzyme (Rose, 1980). This class of inhibitor will be discussed in more detail in chapter five.

1.11.3 Vanadate

The cofactor-dependent, but not the cofactor-independent phosphoglycerate mutases are inhibited by micromolar concentrations of vanadate (Carreras and Bartrons, 1980). It is thought to act by destabilizing the phosphoenzyme, as the hydrolysis of the phosphoenzyme is increased, as is the phosphatase activity (Carreras *et al.*, 1982). The synthase activity, like the mutase activity, is decreased. Stankiewicz *et al.* (1987) showed that divanadate binds with a considerably higher affinity than the mono form, and it has been suggested that the dimer binds at the catalytic site of the phosphoenzyme as a substrate analogue, activating hydrolysis. The same workers have shown that 2-or 3-PGA potentiates the inhibition of PGAM by vanadate, and therefore have suggested that the inhibitor is a complex of monophosphoglycerate and vandate (2-vanadio-3-phosphoglycerate), acting as a transition state analogue for the transfer of the phospho group between the enzyme and monophosphoglycerate (Liu *et al.*, 1992). This complex is a more potent inhibitor than the divanadate, and when incubated with the enzyme-vanadate complex, results in the release of vanadate.

1.12 The mutase/synthase relationship

2,3-BPGA is present only in trace amounts in most mammalian cell types (Grisolia and Joyce, 1959, Chiba *et al.*, 1974), but at a considerably higher concentration in red blood cells (Harkness *et al.* 1969, Brewer and Eaton, 1971). Here the molecule acts as the most important regulator of haemoglobin oxygen affinity, binding preferentially to deoxyhaemoglobin and facilitating the unloading of oxygen in the tissues (Benesch and Benesch, 1968). The synthesis of 2,3-BPGA in red blood cells is catalyzed by the enzyme bisphosphoglycerate synthase (or bisphosphoglycerate mutase), EC 5.4.2.4 (Rapoport and Luebering, 1950). Like monophosphoglycerate mutase from yeast, this enzyme is trifunctional, also catalyzing monophosphoglycerate mutase and bisphosphoglycerate phosphatase reactions. These three reactions have been shown to be catalyzed at a common active site (Ikura *et al.*, 1976). The nucleotide and amino acid sequences of human red cell bisphosphoglycerate mutase have been determined (Joulin *et al.*, 1986, Haggarty *et al.*, 1983), and show that this enzyme shares about 50% sequence identity with yeast PGAM.

Bisphosphoglycerate mutase catalyzes all three reactions at significant rates. The ratio of activities for horse red cell bisphosphoglycerate mutase and chicken muscle monophosphoglycerate mutase are shown below (values taken from Rose, 1980).

	BPGAM	**MPGAM**
	k_{cat} (ratio)	**k_{cat} (ratio)**
mutase	1.7 (1)	1,333 (1)
synthase	12.5 (7.4)	0.4 ($3x10^{-4}$)
phosphatase	2.6 (1.5)	2.78 ($2x10^{-3}$)

The essential difference between the two enzymes is that the monophosphoglycerate mutase releases monophosphoglycerate and regenerates the phospho enzyme, and the bisphosphoglycerate mutase liberates bisphosphoglycerate and regenerates the free enzyme. The relative rates of phosphorylation differ, as does

the preferred phospho donor. The rates have been studied using a continuous flow and quench system (Rose and Dube, 1976). The preferred reaction of monophosphoglycerate mutases correlates with the rates of phosphorylation by the alternative donors. With 2,3-BPGA, the donor in the mutase and phosphatase reactions, the phosphorlyation rate is rapid (greater than 100 s^{-1}), whereas for 1,3-BPGA, the donor in the synthase reaction, the rate is much slower at 1.57 s^{-1}. With the bisphosphoglycerate mutase, the rate is more rapid with 1,3-BPGA (13.5 s^{-1}) than with 2,3-BPGA (2.3 s^{-1}). The rates for each donor are more similar with bisphosphoglycerate mutase than the monophosphoglycerate mutases, which could explain why the levels of activities for this enzyme are closer. Phospho transfer to the acceptor molecule (the second substrate) is very fast (>100 s^{-1}) with both enzymes, but the release of the enzyme-bound phospho group to water in the 2-phosphoglycollate-enhanced phosphatase activity is faster in the monophosphoglycerate mutase than the bisphosphoglycerate mutase (3.6 s^{-1} and 16 s^{-1} respectively). There must therefore be differences between the active sites of these enzymes which are responsible for the differences in the rate of phospho transfer.

Human bisphoshoglycerate synthase has been crystallized (Cherfils *et al.*, 1991), but there is as yet no published structure. However, the residues of the active site can be deduced by comparison with the sequence of the yeast enzyme. There is considerable identity between the two active sites, and many of the residues thought to be involved in the enzyme mechanism are conserved. These include two histidines, His10 and His187 (which correspond to His8 and His181 in the *S. cerevisiae* enzyme). His10 has been shown to be phosphorylated during the catalytic process (Han and Rose, 1979), and the replacement of this residue completely abolishes all three enzyme activities (Garel *et al.*, 1993). The His187 residue is also implicated in the catalytic mechanism by site-directed mutagenesis studies. It has been suggested that the corresponding residue in the *S. cerevisiae* enzyme (His181) donates a proton during formation of the phosphoenzyme and accepts a proton when the phospho group is transferred to the substrates in the mutase reaction (Fothergill-Gilmore and Watson, 1989, White and Fothergill-Gilmore, 1992). However, the formation of the phosphoenzyme in the first step of the synthase

reaction involves the transfer of an acyl phospho group and therefore does not require the transfer of a proton. Garel *et al.* (1993) found that replacing His187 of recombinant human bisphosphoglycerate mutase with aspartate or tyrosine completely removed all three activities, while another mutant, H187N, showed partial preservation of all three. Asparagine is not a proton donor, and so could not perform this role in the mutase and phosphatase reactions. However, all three activities were reduced equally in this mutant - there was no greater effect on the mutase and phosphatase activities as would be expected.

Another conserved residue, Arg89 (Arg87 in *S. cerevisiae* numbering), has been implicated in the reaction mechanism by analysis of the primary structure of bisphosphoglycerate mutase from a patient suffering from decreased 2,3-BPGA levels. This showed that Arg89 was replaced with a cysteine (Rosa *et al.*, 1989). Subsequent site-directed mutagenesis studies have shown that replacement of this positively charged residue with a neutral amino acid leads to an absence of synthase activity, a decrease in mutase activity and a decrease in the stimulation of the phosphatase activity by 2-phosphoglycollate. However, the unstimulated phosphatase activity was conserved or even increased (Garel *et al.*, 1993). Replacement of Arg89 with lysine on the other hand preserves some of the properties of the wild type enzyme. Synthase and phosphatase activities are maintained, and mutase and 2-phosphoglycollate stimulation are only moderately decreased.

As only the unstimulated phosphatase activity is unaffected when this positive charge is removed, it would suggest that the binding of monophosphoglycerates only is affected by the substitution. This is the only activity where the binding of a monophosphoglycerate is not involved. This gives weight to the theory that monophosphoglycerates and 2-phosphoglycollate bind at a site distinct from the bisphosphoglycerate binding site, although these would be likely to overlap at a single phosphorylation site at His8 of *S. cerevisiae* monophosphoglycerate mutase, and His10 of human bisphosphoglycerate mutase (Rose, 1980, Garel *et al.*, 1993, Ravel *et al.*, 1996).

The two histidines and the arginine are conserved in mono- and bisphosphoglycerate mutase. We would expect unconserved residues to be responsible for the specific functioning of the enzyme as predominantly a mutase or a synthase.

As described above, studies on the bisphoshoglycerate mutase from human erythrocytes have suggested the mono- and bisphosphoglycerate substrates bind at separate sites in the catalytic cleft. The postulated binding site for monophosphoglycerates involves (using *S. cerevisiae* numbering) residue 11 (Ser in monophosphoglycerate mutase and Gly in bisphosphoglycerate mutase), Glu15 and Lys245. The suggested binding site of bisphosphoglycerates involves residue 21 (Gly in monophosphoglycerate mutases and Ser in bisphosphoglycerate mutases), and Arg87 (Ravel *et al.*, 1996). These sites would therefore differ between the mono- and bisphosphoglycerate mutases. The former would have an extra phospho ligand for monophosphoglycerates (Ser11), and the latter would have an extra ligand for the binding of bisphosphoglycerates. This idea is partially supported by the new *S. cerevisiae* PGAM structure (Rigden *et al.*,1997) which shows that Gly21 and Arg87 are close together, as are Ser11 and Glu15. However, Glu15 is not solvent-exposed within the catalytic site cleft but on a different face of the protein, and therefore its role in substrate binding, at least in the *S. cerevisiae* enzyme, must be in question.

This structure also suggests that there may be a significant difference between the two catalytic sites in a least one area. The *S. cerevisiae* structure shows that Gly21 is hydrogen bonded by Arg59. This glycine residue has unusual torsion angles and it is unlikely that the corresponding serine residue in bisphosphoglycerate mutases adopts the same backbone conformation.

1.13 The histidine phosphatase family of enzymes

The cofactor-dependent phosphoglycerate mutases show significant sequence similarity with some other enzymes that catalyze different reactions. Rat prostatic acid phosphatase (RPAP) and the C-terminal phosphatase domain of the bifunctional enzyme 6-phosphofructo-2-kinase/fructose-2,6-bisphosphatase have been shown to

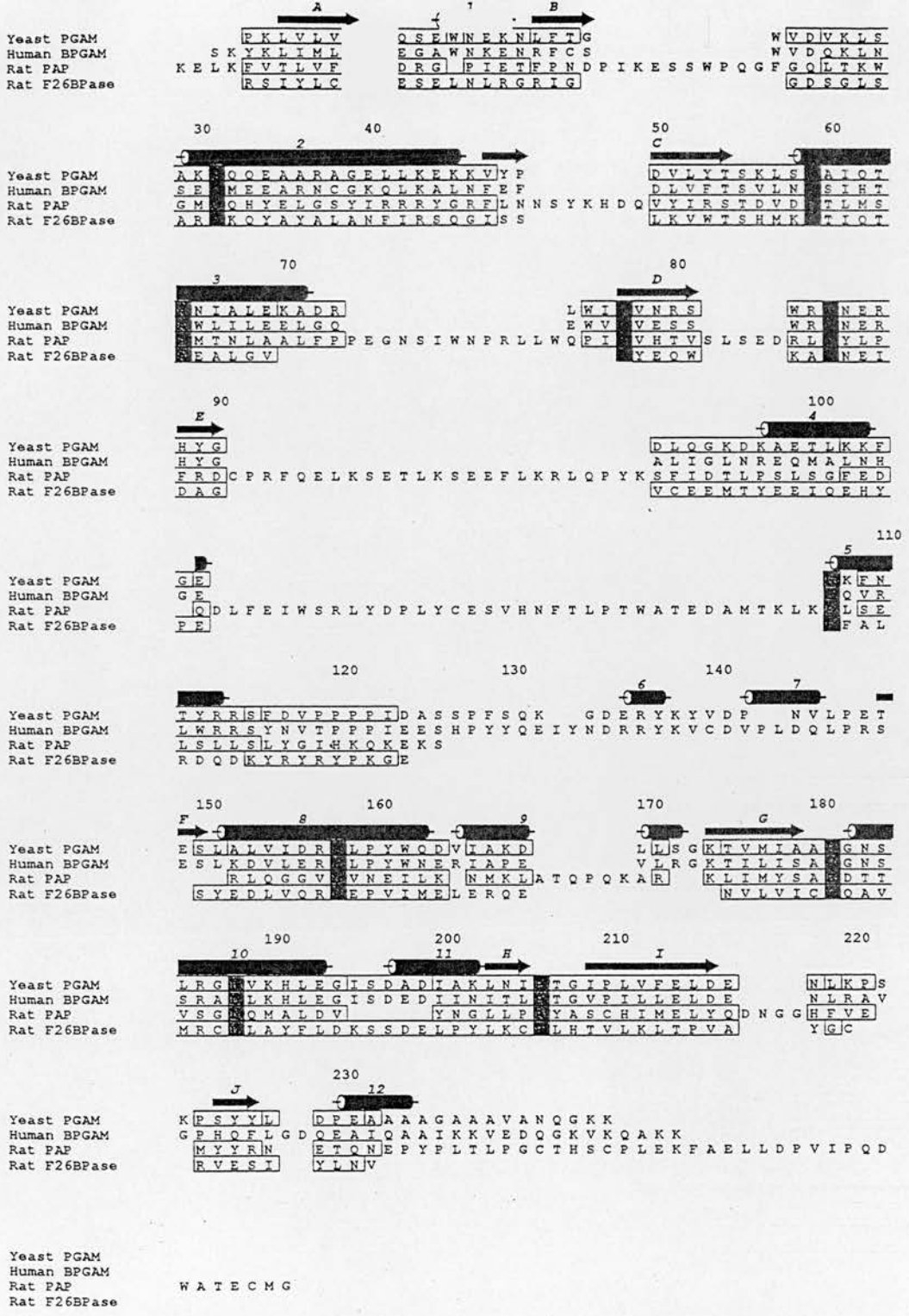

Figure 1.12

Structure-based alignment of members of the histidine phosphatase family. The helices and strands are indicated above the sequences. Residues identical in the four sequences are shaded. Abbreviations: Yeast PGAM, S. cerevisiae PGAM (White and Fothergill-Gilmore, 1988); Human BPGAM, bisphosphoglycerate mutase (E isoenzyme) from human erythrocytes (Joulin *et al.*, 1986); rat PAP, rat prostatic acid phosphatase (Roiko et al., 1990); rat F26BPase, fructose-2,6-bisphosphatase from rat liver (Lively et al., 1993). Figure from Rigden *et al.*, 1997).

have functional similarity with the mutases (Van Etten 1982, Bazan *et al.* 1989), and the catalytic mechanisms involve a phosphohistidine intermediate. Together with the phosphoglycerate mutases, they are sometimes known as the histidine phosphatase family. The crystal structures of both RPAP and the recombinant C-terminal phosphatase domain of 6-phosphofructo-2-kinase/fructose-2,6-bisphosphatase have been solved (Schneider *et al.*, 1993, Lee *et al.*, 1996), and have been compared with the 2.3Å structure of *S. cerevisiae* PGAM (Rigden *et al.*, 1997). Figure 1.12 shows a structure-based alignment between *S. cerevisiae* PGAM, BPGAM from human erythrocytes, RPAP and rat Fru-2,6-BPase. The catalytic site residues His8, His181, Arg7, Arg59 and Gly9 are conserved. Also conserved are residues which may be involved in maintaining the tertiary structure of the enzymes. The structural information, together with the results of site-directed mutagenesis studies on the enzymes may give valuable insight into the mechanism of the related phosphoglycerate mutases.

1.13.1 6-phosphofructo-2-kinase/fructose-2,6-bisphosphatase.

This bifunctional enzyme is responsible for the synthesis and hydrolysis of fructose-2,6-bisphosphate (Fru-2,6-P_2). This molecule, not itself an important metabolic intermediate, acts as an allosteric modulator of two important enzymes in sugar metabolism. An increase in cellular concentrations of Fru-2,6-P_2 leads to activation of 6-phosphofructo-1-kinase and inhibition of fructose-1,6-bisphosphatase. A decrease in Fru-2,6-P_2 reduces the activation of the kinase and the inhibition of the bisphosphatase. These enzymes are usually considered to be rate-limiting in the pathways of glycolysis and gluconeogenesis, and therefore an increase in Fru-2,6-P_2 leads to a net increase of glycolysis versus gluconeogenesis (Pilkis *et al.* 1995).

The rat liver enzyme is a dimer, each subunit consisting of a single polypeptide chain of 55,000 molecular weight. Residues 1-250 constitute the kinase domain and 251-470 the bisphosphatase domain. This C-terminal domain has 36% sequence identity with yeast PGAM. The crystal structure of the recombinant bisphosphatase domain has been determined (Lee *et al.* 1996), and shows a similar core structure to the yeast enzyme. The active site contains two histidines close to

each other (4.2 A) but not parallel. Other key active site residues are conserved in both the yeast PGAM and the bisphosphatase domain. A glutamic acid residue (Glu86 in yeast PGAM, Glu 327 in fructose-2,6-bisphosphatase) has been shown by site-directed mutagenesis to be important in the catalysis of the fructose-2,6-bisphosphatase reaction (Lin *et al.* 1992). On the basis of these studies, a mechanism has been proposed, involving nucleophilic attack by one of the histidines (that corresponding to His8 in yeast PGAM) on the 2-phospho group of the substrate, giving rise to the phosphohistidine intermediate The second His (corresponding to His181 in PGAM) donates a proton to the leaving group. The unprotonated Glu then leads to the formation of a OH^- ion from a water molecule, which then breaks down the phosphohistidine by nucleophilic attack on the phospho group, producing a molecule of inorganic phosphate.

1.13.2 Acid Phosphatases

The hydrolysis of phosphoric monoesters is catalyzed by several non-related enzymes, of which the acid phosphatases are one group. A conserved sequence motif in these enzymes is also found in phosphoglycerate mutase and in the phosphatase domain of 6-phosphofructo-2-kinase/fructose-2,6-bisphosphatase (Roiko *et al.* 1990). Crystallographic studies have shown that these enzymes have a similar core structure (Schneider *et al.* 1993), and site-directed mutagenesis studies on the enzyme from *E. coli* have shown that several residues which are located in the active site are important for catalysis, including the two histidines, three arginines and an aspartate (Ostanin *et al.* 1992). These, with further crystallographic studies on the rat prostatic enzyme complexed with vanadate and molybdate (which are thought to act as transition state analogues) have suggested a mechanism similar to that of the bisphosphatase reaction of the bifunctional enzyme (Lindqvist *et al.* 1994). Nucleophilic attack on the P atom of the phospho group of the substrate by an unprotonated histidine leads to the cleavage of the P-O bond. The oxygen atom of the ester is protonated to prevent the formation of a high energy alkoxide species. There are two candidates for the proton donor - a His residue analogous to that implicated in the PGAM and Fru-2,6BPase, and an Asp residue. The low optimum pH and the

orientations of these residues make the Asp (Asp258) the more likely donor, and the His is presumed to have a role in substrate binding. The proposed mechanism for this enzyme does therefore differ from those proposed for the other histidine phosphatases discussed. If they are indeed homologous, it is likely that this change occurred during adaptation to different conditions, in particular the change in the pH at which the enzyme functions.

1.14 Background to the project and aims

The PGAM from *S. cerevisiae* is the most extensively characterized of all the cofactor-dependent phosphoglycerate mutases. The availability of complete nucleotide and aminoacid sequences and the X-ray crystal structure (the only structure of a PGAM available) gave a good background for the study of this enzyme using protein engineering techniques. An expression system was developed by Dr Malcolm White, who constructed a phagemid vector carrying the *pgm* gene from *S. cerevisiae*. The vector (pVT-gpm) is shown in figure 1.13. There are a number of features which allow the production of single-stranded DNA for site-directed mutagenesis, the transformation of yeast and overexpression of phosphoglycerate mutase to be carried out without subcloning. The gene is under the control of its own promotor, and is expressed in a strain of *S. cerevisiae* from which the chromosomal copy of the phosphoglycerate mutase gene had been deleted and replaced with a marker gene HIS3, thereby removing the possibility of comtamination by wild type PGAM when mutant copies of the gene are expressed. Using this system, Dr White constructed a number of mutants designed for use in investigating the roles of several specific residues. Some of these were fully characterized, including a mutant in which His181 was replaced with Ala (White and Fothergill-Gilmore, 1992, White *et al.*, 1993). However, several other mutants that were constructed had not been characterized. These included a set of mutants where the C-terminal lysines were replaced by alanines, which were designed to investigate the roles suggested for the tail (see section 1.9.4). In addition, there was a set of mutants which were constructed with the intention of studying the mutase/synthase relationship. As described in

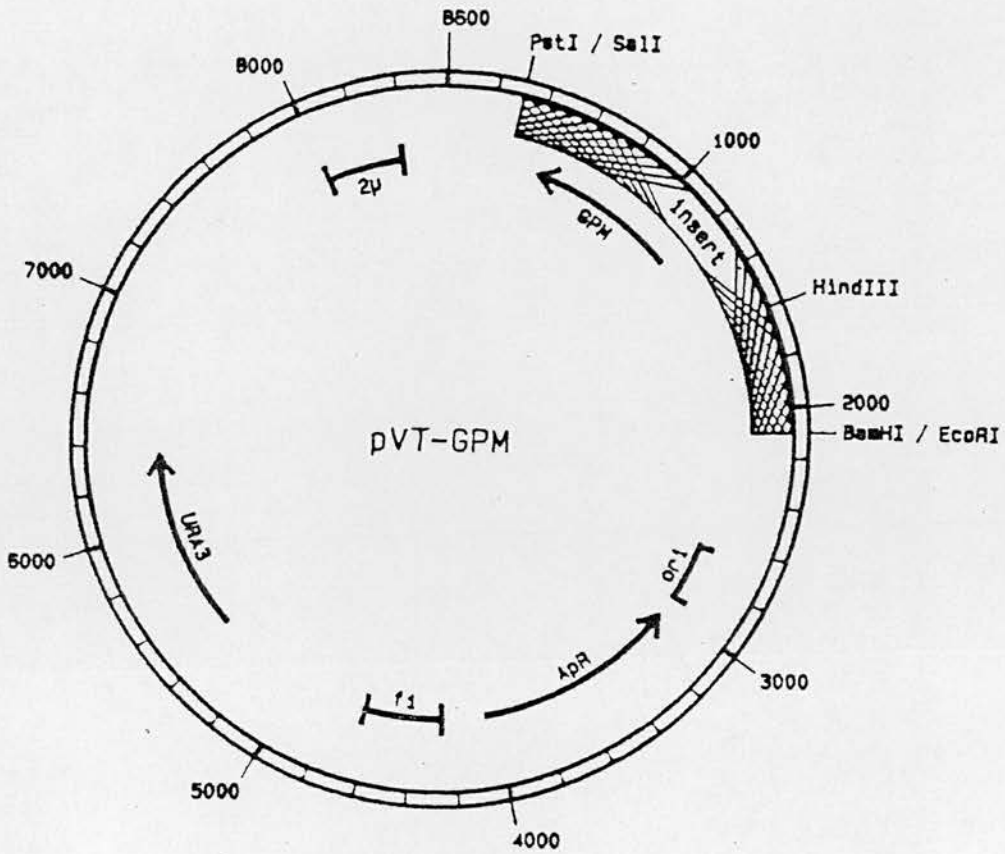

Figure 1.14

The phagemid vector pVT-gpm (White and Fothergill-Gilmore, 1992).

GPM: the phosphoglycerate mutase gene, expressed under its own promoter; ori: origin of replication; ApR: ampicillin resistance for selection in *E. coli*; f1: phage origin of replication for the production of single-stranded DNA; URA3: for selection in *S. cerevisiae*.

section 1.12, certain residues conserved in the monophosphoglycerate mutases differ in the bisphosphoglycerate mutases. These include Ser11 (Gly in BPGAM) and Ala60 (Ser in BPGAM). The mutants have the residues of monophosphoglycerate mutase replaced by the residues found in BPGAM. The primary aim of this project was to express, purify and characterize these mutant enzymes. In addition, the role of the C-terminal tail could be further studied using limited proteolysis, which has been used previously to remove the C-terminal region of rabbit muscle PGAM (Price *et al.* 1985). During the course of this project, a final-year research project was undertaken in this laboratory by four Honours students, who constructed a mutant in which Glu86 was replaced with a glutamine. Subsequently, the mutant was overexpressed in the mutase-deficient yeast strain, purified and characterized.

Chapter Two

Materials and Methods

2.1. MATERIALS

2.1.1. Strains

E.coli :

TG1	*supE hsd*ΔS *thi* Δ(*lac-pro AB*)
	F'[*traD*36 *proAB*$^{+}$ *lacI*^{q} *lacZ* ΔM15]
CJ236	*dut*1 *ung*1 *thi*-1 *relA*1 / pCJ105 (camr F')

S.cerevisiae:

S150-gpm::HIS3	MAT **a**, ura3, leu2, trp1, his3, **gpm::HIS3**
	(White and Fothergill-Gilmore 1992).

2.1.2. Vectors

The following were made by Dr. Malcolm White.

pVT-gpm	(White and Fothergill-Gilmore 1992).
pVT-K245G	
pVT-K246G	
pVT-K245G/K246G	

2.1.3. Growth Media

Oxoid Ltd., Haverhill, Suffolk.

Tryptone, bacteriological peptone, yeast extract, agar No.1.

Difco Ltd., Central Avenue, East Molesly, Surrey.

Yeast nitrogen base without amino acids.

Sigma Chemical Company, Fancy Road, Poole, Dorset.

Ampicillin, kanamycin, tetracyclin, tryptophan.

2.1.4. Radiochemicals

Amersham plc, Lincoln Place, Aylesbury, Bucks.

Deoxyadenosine 5'-(α-^{35}S)thiotriphosphate, triethylammonium salt, stabilized aqueous solution >300Ci/mmol.

2.1.5. Plasmid preparation.

Qiagen Ltd. Unit 1, Tillingbourne Court, Dorking Business Park, Dorking, Surrey.

Qiaprep-spin plasmid kit.

2.1.6. Enzyme Assays and Purification

Boeringher Mannheim, Bell Lane, Lewes, East Sussex.

Enolase, pyruvate kinase, lactate dehydrogenase, glyceraldehyde-3-phosphate dehydrogenase, triose phosphate isomerase, aldolase, 3,4-dichloroisocoumarin, fructose1,6-bisphosphate, NAD, NADH, ATP, ADP.

Sigma Chemical Company, Fancy Road, Poole, Dorset.

3-phosphoglycerate grade I, 2,3-bisphosphoglycerate, 2-phosphoglycollate, E64.

Aldrich Chemical Company Ltd, New Road, Gillingham, Dorset.

1,10-phenanthroline.

BDH, Merck Ltd, Hunter Blvd, Magna Park, Lutterworth, Leics.

Polyethyleneimine.

0.5mm diameter glass beads.

Whatman, Maidstone, Kent.

QA52-cellulose.

Pharmacia Ltd, Midsummer Blvd, Central Milton Keynes, Bucks.

Superose HR12 prepacked FPLC column.

Biospec Products.

Bead Beater.

2.1.7. Other enzymes

Northumbria Biologicals Ltd., South Nelson Industrial Estate, Cramlington, Northumbria.

T4 polynucleotide kinase, T4 DNA ligase.

Boeringher Mannheim, Bell Lane, Lewes, East Sussex.

RNase A.

Sigma Chemical Company, Fancy Road, Poole, Dorset

Lyticase.

2.1.8. Oligonucleotides

Synthesised by OSWEL DNA Service, Dept. Chemistry, University of Edinburgh, West Mains Road, Edinburgh.

2.1.9. DNA Sequencing

Amersham plc, Lincoln Place, Aylesbury, Bucks.

Sequenase Version 2.0™ DNA sequencing kit

Flowgen Instruments Ltd, Broad Oak Enterprise Village, Broad Oak Road, Sittingbourne, Kent.

Sequagel reagents.

2.1.10. Miscellaneous

Amersham plc, Lincoln Place, Aylesbury, Bucks.

Hyperfilm MP X-ray film.

Sigma Chemical Company, Fancy Road, Poole, Dorset.

Polaroid 665 film

Millipore (UK) Ltd., Peterborough Road, Harrow, Middlesex.

Millex-GS 0.22μm filter units.

A & J Beveridge Ltd., Bonnington Rd Lane, Edinburgh.

15 and 50ml Falcon tubes.

All other chemicals supplied by BDH or Sigma.

2.2. METHODS

Note - unless otherwise specified, "yeast" refers to *Saccharomyces cerevisiae*.

2.2.1. Growth of yeast

Yeast can be grown in either a rich, non-selective medium or in a synthetic medium which allows the selective growth of cells which can synthesize a specific amino acid or nucleotide. For example, the strain of yeast used for expressing the mutant PGAMs in this work, S150-2B GPM::HIS3, is ura3-, and can only grow in a selective ura- medium if it has been transformed with a plasmid carrying a functional URA3 allele (here the pVT-103U vector). Usually glucose is supplied as a carbon source, but as S150-2B GPM::HIS3 cannot use the glycolytic pathway, it must be grown on a non-fermentable carbon source. In this work glycerol and ethanol are used. Using glucose instead of glycerol and ethanol in the plates after yeast transformation therefore also acts as a selection for transformants, as non-transformed cells would not be able to utilize this carbon source.

2.2.1.1 Growth Media

(Percentages are expressed as w/v)

YEPD	Yeast extract	1%
	Bactopeptone	2%
	Glucose	2%
YEPGE	Yeast extract	1%
	Bactopeptone	2%
	Glycerol	2%
	Ethanol	2%

The above were made up to the desired volume with distilled water and sterilized by autoclaving at 15lb/in^2 for 15 minutes. For YEPD/YEPGE agar, 2% agar was added before autoclaving.

YOD ura-	Yeast Nitrogen Base w/o amino acids	0.67%
	Casamino acids	1%
	Glucose	2%
YOGE ura-	Yeast Nitrogen Base w/o amino acids	0.67%
	Casamino acids	1%
	Glycerol	2%
	Ethanol	2%

Casamino acids are the product of the hydrolysis of casein, and provide the necessary amino acids to supplement the medium with the exception of tryptophan, which must be added separately. A stock solution of 0.2% tryptophan was made up with distilled water, sterilized by autoclaving and kept in the dark at 4°C. It was added to the medium in a 100-fold dilution. For YOD/YOGE agar, 2% agar was added before autoclaving.

2.2.2. Transformation of gpm-disrupted strain

A single colony of S150-2B GPM::HIS3 was transferred on a sterile loop to 5ml of YEPGE and grown overnight at 30°C in a shaking incubator. This was then subcultured into 50ml of fresh medium and grown to an OD_{600} of between 0.4 and 0.6.

The cells were harvested by centrifugation (4°C, 2000g, 5min), washed in 10ml TE (10mM Tris-HCl pH8.0, 1mM EDTA pH8.0), and centrifuged again as before. The washed cells were resuspended in 5ml LA (0.1M lithium acetate in TE).

20µl of miniprep DNA (approximately 4µg) was mixed with 200µl of cells. 300µl of 50% PEG4000 was added, mixed well and incubated at 30°C in a shaking incubator for one hour. The cells were then subjected to heat shock at 42°C for 15 minutes.

The transformed cells were grown overnight in 3ml YEPGE, then spread onto selective plates (YODura$^-$) and incubated at 30°C. Transformant colonies typically

began to appear after 14 days. The transformation efficiency was low using the deleted strain - typically 10-15 colonies from the above quantities.

2.2.3. Analysis of protein expression levels in yeast

The transformant colony was transferred on a sterile loop to 5ml YEPD and grown overnight at 30°C in a shaking incubator. 1ml of the overnight culture was taken and the cells pelleted by centrifugation (2500g, 2 minutes). The cells were resuspended in 70µl of 50mM Tris-HCl pH8.0 and glass beads (0.5mm diameter) were added to 1-2mm below the meniscus. The sample was cooled on ice for 5 minutes, then vortexed twice for one minute with one minute cooling on ice in between. The cell debris was pelleted by centrifuging the sample for 2 minutes at 12,000g. 20µl of the supernatant was removed and analysed using SDS-PAGE.

2.2.4. Small-scale plasmid preparation from yeast

A single colony of the yeast was transferred on a sterile loop to 5ml of selective medium (YODura$^-$) and grown overnight at 30°C in a shaking incubator. The overnight culture was centrifuged (2500g, 2 minutes), and the supernatant was discarded. The pellet was resuspended in 400µl of SCEM (1M sorbitol, 0.1M sodium citrate pH 5.8, 10mM EDTA, 30mM 2-mercaptoethanol). 50 units of lyticase were added and the sample was incubated for 20 minutes at 30°C. The level of spheroplast formation was checked by mixing 5µl of cells with 5µl of 10% SDS and looking for more than 50% lysis under a microscope. The spheroplasts were collected by centrifuging at low speed for 10 seconds, and resuspended in 450µl of TE (10mM Tris.HCl pH7.5, 1mM EDTA). 50µl of 10% SDS was added and the sample was incubated for 30 minutes at 65°C. After incubation, 80µl of 5M potassium acetate was added. The sample was kept on ice for one hour, then centrifuged (12,000g, 15 minutes) and the supernatant transferred to a clean tube. The plasmid DNA was precipitated by the addition of 1ml of ice-cold ethanol and collected by centrifugation (13,000rpm, 5 minutes). The pellet was rinsed with 0.5ml 70% ethanol and allowed to air dry, then resuspended in 20µl of TE. 10µl was used to transform *E.coli* to

allow sufficient amplification for analysis using agarose gel electrophoresis and DNA sequencing.

2.2.5. Purification of *S.cerevisiae* phosphoglycerate mutase

NB - this method was followed for wild type mutase and all the mutants except S11A/A60S.

2.2.5.1. Growth and cell lysis.

A single colony of the yeast expressing the PGAM to be purified was taken on a sterile loop and used to inoculate 10ml of YEPD, and grown overnight at 30°C in a shaking incubator. The following day this was used to inoculate 200ml of YEPD. This was grown as before and used the next day to inoculate 2 litres of YEPD in four 2L flasks. The cells were harvested in early stationary phase (after approximately 18 hours' growth) by centrifugation. The cells were washed in a small volume of ice-cold 50mM Tris-HCl pH8.0 and collected by centrifugation (2000rpm, 10 minutes, 4°C). The packed cell volume was estimated and the cells were resuspended in an equal volume ice-cold 50mM Tris-HCl pH8.0. Protease inhibitors (see section 2.2.6.7) were added. The cell suspension was transferred to the pre-cooled chamber of the bead-beater apparatus and an equal volume of 0.5mm diameter glass beads was added. The cells were lysed by five one minute pulses with one minute cooling on ice in between each pulse. The beads were then washed in ice-cold 50mM Tris-HCl pH8.0 and allowed to settle out. The supernatant was centrifuged at 30,000g at 4°C for one hour in an ultracentrifuge to remove cell debris, and the supernatant collected.

2.2.5.2. Ammonium sulphate fractionation.

Solid ammonium sulphate was added to the cleared lysate to 50% saturation, slowly and with stirring. This was carried out at room temperature (18-20°C). The sample was centrifuged (17,400g, 30min, 4°C), the supernatant collected and ammonium

sulphate added to 80% saturation. The sample was then centrifuged as above and the pellet resuspended in 15ml 10mM Tris-HCl pH8.0 and dialysed against 5 litres of 10mM Tris-HCl pH8.0 overnight at 4°C.

2.2.5.3. Anion exchange chromatography

The dialysed sample was applied to a QA52-cellulose column (20cm x 1.7cm^2) equilibrated overnight with 10mM Tris-HCl pH8.0 at 4°C. Wild type PGAM, K245G, K246G, K245G/K246G and A60S bound to the column under these conditions, and were eluted with a 500ml linear gradient of 0 - 75mM NaCl in 10mM Tris-HCl pH8.0. The flow rate was approximately one column volume per hour. S11A did not bind to the QA52-cellulose column under these conditions and was collected when the column was washed with 10mM Tris-HCl pH8.0.

2.2.5.4. Size exclusion chromatography

The fractions showing peak mutase activities were pooled and further purified by FPLC gel filtration on a Superose HR12 column equilibrated in 50mMTris-HCl pH8.0, using a flow rate of 0.3ml/min.

The purified protein was analysed using SDS-PAGE and enzyme activity assays.

2.2.5.5. Partial Purification of S11A/A60S

The cells were grown and lysed as for wild type mutase, but the buffer used was 30mM Tris.HCl pH8.0 containing 25% glycerol. The cell debris was spun out at a lower speed (17,400g, 20 min, 4°C).

An equal volume of 0.2% polyethyleneimine, 25% glycerol (pH adjusted to 8.0) was added and the mixture stirred for 30 minutes at 4°C. After centrifugation (17,400g, 30minutes) the supernatant was loaded directly onto a QA52-cellulose column equilibrated with 15mM Tris-HCl, 25% glycerol pH 8.0 at 4°C, using a flow rate of 0.1ml/min.

2.2.5.7. Protease Inhibitors

The following inhibitors were added to the cell slurry to prevent the degradation of PGAM by endogenous proteases released when the cells were disrupted.

- 3,4-dichloroisocoumarin (inhibits serine proteases)

Stock - 5mM in DMSO. Diluted x 50 for use into the lysis buffer.

- E64c (inhibits cysteine proteases)

Stock - 1mM in SDW. Diluted x 50 for use

- 1,10-phenanthroline (inhibits metalloenzymes)

Stock - 100mM in DMSO. Diluted x 1000 for use.

2.2.6. Purification of *S.pombe* phosphoglycerate mutase.

The sample of *S.pombe* PGAM was obtained in a partially purified condition from Dr. J. Nairn, Department of Biological and Molecular Sciences, University of Stirling, Stirling FK9 4LA. It was purified to homogeneity by a Superose 12 gel filtration step, exactly as described for the *S.cerevisiae* PGAM in section 2.2.6.4.

2.2.7. Protein assays

The concentration of total protein in crude samples was determined by a Coomassie Blue binding method (Sedmak and Grossberg, 1977), using bovine serum albumin as a standard.

The concentration of pure enzyme was determined spectrophotometrically, using a value of 1.45 for the A_{280} of a 1mg/ml solution (Edelhoch *et al.*, 1957).

2.2.8. Enzyme Activity Assays

2.2.8.1 Mutase assay

The mutase activity was coupled to the activity of enolase, pyruvate kinase and lactate dehydrogenase.

The reaction was monitored by the decrease in absorbance at 340nm due to the oxidation of NADH in the reaction catalyzed by lactate dehydrogenase.

The activity was monitored using a Phillips 8720 UV/VIS spectrophotometer. 1 unit of PGAM was defined as 1μmol NADH oxidized/min/mg PGAM i.e. (ΔA_{340} /6.22) / min / mg.

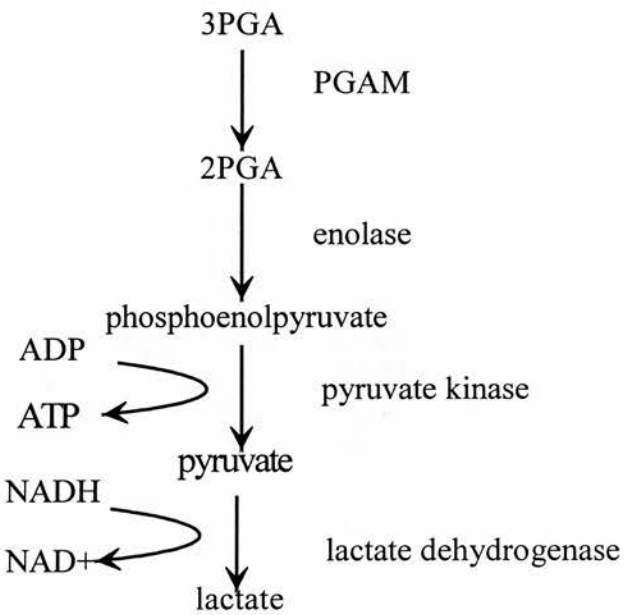

Assay mix;

30mM	Tris.HCl pH7.0
20mM	KCl
5mM	$MgSO_4$
0.2mM	NADH
0.15mM	ADP
0.08 units	enolase
0.5 units	pyruvate kinase
0.5 units	lactate dehydrogenase

The concentrations of 3PGA and 2,3BPGA could be varied. Saturating concentrations (5mM 3PGA, 0.2mM 2,3BPGA) were used when assaying for specific activity,

The above components were mixed and allowed to equilibrate at 30°C for 5 minutes. The reaction was started by the addition of PGAM.

For pure wild type PGAM, 20-50ng can conveniently be assayed, giving an activity of approximately 1000U/mg. Mutase samples were diluted in 30mM Tris.HCl pH7.0 containing 1mg ml^{-1} bovine serum albumin.

2.2.8.2 Phosphatase assay

The phosphatase activity was coupled (like the mutase activity) through enolase, pyruvate kinase and lactate dehydrogenase.

The assay was carried out in 30mM Tris-HCl pH8.0, and KCl and 3PGA were omitted, otherwise the conditions were as for the mutase assay.

10-20μg of pure wild type PGAM can conveniently be assayed, giving a specific activity of approximately 0.002U/mg.

2.2.8.3 Synthase Assay

The synthase activity was measured using the method of Rosa *et al.*, 1989.

It is coupled to the activities of aldolase, triosephosphate isomerase (TIM) and glyceraldehyde-3-phosphate dehydrogenase (GAPDH), and followed by monitoring the increase in absorbance at 340nm due to the reduction of NAD^+ by GAPDH.

Assay mix; 50mM Tris-HCl pH8.0
7mM KH_2PO_4
1mM NAD^+
2mM 3PGA
7mM fructose-1,6-bisphosphate
0.18 unit aldolase
0.1 unit TIM
0.32 unit GAPDH

The above components were mixed and allowed to equilibrate at 30°C for 5 minutes. The reaction was started by the addition of PGAM.

10-20μg of pure wild type PGAM can conveniently be assayed, giving a specific activity of approximately 0.002U/mg.

2.2.9. Kinetic analysis.

The kinetic parameters of the enzyme were measured by varying the concentrations of 3-PGA and 2,3-BPGA in the assay mixture, measuring rates and plotting them on a Hanes plot, as described in Cornish-Bowden, 1979. Each assay was repeated in triplicate and the data point shown is the mean of the three values obtained (which differed by less than 5% standard error). The graphs were drawn using the application Cricketgraph on an Apple Macintosh computer, which provided linear regression analysis of the data. For each line of best fit, the R^2 value obtained was greater than 0.96.

2.2.10 Inhibitor studies.

The effect of inhibitors on mutase activity was carried out as described in section 2.2.8.1. 3-PGA was added to the assay mix at 5mM, and the concentrations of 2,3-BPGA and inhibitor were varied. The amount of coupling enzymes was doubled (0.16 units enolase, 1 unit pyruvate kinase, 1 unit lactate dehydrogenase per assay). See section 5.3. These were incubated at 30°C for five minutes, and the reaction was started by the addition of PGAM. The results were plotted and regression analysis performed using Lotus123 for Windows.

2.2.11. Protein crosslinking

The subunits of PGAM were cross-linked with glutaraldehyde using the method of Jaenicke and Rudolf (1986). 40μl of 25% (w/v) glutaraldehyde (Sigma Grade 1) was added to a 1ml solution containing 10-50μg of protein in 50mM sodium phoshpate buffer pH7.0. After two minutes at room temperature the reaction was quenched by the addition of 50μl of 2M sodium borohydride in 0.1M NaOH, and incubated for 20

minutes at room temperature. After incubation, 3µl of 10% aqueous sodium deoxycholate was added, followed by 45µl of 78% trichloroacetic acid, added slowly to minimize bubbling. The mixtures were incubated for five minutes on ice, and then centrifuged for 10 minutes at full speed in a microcentrifuge at 4°C. The supernatant was discarded and the pellet was washed in 600µl of cold acetone, dispersed with a pipette tip, and centrifuged again as before. The supernatant was discarded and the pellet resuspended in 10µl of loading buffer (0.1M Tris-HCl pH8.0, 0.1% SDS, 50mM DTT, 10% glycerol, 5mg/100ml bromophenol blue). The samples were electrophoresed on a 15% SDS-PAGE gel.

2.2.12 Limited proteolysis

The proteolysis of PGAM by thermolysin was studied at 20°C in 50mM Tris-HCl pH8.0. Solutions of thermolysin were prepared fresh each day in the same buffer. For studying the effect of proteolysis on activity, thermolysin was added at different concentrations to a 100µg/ml solution of PGAM, and samples removed at intervals and diluted into buffer containing 5mM EDTA to inactivate the thermolysin (Girg *et al.* 1981). For studying the proteolysis using SDS-PAGE, 500µg/ml of PGAM was incubated with thermolysin at 200µg/ml and 50µg/ml. Samples were removed at intervals and EDTA added to 5mM. The samples were electrophoresed as detailed in section 2.2.19.

2.2.13 Protein Sequencing

Sequencing studies on *S. cerevisiae* PGAM were done on an Applied Biosystems 477A microsequencer. Samples containing approxiamately 1 nmol of PGAM were taken at zero time and after a ten minute treatment with thermolysin and spotted directly onto glass fibre disks for sequencing.

2.2.14 Circular Dichroism.

C.d. measurements were performed on a JASCO J-600 spectropolarimeter at 20°C. The molar ellipticities were calculated assuming a value of 112 for the mean residue weight of each enzyme (White and Fothergill-Gilmore, 1988).

2.2.15 Mass Spectrometry

Mass spectrometry analysis was performed on a VG Platform quadropole mass spectrometer (2-3000 amu range) fitted with a pneumatically assisted electrospray source and controlled via the VG Mass-Lynx software (VG Biotech Ltd, Altrincham, Cheshire, UK.).

2.2.16 Site-Directed Mutagenesis

Site-directed mutagenesis was carried out using the method of Kunkel (1987). The single-stranded template was prepared from CJ236 cells transformed with pVT-gpm using the standard methods described above. The helper phage used in production of single-stranded DNA was M13K07. Sequenase version 2.0 purchased from Amersham was used as the DNA polymerase, and the method given in Sambrook *et al.* (1989) for mutagenesis using this enzyme was followed. The mutagenesis reaction mix was used to transform competent TG1 cells. The resulting colonies were then pooled and grown overnight. Plasmid DNA was then prepared from the pooled cells and again used to transform TG1. This ensured that a single colony only contained either a wild type or a mutant copy of the plasmid. The colonies were then screened for mutants using DNA sequencing.

2.2.17 DNA sequencing.

Sequencing was done using the Sequenase version 2.0 kit from Amersham, using the modifications described in Hsaio (1991) for a double stranded DNA template.

The reactions were electrophoresed on a 6% acrylamide/urea gel made up using Sequagel solutions from Flowgen Instruments Ltd. The gel was fixed and dried and an autoradiograph obtained using the standard procedure given above.

2.2.18 Standard Procedures.

The following procedures were carried out as described in *Molecular Cloning - A Laboratory Manual (Second Edition). Sambrook, J., Fritsch, E.F. & Maniatis, T.(1989) Cold Spring Harbour Laboratory Press.*

- Preparation and purification of single-stranded phagemid DNA.
- Extraction and purification of plasmid DNA from *E.coli.* (To obtain high quality templates for DNA sequencing, the Qiaprep spin plasmid kit from Qiagen was used)
- Preparation and transformation of competent *E.coli* using calcium chloride.
- Autoradiography of Sequencing gels.
- SDS-polyacrylamide gel electrophoresis of proteins.

Chapter Three

The Effects of Limited Proteolysis on Phosphoglycerate Mutase

3.1 Introduction

The susceptibility of proteins to proteolysis has been widely used to study their domain structures. Particularly susceptible are "flexible loops" in the polypeptide chain. As described in section 1.8.4 the 14 residues nearest the C-terminus of phosphoglycerate mutase from *S.cerevisiae* are not seen in the electron density map and are therefore assumed to form one of these highly flexible regions (Winn *et al.* 1981).

Early attempts to purify the enzyme from yeast gave a mixture of enzyme forms with differing electrophoretic mobilities (Chiba and Sugimoto 1959, Chiba *et al.* 1960*a*). The component with the lowest electrophoretic mobility had the highest specific activity and *vice versa*. Chiba *et al.* (1960*b*) showed that the formation of the lower activity components was dependent on the length of time the yeast was subjected to autolysis during enzyme purification. The endogenous protease was partially purified by Sasaki *et al.* (1966) and was shown to cause the loss of nine or ten residues per subunit of PGAM. Comparison of the amino acid composition of the native and modified enzyme showed that they were similar, but that the proteolyzed protein contained less alanine, lysine, glycine, valine, aspartic acid and glutamic acid. The difference between the two corresponded closely to the number of residues liberated during modification. Alanine, glycine, lysine and valine are all found at the C-terminus of the protein (the tail region). Removal of these residues did not alter the optical rotary dispersion pattern of the enzyme, and although the mutase activity was severely affected, the 2,3BPGA phosphatase activity was unchanged. This activity was not however stimulated by the substrate analogue 2-phosphoglycollate in the modified enzyme, compared with the 20-fold increase seen with the native enzyme.

More recently, the enzyme from rabbit muscle has been shown to be inactivated by limited proteolysis with thermolysin (Price *et al.* 1985). Again the inactivation was not accompanied by a change in overall conformation as measured using circular dichroism, although when analyzed using SDS-PAGE, a change in electrophoretic mobility was seen, which was thought to be due to the loss of a peptide corresponding to the C-terminal tail of the yeast enzyme.

Similar experiments were done on the yeast enzyme to try to elucidate the role of the tail.

3.2 Effect of different thermolysin concentrations on mutase activity

PGAM (100μg/ml) was incubated with various concentrations of thermolysin (0, 10, 50 and 100μg/ml) and samples removed at intervals. These were assayed for mutase activity, and the results are shown in figure 3.1. Clearly thermolysin has a significant effect, with activity lost rapidly over the first 10-20 minutes and continuing to decrease at a slower rate for at least 2 hours. When the reaction is complete (i.e. the activity no longer changes with time) around 10% of activity remains. This pattern is seen for all concentrations of thermolysin, with the higher concentrations reaching this level more quickly.

Further investigations were carried out using the 10:1 PGAM to thermolysin ratio.

3.3 Effect on phosphatase activity

The phosphatase activity is largely unaltered by treatment with thermolysin, as can be seen in figure 3.2. However, the stimulatory effect of 2-phosphoglycollate is decreased, from 18-fold with untreated PGAM to 1.8 fold after 2 hours incubation. Specific mutase and phosphatase activities are given in the table below.

	untreated	**10min incubation**	**120min incubation**
mutase	970	630	95
phosphatase	0.02	0.02	0.03
phosphatase + 1mM 2-PG	0.35	0.12	0.05
fold stimulation by 1mM 2-PG	18	6.2	1.8

Table 3.1
Specific activities (units, see 2.2.8.1) of untreated and proteolyzed PGAM from *S. cerevisiae*.The PGAM:thermolysin ratio used was 10:1 (100μg/ml PGAM, 10μg/ml thermolysin).

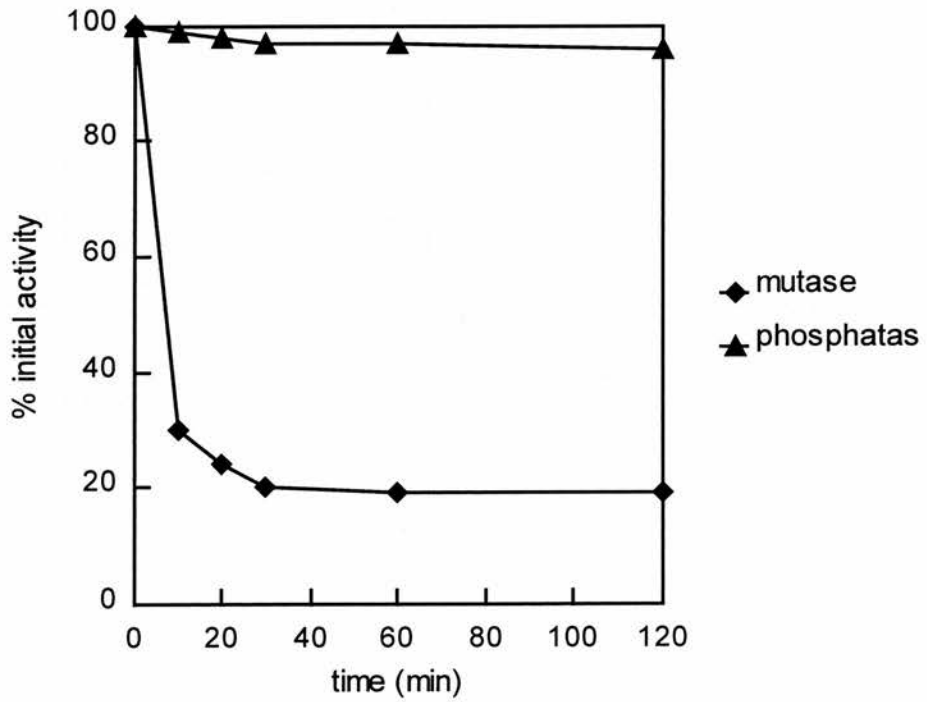

Figure 3.2
The effect of thermolysin on the mutase and phosphatase activities of PGAM. PGAM was added at 100μg/ml and thermolysin at 10μg/ml.

3.4 Effect of thermolysin on PGAM monitored by SDS-PAGE

Figure 3.3 shows the pattern seen on SDS-PAGE when 500μg of PGAM was treated with 200μg thermolysin. A second band (with higher electrophoretic mobility) becomes visible after 10 minutes, becoming more prominent with time. However, the total amount of protein present clearly decreases, and almost no protein is visible after 120 minutes. When the 10:1 PGAM to thermolysin ratio was used (Figure 3.4), again a second band appears (after 20 minutes), but the band corresponding to native PGAM remains the major component. As this does not correlate with the large decrease in activity observed, it is unlikely that this band is the tailless enzyme (see Section 3.6).

3.5 The effect of ligands

Limited proteolysis was carried out as before, but with the addition of saturating concentrations of substrates 3PGA and 2,3BPGA (10mM and 0.5mM respectively - the concentrations used in the standard activity assays). The results can be seen in figure 3.5. In the presence of 3PGA alone, the loss of activity seen over time was very similar to that seen when no substrates were added. However, when 2,3-BPGA was included (either alone or with 3PGA), the initial decrease in activity (over 20 minutes) was seen to be slower, whereas the more gradual decrease from 30 minutes to 2 hours was at approximately the same rate.

3.6 Separation and sequencing of peptides

The 2 hour sample was run on a reverse phase hplc column, and a complex pattern of many peptides emerged, suggesting more than a single clip near the C-terminus (see figure 3.6). One of the largest peaks (fraction 23) was subjected to N-terminal sequence analysis. 10 cycles gave the following sequence:

S F D V P P P P I D

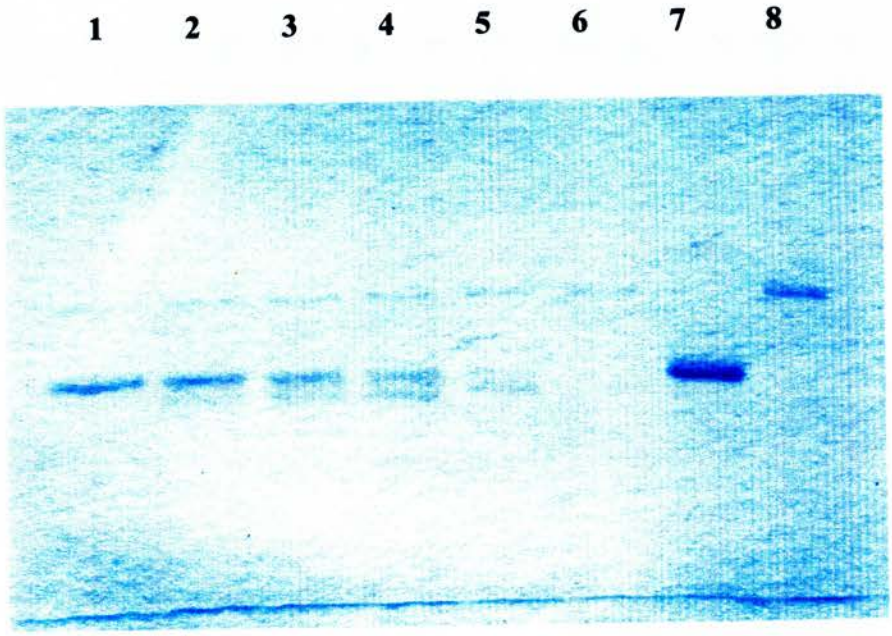

Figure 3.3

SDS-PAGE analysis of the effect of thermolysin on PGAM.
500μg/ml PGAM, 200μg/ml thermolysin.

Lane	1	0 min incubation
	2	10 min
	3	20 min
	4	30 min
	5	60 min
	6	120 min
	7	PGAM only
	8	thermolysin only

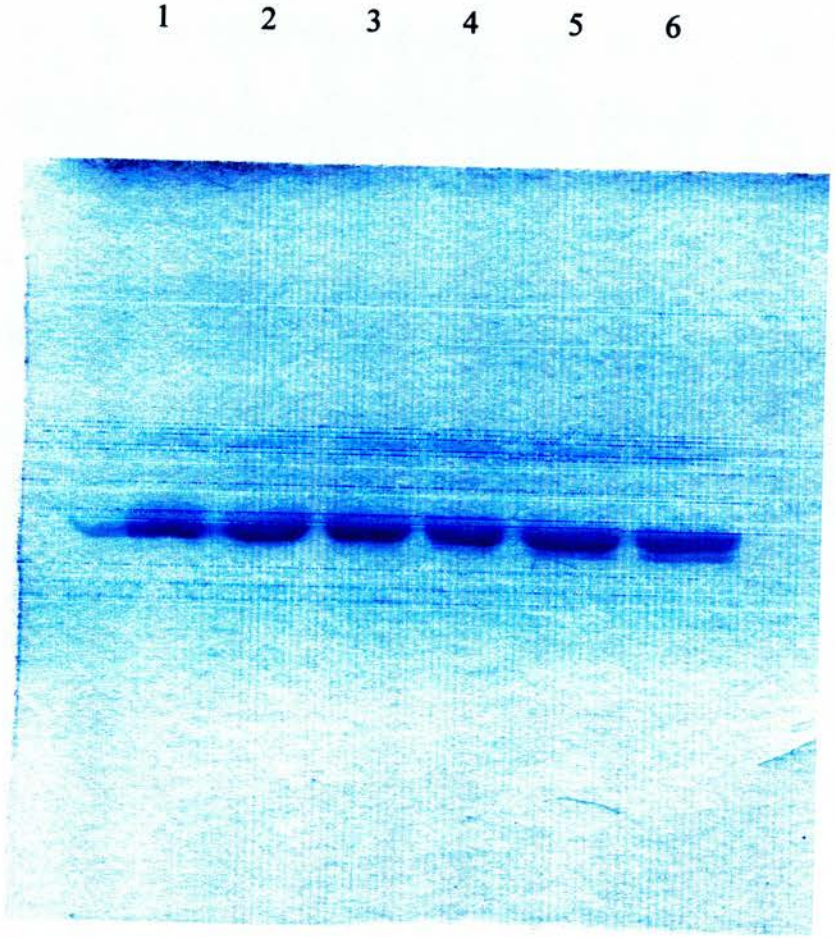

Figure 3.4
500μg/ml PGAM, 50μg/ml thermolysin.

Lane		
	1	0 min incubation
	2	10 min
	3	20 min
	4	30 min
	5	60 min
	6	120 min

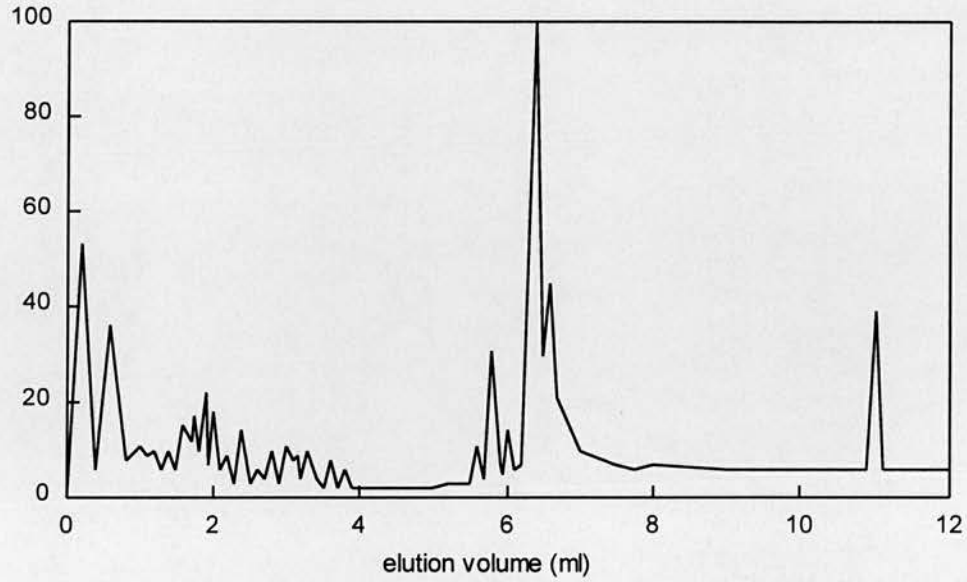

Figure 3.6

Peptides eluted from a 2.1 mm x 30 mm, reverse phase C_{18} Aquapore RP300 hplc column after incubating PGAM and thermolysin in a 10:1 ratio for 2 hours. The most abundant peptide (peak 23) was collected and sequenced.
(Applied Biosystems Microbore hplc system, model 130.)

This corresponds with the internal sequence of residues 115-124. Taken together with the number of peptides generated, this suggests that thermolysin is attacking at sites other than the tail. These results were obtained with the sample incubated with thermolysin for 2 hours, however most of the loss of activity occurs within 20 minutes, and it is not until this time that the second band appears on the SDS gel. It is possible that the clipping of the readily available tail could account for the initial sharp decline in activity, and then further cleavages elsewhere on the protein which give rise to the subsequent slow activity loss and the protein species with higher electrophoretic mobility.

3.7 Sequence analysis of the complete incubation mixture

N-terminal sequence analysis was done on the complete incubation mixtures at zero time and at 10 minutes.

6 cycles of the zero time incubation gave the following 2 sequences:

Sequence	initial yield	identity
P K L V L V	400pmol	PGAM residues 1-6
I T G T S(?)T	80pmol	thermolysin residues 1-6

(?) indicates that the residue cannot be assigned unambiguously.

After 10 minutes, the sequences above were seen in the same yields, and also a third sequence:

V A N Q G K(?)	500pmol	PGAM residues 240-245

As is usual with small peptides, the yields fell away significantly between cycles as the peptide is washed off the disc in the sequencer. The yields for the larger fragments remained more constant.

If all PGAM molecules lost the 7 residue peptide within 10 minutes, the initial yield of peptide would be expected to be equal to the initial yield for the protein's N-terminal sequence. Given the activity results, it is unlikely that this is the case. Obviously 400pmol of PGAM cannot yield 500pmol of peptide, but it is known that certain residues such as proline give low yields in N-terminal sequencing. Valine by contrast, is typically recovered in very high yield.

3.8 Proteolysis studied by Mass Spectroscopy

The removal of these 7 residues was confirmed using electrospray mass spectroscopy. The results are shown in figure 3.7.

At zero time, the major peak is at a mass of 27,475 (the intact PGAM monomer), and there is is a much smaller peak at 26,748. After 5 minutes the lower mass peak is the most abundant, and after 15 minutes the peak corresponding to the intact monomer has disappeared.

The difference between these two masses (727) corresponds to the loss the of the 7 C-terminal residues (**V A N Q G K K**).

N.B. The presence of the small lower mass peak in the zero time sample is probably due to the delay in loading the sample into the machine (i.e. zero time is not exactly zero time).

3.9 Discussion

Previous experiments on PGAM from rabbit muscle have indicated that a portion of that enzyme which corresponds to the flexible C-terminal tail of the yeast PGAM can be cleanly removed by treatment with thermolysin. Attempts to replicate this simple removal of the tail from the yeast enzyme have not been completely successful. The digestion of PGAM by thermolysin can be divided into two main stages. Immediately on addition of the protease, a seven residue peptide is removed from the C-terminus, which leads to a significant decrease in the level of mutase activity. The removal of the peptide is confirmed by peptide sequencing and mass spectrometry. It does not however give rise to an obvious change in electrophoretic

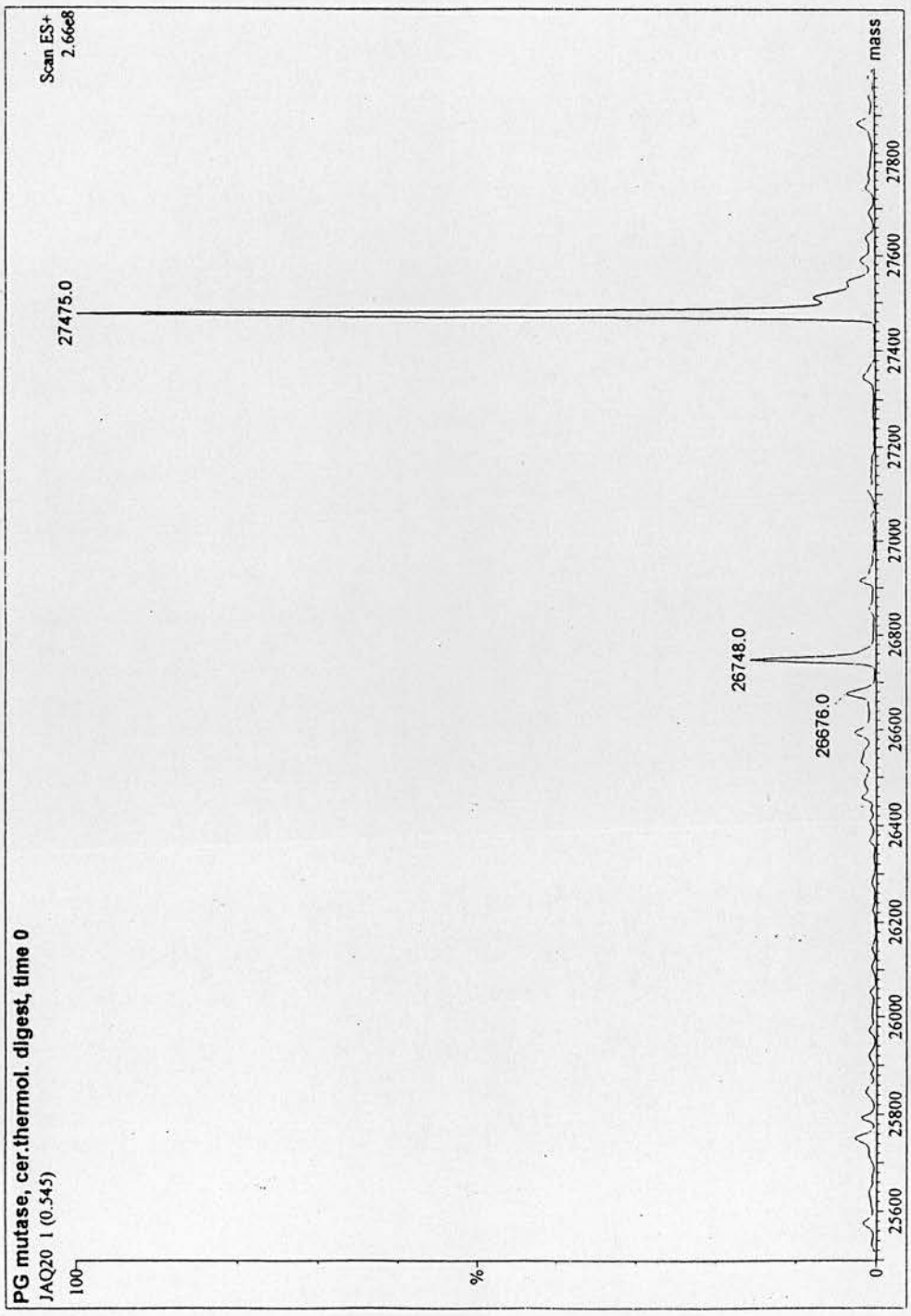

Figure 3.7

Results obtained from mass spectrometry at 0 min incubation.
The mass of each fragment detected is given above the peak.

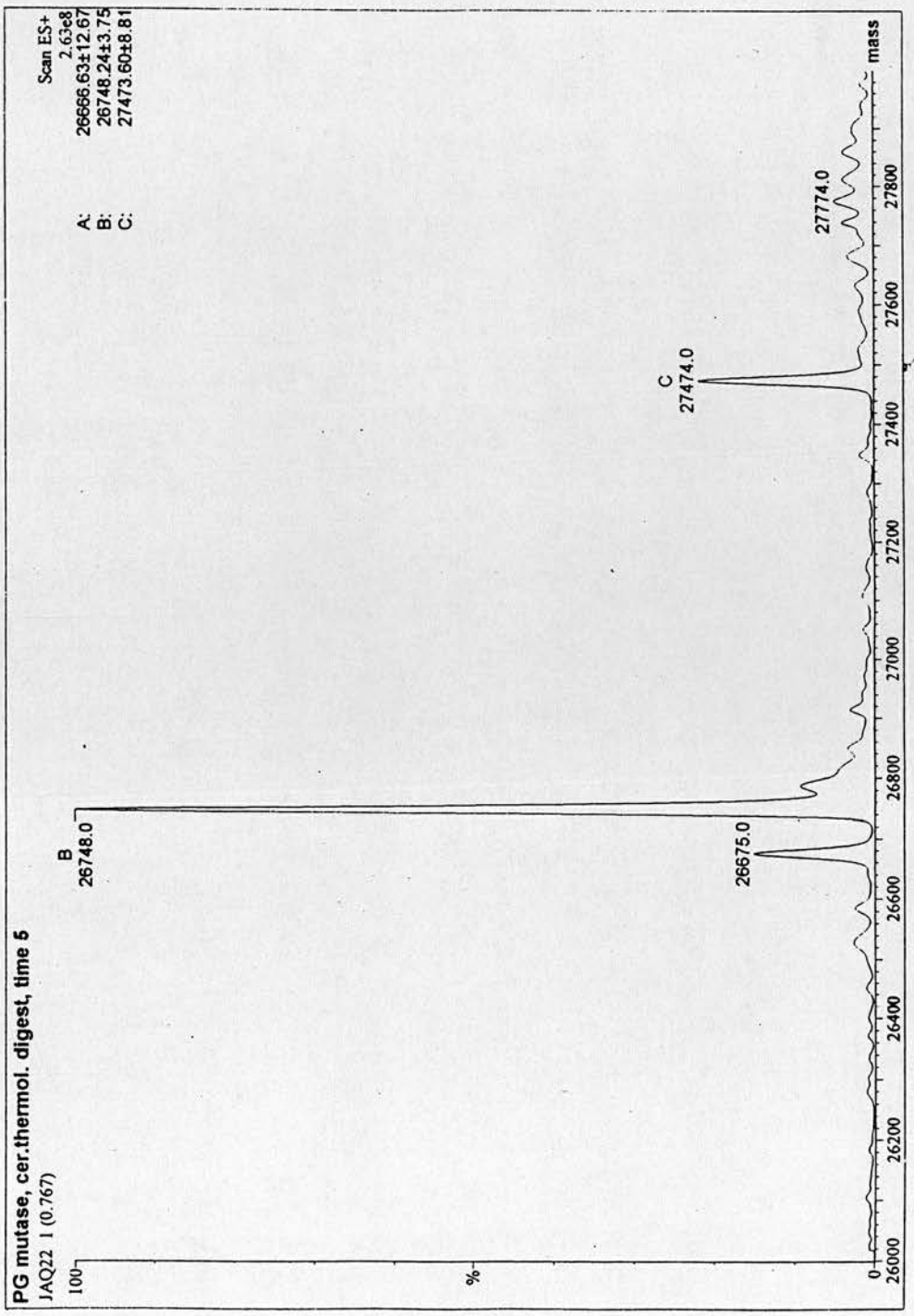

Figure 3.8

Results obtained from mass spectrometry at 5 min incubation..
The mass of each fragment detected is given above the peak.

mobility. The second stage begins after about five minutes incubation, and involves more extensive proteolysis, giving rise to a number of peptides as seen on the HPLC. This degradation also leads to a decrease in mutase activity, although less dramatic than that observed with the loss of part of the tail. Throughout, the phosphatase activity remains fairly constant, and so it is unlikely that the tail is involved in catalysing this reaction.

These results clearly show the importance of the tail in the mutase reaction. The protein sequencing and mass spectrometry results show that the initial loss of over 60% of activity is due to the removal of a seven residue peptide from the C-terminus only - the rest of the enzyme remains intact. This peptide represents the majority of the highly flexible region of the tail beyond the short helix seen in the new 2.3Å structure (see figure 1.8), and therefore this region is crucial in maintaining a high level of mutase activity. It is not however important in maintaining the phosphatase activity. It has also been proposed that the tail is responsible for maintaining a low level of phosphatase activity by excluding water from the active site, thereby preventing the hydrolysis of the phospho enzyme and the transfer of the phospho group to water (see section 1.8.4). However, if this were the case, we would expect to see the removal of a significant proportion of the tail accompanied by an increase in the phosphatase activity. In fact, the phosphatase activity remains almost constant during removal of the tail.

Chapter Four

The Role of the C-terminal Lysine Residues

4.1 Introduction

As described in section 1.8.4, the two C-terminal residues of the *S. cerevisiae* mutase are lysine (K245 and K246). These are therefore at the end of the C-terminal tail - the region not seen in the electron density map of PGAM and assumed to be flexible. The position of one of the lysines (K245) is conserved in most PGAM sequences (bis- and monophosphoglycerate mutases) with the exception of the *S. pombe* PGAM, which lacks the residues thought to constitute the tail.

Figure 4.1. The C-terminal regions of PGAMs from different organisms.

Ref.	S.cerevisiae numbering	233	234	235	236	237	238	239	240	241	242	243	244	245	246					
1	*S.cerevisiae*	A	A	A	G	A	A	A	V	A	N	Q	G	K	K					
2	*S.coelicolor*	A	A	A	A	I	E	A	V	K	N	Q	G	K	K	K				
3	*E.coli*	I	A	A	K	A	A	A	V	A	N	Q	G	K	A	K				
4	human-B	V	R	K	A	M	E	A	V	A	A	Q	G	K	A	K	K			
5	human-M	V	R	K	A	M	E	A	V	A	A	Q	G	K	A	K				
6	rat-B	V	R	K	A	M	E	A	V	A	A	Q	G	K	V	K	K			
7	rat-M	V	R	K	A	M	E	A	V	A	A	Q	G	K	A	K				
8	human-E	I	Q	A	A	I	K	K	V	E	D	Q	G	K	V	K	Q	A	K	K
9	rabbit-E	I	Q	A	A	I	K	K	V	E	D	Q	G	K	V	K	R	A	E	K
	Human E-type numbering	239	240	241	242	244	245	246	247	248	249	250	251	252	253	254	255	256	257	258

In order to investigate the role of the C-terminal lysines of *S.cerevisiae* PGAM, a number of mutants had been constructed previously by Dr. Malcolm White and expressed in the gpm-disrupted strain as described in section 1.14. The mutants have the lysines replaced with glycines which are neutral and therefore have different charge properties to the wild type enzyme.

Figure 4.2 The C-terminal sequences of the lysine tail mutants, showing charges.

wild type - A A A V A N Q G K^+ K^+_{COO-}

K246G - A A A V A N Q G K^+ G $_{COO-}$

K245G - A A A V A N Q G G K^+_{COO-}

K245G/K246G - A A A V A N Q G G G $_{COO-}$

This chapter describes the purification and characterization of these mutants.

4.2 Expression of the tail mutants.

The wild type and mutant proteins were expressed in the gpm-disrupted strain of *S. cerevisiae*. All grew on YEPD, using glucose as a carbon source, which demonstrates that the mutant PGAMs do show some mutase activity. After overnight growth, the yeast was lysed using glass beads and the proteins run on an SDS-PAGE gel (Figure 4.3). Wild type and mutant PGAM proteins were expressed to high levels. The wild type, K246G and K245G/K246G proteins represented around 20-30% of total cell protein, as estimated from the SDS-PAGE gel. The K245G protein was expressed to a lesser extent. It was thought that perhaps the phagemid had established at a lower copy number than usual in the original colony. Different transformants may express to a higher level, so the pVT-K245G phagemid was used to transform the disrupted strain again. Several transformants were screened, but each showed a similar level of expression (see figure 4.4.).

4.3 Growth of the tail mutants

The growth characteristics of the wild type and mutant strains were investigated. Growth curves are shown in Figure 4.5. There are no significant differences between wild type and mutants. The mutase gene carried on the phagemid is overexpressed, so a decrease in activity would not necessarily cause the cells to grow more slowly as the increased number of PGAM molecules could balance the lower activity. However, it has been shown previously that where the change in activity is very great, there can be changes to parts of the growth curve, as for the active site H181A mutant (White and Fothergill-Gilmore, 1988).

4.4 Purification of wild type and tail mutants

The wild type and mutant proteins were purified as described in Section 2.2.6. This is based on the method previously used to purify overexpressed recombinant

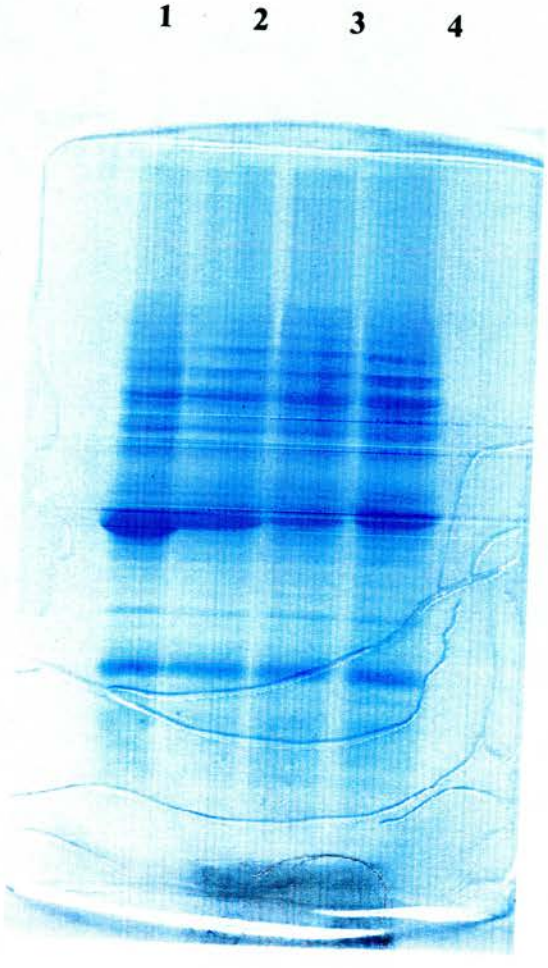

Figure 4.3

12% SDS-PAGE showing the levels of expression of the wild type and mutant PGAM (see section 2.2.3)

Lane	1	S150-2B GPM::HIS3 + pVT-gpm
	2	S150-2B GPM::HIS3 + pVT-K246G
	3	S150-2B GPM::HIS3 + pVT-K245G
	4	S150-2B GPM::HIS3 + pVT-K245G/K246G

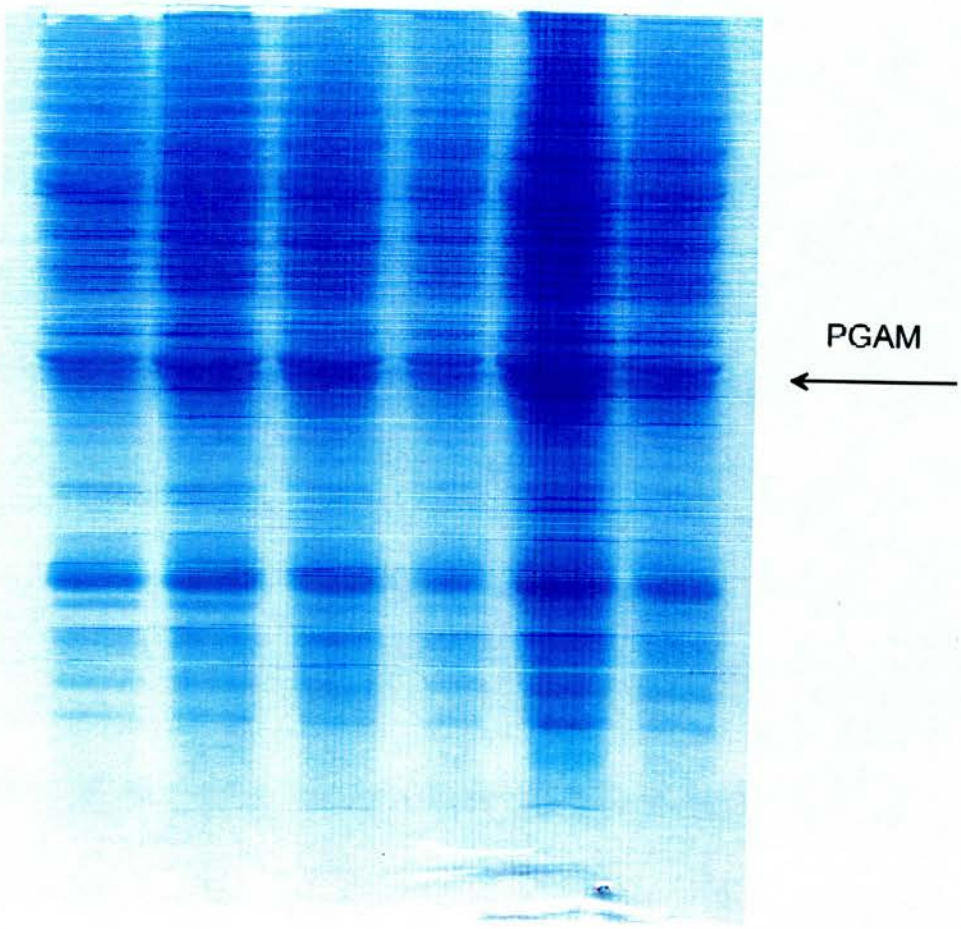

Figure 4.4
SDS-PAGE showing the screening of K245G transformants for overexpression.

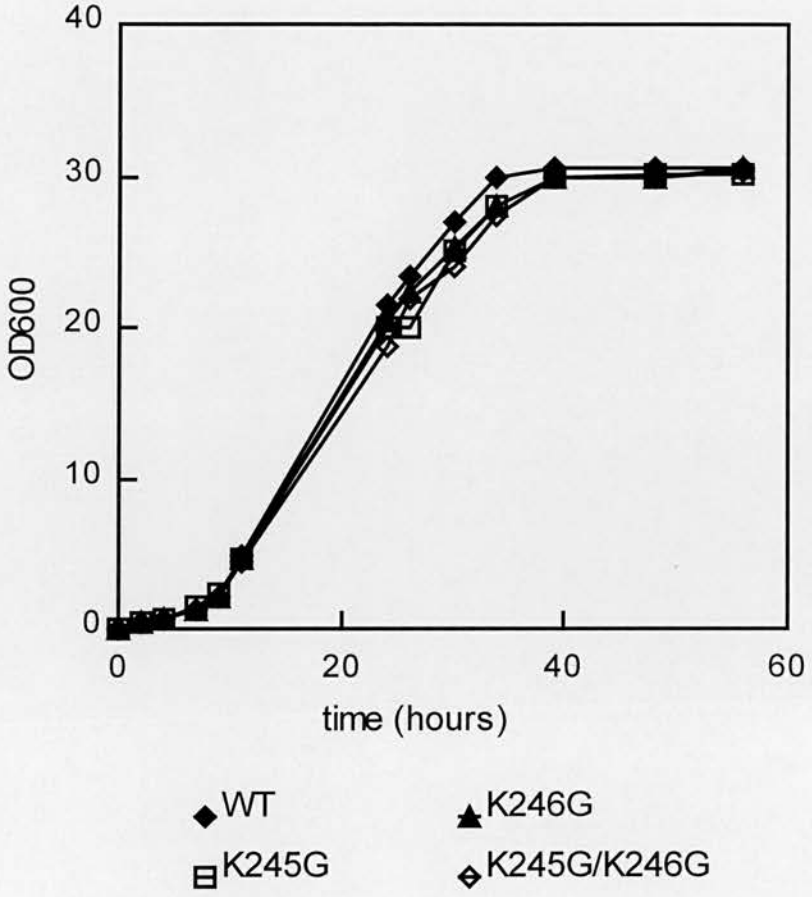

Figure 4.5

Growth curves for S150-2B GPM::HIS3 expressing wild type or mutant PGAM. An overnight culture of each was used to innoculate 500ml YEPD (section 2.2.2.1) to 0.1 OD_{600}. This was then incubated (with shaking) at 30°C, and small samples taken at intervals to determine optical density. Each point represents the mean value obtained from three cultures.

PGAM (White and Fothergill-Gilmore 1992), with the addition of a final FPLC Superose 12 gel filtration step. Each protein was purified to homogeneity as indicated by a single band on an SDS-PAGE gel (see Figure 4.6).

Proteolytic degradation of yeast PGAM during purification is well-documented (Sasaki *et al.* 1976) and it is thought that the tail is particularly susceptible. Care must be taken at every stage to ensure that the enzyme is purified intact, especially when a study of the role of specific tail residues is being undertaken! A combination of inhibitors shown to be effective in previous work (White and Fothergill-Gilmore, 1989, details of inhibitors given in section 2.2.6.7) was added before cell lysis. The preparations were kept on ice in between steps and most steps were carried out at 4°C. The final gel filtration step had to be carried out at room temperature because it involved the use of an FPLC system. However, this step is very quick (PGAM elutes from the column in less than two hours) and did not appear to have any deleterious effects on the enzyme.

4.5 Purification tables

Wild type

Purification step	Volume ml	Total protein mg	Total EU	EU/mg	Yield %	Fold purification
lysate	250	1,225	425,000	347	100	1
dialysate	100	590	350,000	593	82	1.7
QA52- cellulose	56	73	44,800	615	11	1.8
Superose 12	5	40	40,500	1,013	10.5	3

Table 4.1
Purification of wild type PGAM from *S. cerevisiae*. EU (enzyme units) defined as μmol NADH oxidized/min.

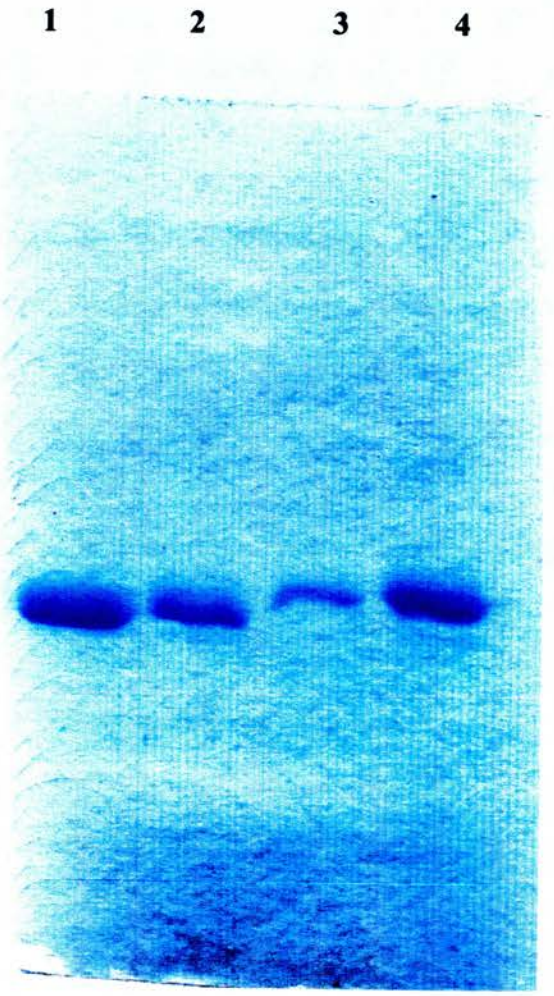

Figure 4.6
12% SDS-gel of purified wild type and mutant phosphoglycerate mutases.

Lane	1	Wild type
	2	K246G
	3	K245G
	4	K245G/K246G

K246G

Purification step	Volume ml	Total protein mg	Total EU	EU/mg	Yield %	Fold purification
lysate	255	1,097	372,810	340	100	1
dialysate	100	500	240,000	430	64	1.4
QA52- cellulose	63	58	34,970	603	9.4	1.8
Superose 12	4.5	38	32,300	850	8.7	2.5

Table 4.2

Purification of K246G PGAM. EU (enzyme units) defined as μmol NADH oxidized/min.

K245G

Purification step	Volume ml	Total protein mg	Total EU	EU/mg	Yield %	Fold purification
lysate	250	1,134	238,140	210	100	1
dialysate	100	525	181,125	345	76	1.6
QA52- cellulose	59	80	37,120	464	16	2.2
Superose 12	5	42	23,730	565	10	2.7

Table 4.3

Purification of K245G PGA. EU (enzyme units) defined as μmol NADH oxidized/min.

K245/K246G

Purification step	Volume ml	Total protein mg	Total EU	EU/mg	Yield %	Fold purification
lysate	245	1,010	270,545	268	100	1
dialysate	100	460	202,909	441	73	1.6
QA52- cellulose	56	51	40,582	796	15	2.9
Superose 12	4.5	32	29,760	930	11	3.5

Table 4.4

Purification of K245G/K246G PGAM. EU (enzyme units) defined as μmol NADH oxidized/min.

The yield was consistently around 10% as not all the fractions in the mutase peak eluting from the QA52-cellulose column were pooled and taken on to the next step. The decision was taken to sacrifice some of the yield in this step in order to collect a purer sample which could be purified to homogeneity on the Superose 12 column. When all the fractions showing mutase activity were pooled, at least one other protein was also collected which could not be separated from PGAM on the gel filtration column. As the mutase is so overexpressed, even a 10% yield gave tens of milligrams of protein, sufficient for most purposes.

4.6 Storage and stability of phosphoglycerate mutase

The PGAM was eluted from the Superose column in 50mM Tris.HCl pH8.0. Wild type PGAM is stable in this buffer for at least one week when stored at 4°C, after which time activity begins to decrease slowly (a graph showing wild type activity over 20 days is given in figure 6.7). For longer term storage, the enzyme is kept in 80% saturated ammonium sulphate at 4°C. Under these conditions it is stable for at least two months. The K246G, K245G and K245G/K246G mutants do not show any significant differences to wild type mutase in storage and stability.

4.7 Circular Dichroism Spectra

The mutants had very similar far u.v and near u.v spectra to the wild type (Figures 4.7 and 4.8), indicating that the mutations had very little effect on the secondary and tertiary structure of the enzyme.

4.8 Specific activities

Each of the three activities of PGAM were measured,and the results given in Table 4.5.

Figure 4.7

Far u.v. spectra of wild type and mutants.
Key: Green, wild type; Red, K246G; Black, K245G; Blue, K245G/K246G.

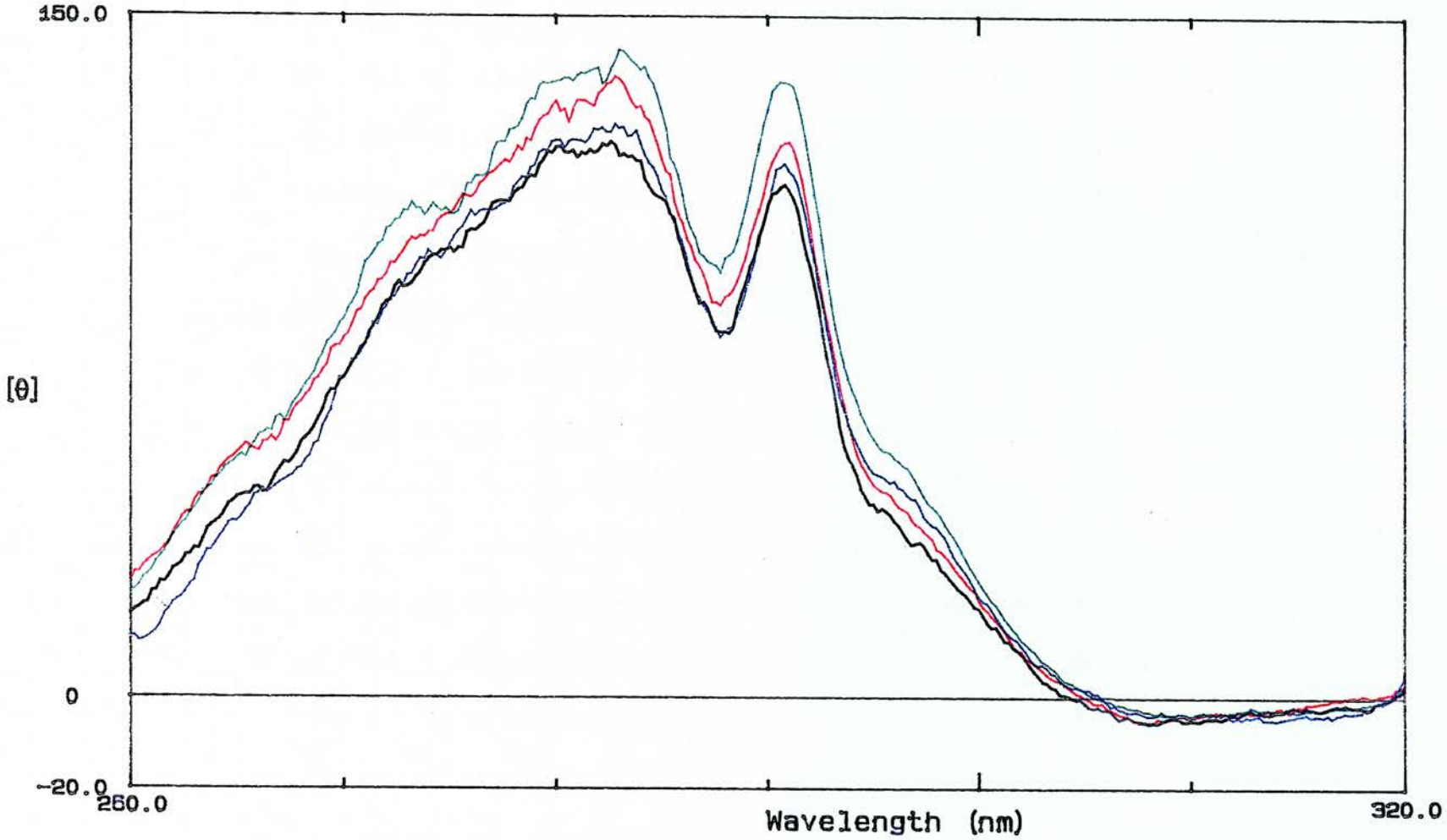
150.0
[θ]
0
-20.0
260.0
Wavelength (nm)
320.0

Figure 4.8
Near u.v.spectra of wild type and mutants.
Key: Green, wild type; Red, K246G; Black, K245G; Blue, K245G/K246G.

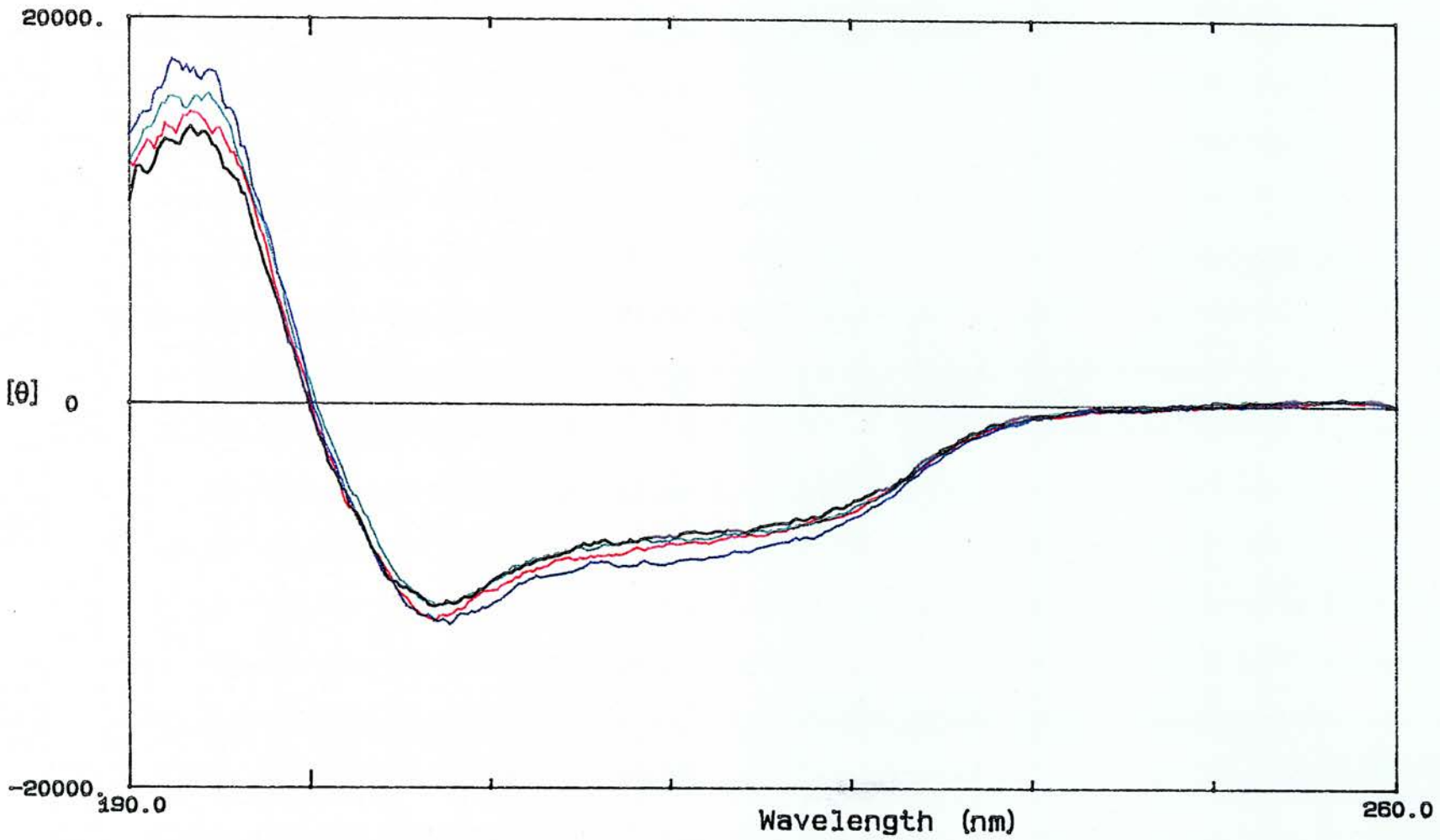
20000.
[θ]
0
-20000.
190.0
Wavelength (nm)
260.0

	mutase EU/mg	phosphatase EU/mg	synthase EU/mg
WT	970	0.02	0.01
K246G	850	0.02	0.02
K245G	565	0.02	0.02
K245G/K246G	930	0.02	0.02

Table 4.5
Specific activities of wild type, K245G, K246G and K245G/K246G PGAM. EU (enzyme units) defined as μmol NADH oxidized/min. All values are determined from three different experiments and given as means with less than 5% standard error.

The mutants show mutase activity of between 60 and 100% of the wild type, and phosphatase and synthase activities are apparently almost unaltered. However, with such low levels of activity, changes are difficult to detect accurately.

The stimulation of phosphatase activity by 2-phosphoglycollate was also measured.

	Phosphatase	Phosphatase + 1mM 2-PG	fold stimulation
wild type	0.02	0.35	18
K246G	0.02	0.39	16
K245G	0.02	0.09	4.1
K245G/K246G	0.02	0.09	4.0

Table 4.6
The stimulatory effect of 2-phosphoglycollate (2-PG) on the phosphatase activity of wild type, K246G, K245G and K245G/K256G PGAM. The activities are given as EU (defined as μmol NADH oxidized/min).

The stimulation of the K246G mutant is similar to the wild type enzyme, but where Lys-245 is replaced by glycine, the stimulation is reduced (from 18-fold to 4-fold).

4.9 Kinetic data

The K_m values for 3-PGA and 2,3-BPGA in the mutase reaction were determined for the wild type and each mutant. Hanes plots are shown in Figures 4.9 - 4.12. All show ping-pong kinetics as described for the wild type. The kinetic data are shown in the table below.

	$K_m^{3\text{-PGA}}$ μM	K_m^{BPGA} μM	k_{cat} s^{-1}
wild type	470	3.2	530
K246G	630	3.2	520
K245G	400	2.4	210
K245G/K246G	1,430	7.9	560

Table 4.7
The kinetic constants of wild type, K246G, K245G and K245G/K246G PGAM, calculated using Hanes plots.

The results for wild type are in close agreement with previously published values (White and Fothergill-Gilmore 1992).

4.10 Limited proteolysis

The interaction of the tail lysines with substrates was further studied using the limited proteolysis by thermolysin described in chapter three. The effect of thermolysin concentration on the activity of K245G/K246G was measured (Figure 4.13B) and is similar to the pattern seen with wild type (see Figure 4.13A). The mutant is however affected more quickly than the wild type at all concentrations of thermolysin.

Wild type and mutant PGAMs were incubated with concentrations of substrate used in specific activity assays (10mM 3-PGA and 0.5mM 2,3-BPGA) and subjected to limited proteolysis. For wild type PGAM, the addition of 3-PGA does not have any significant effect on the extent of proteolysis. When 2,3-BPGA is added however, the rate of activity loss is decreased and indeed never reaches the same level as in the unligated enzyme or that incubated with 3-PGA (around 45% of

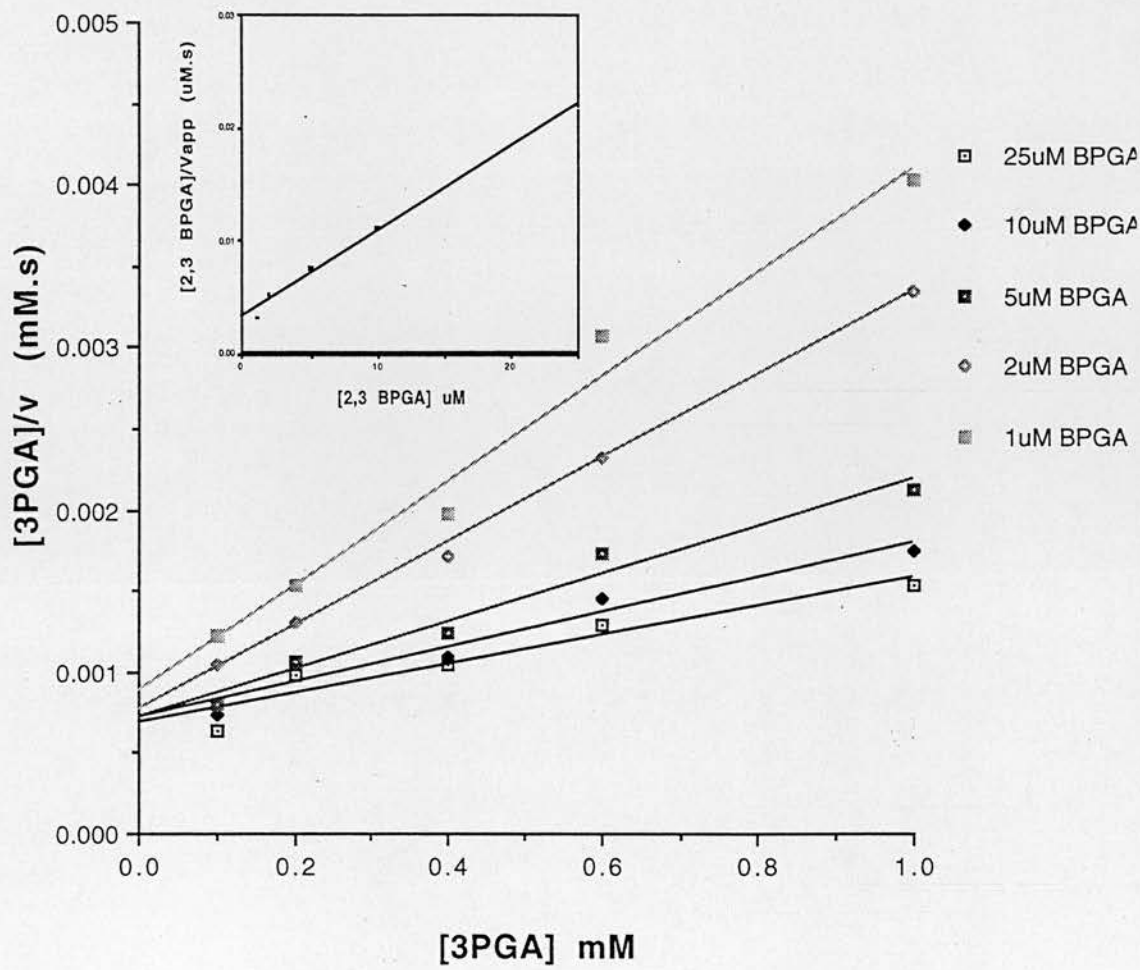

Figure 4.9

Hanes plots showing kinetic data obtained for wild type PGAM. The pattern seen in the primary plot corresponds to a ping-pong mechanism. The inset graph is the secondary plot required for calculating the kinetic constants. Assays were carried out as described in section 2.2.9.

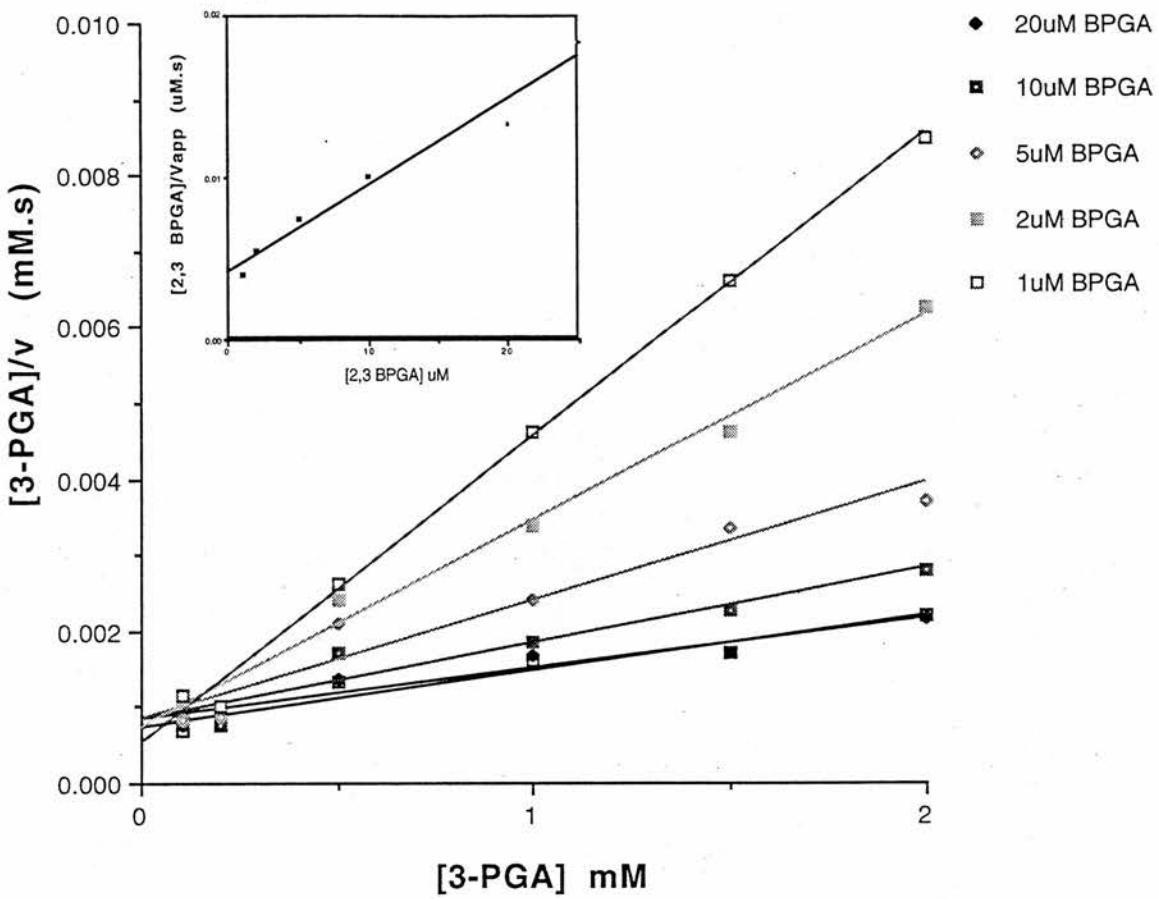

Figure 4.10
Hanes plots for K246G PGAM.

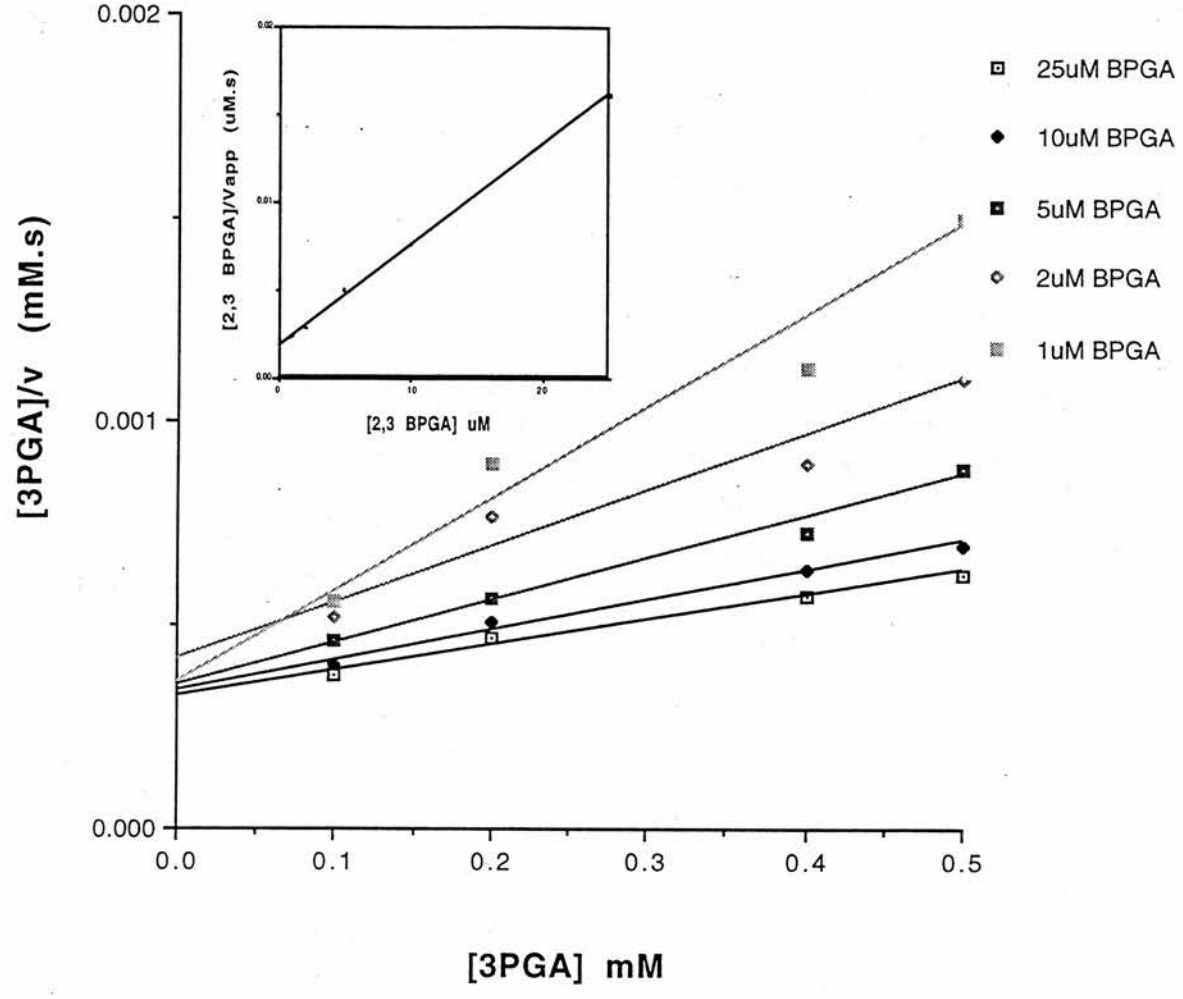

Figure 4.11
Hanes plots for K245G PGAM.

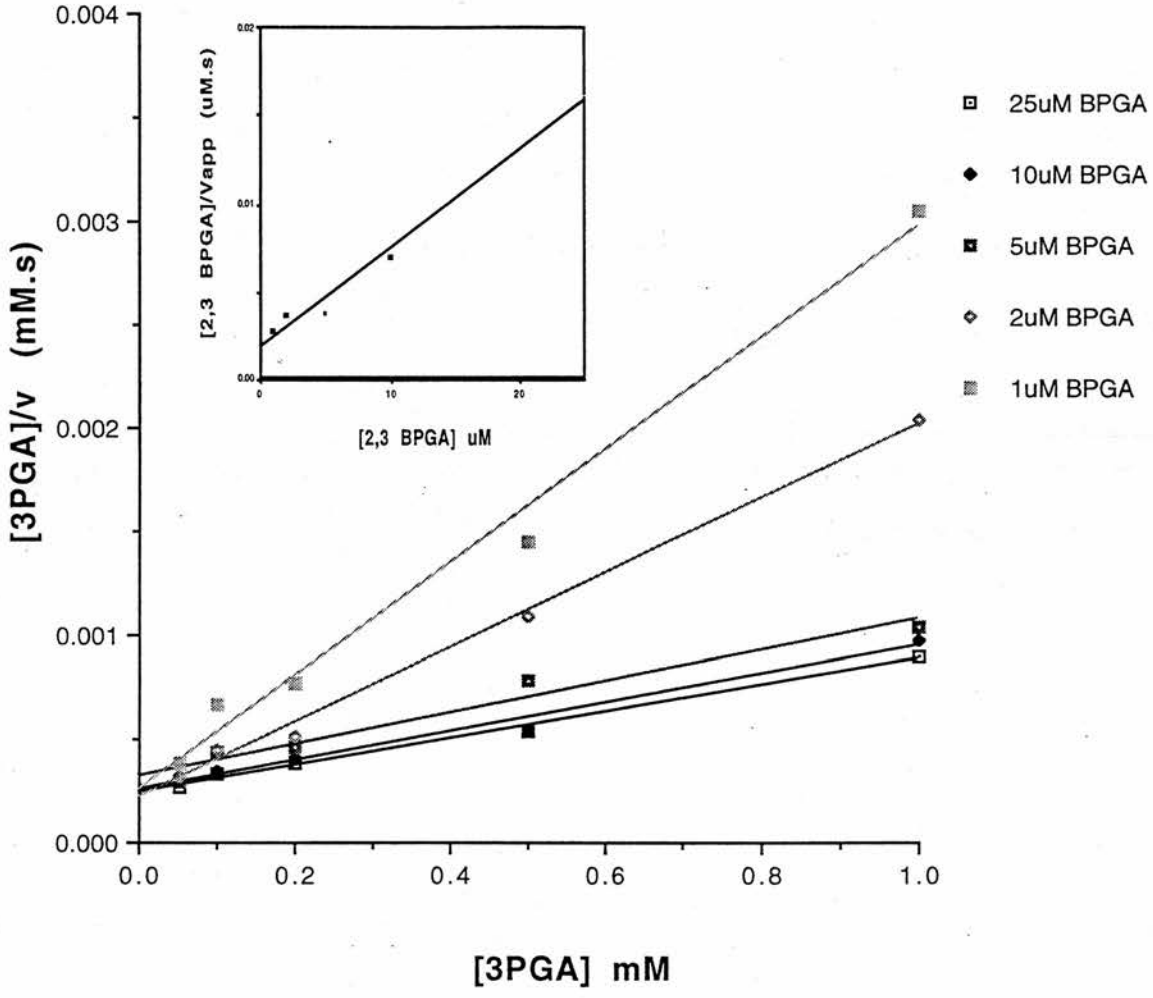

Figure 4.12
Hanes plots for K245G/K246G PGAM.

A

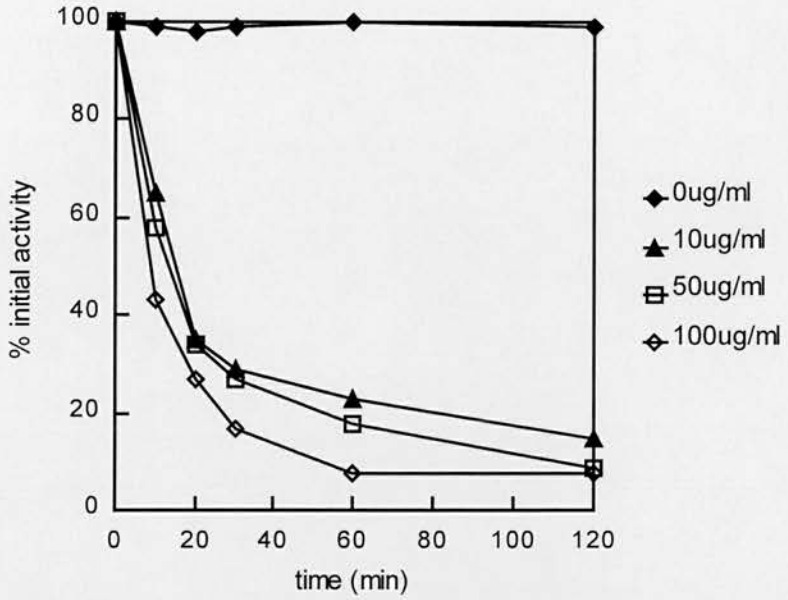

B

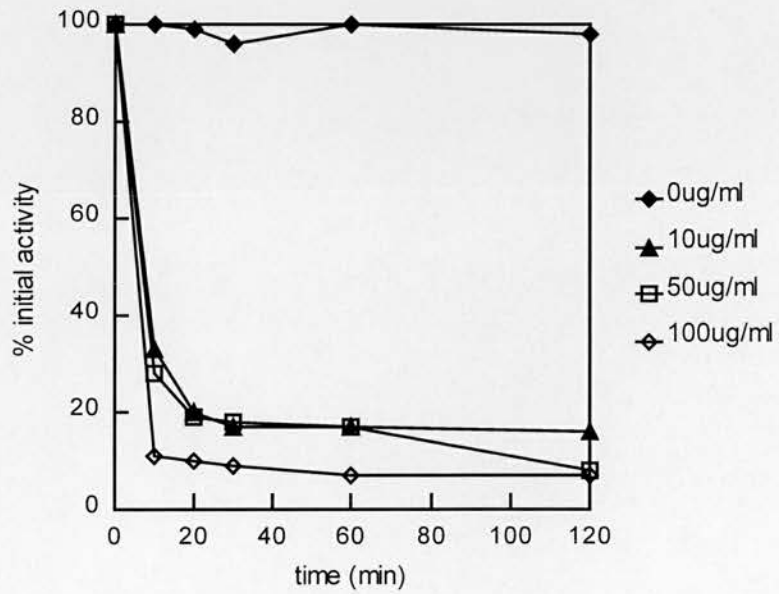

Figure 4.13

The effect of different concentrations of thermolysin on the activity of **A**. Wild type PGAM and **B**. K245G/K246G. The concentration of mutase was 100μg/ml.
Figure A is reproduced here from chapter three in order to facilitate close comparison with the results for the mutant.

activity remaining as opposed to around 25%). When the same experiments are carried out with the K245G/K246G enzyme, this pattern is not repeated; the addition of ligands has no significant effect on the extent of activity loss due to proteolysis (see Figure 4.14). In addition, the inactivation is more rapid with the mutant, which suggests that it is more susceptible to proteolysis.

4.11 Discussion

The mutase, phosphatase and synthase activities are all unaffected by the replacement of the C-terminal lysines. In addition, the kinetic constants for the wild type and mutants are also similar. Where both lysines are replaced (leaving an overall negative charge at the C-terminus), the K_M values for 2,3-BPGA and 3-PGA are slightly higher than with the wild type enzyme (3x and 2.5x wild type values respectively), although none of the differences are consistent with crucial charge interactions with negatively charged phospho groups of bound substrates or intermediates that have previously been suggested (Fothergill-Gilmore and Watson, 1989). However, some degree of interaction with the bisphosphoglycerate substrate bound to the enzyme is suggested by the results of the limited proteolysis experiments.

As has been previously shown with the rabbit muscle enzyme (Price *et al.* 1985), the presence of 2,3-BPGA offers some protection against thermolysin for the wild type enzyme. It suggests that the tail adopts a less flexible conformation when this molecule is bound in the active site. 3-PGA does not have this protective effect, indicating that both phospho groups are necessary to draw the C-terminus towards the active site in this way. No ligand protection is seen in the K245G/K246G mutant, either with 3-PGA or 2,3-BPGA. As would be expected then, the positive charge associated with the C-terminal lysines is necessary for the interaction between enzyme-bound BPGA and the tail.

Another difference between the mutants and wild type is seen in the enhancement of phosphatase activity in the presence of the substrate analogue 2-phosphoglycollate. This effect is thought to be due to the two carbon substrate

A

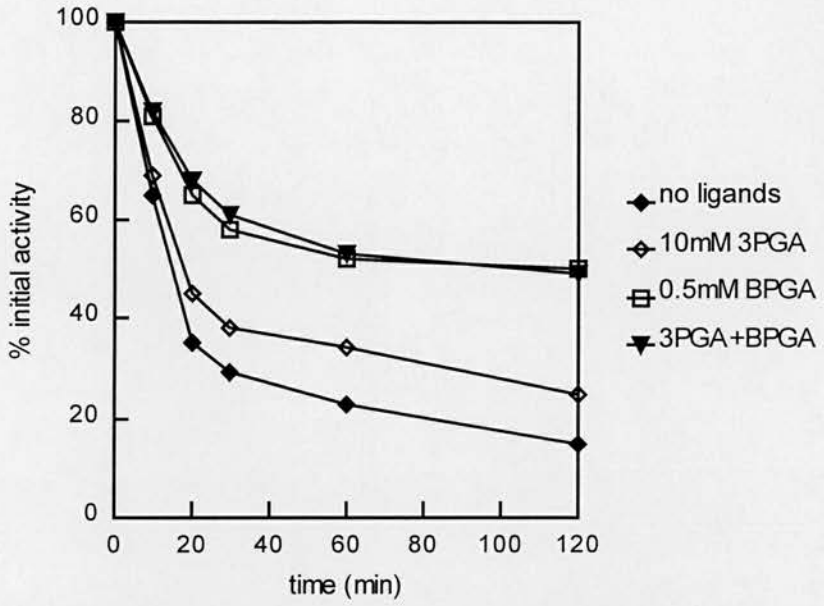

B

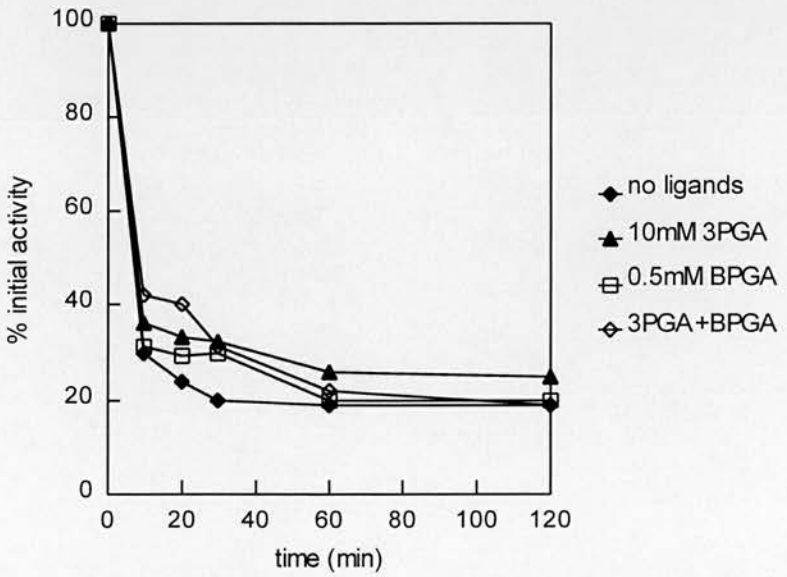

Figure 4.14

The effect of ligands on the limited proteolysis of wild type PGAM (A) and K245G/K246G (B).
PGAM at 100μg/ml, thermolysin at 10μg/ml.

analogue binding to the phosphorylated enzyme along with a molecule of water,facilitating the transfer of the phospho group to water. The stimulated activity when lysine 245 is replaced is only a quarter of that observed for the wild type and K246G enzymes. The positive charge associated with the C-terminus therefore appears to be important for the maximal stimulatory effect of 2-phosphoglycollate.

The role of the C-terminal tail can also be investigated by comparing the properties of the enzyme from *S. cerevisiae* and that from the fission yeast *S. pombe* which lacks the residues that constitute this region. The *S. pombe* enzyme catalyzes the mutase reaction with a significantly lower mutase activity than the *S. cerevisiae* mutase (210 μmol/min/mg compared with 970 μmol/min/mg). The phosphatase activity is about 3x higher than the *S. cerevisiae* PGAM, but still significantly lower than the mutase activity. The ratios of phosphatase and mutase activites are given in the table below.

	Specific activities (μmol/min/mg)			
	mutase	**phosphatase**	**phosphatase +1mM 2-PG (fold stimulation)**	**phosphatase /mutase ($x10^5$)**
***S. cerevisiae* PGAM**	970	0.02	0.35 (18)	2.1
thermolysin-treated *S. cerevisiae* (10 min)	630	0.02	0.12 (6.2)	3.2
***S. pombe* PGAM**	220	0.06	0.14(2.3)	28

Table 4.8
Specific activities of S. cerevisiae and S. pombe PGAM, and the ratios of phosphatase to mutase activities. Values for *S. pombe* PGAM are taken from Nairn *et al*, 1996.

The results from the *S. pombe* mutase are in agreement with the results for the proteolyzed *S. cerevisiae* mutase. They support the the conclusion that the residues

found in the tail are responsible for the maximal stimulatory effect of 2-phosphoglycollate on the phosphatase activity. The levels of phosphatase activity are very low compared to the mutase activity, even in the absence of the tail. It is therefore unlikely that the exclusion of water by the tail is responsible for the low phosphatase activity of *S. cerevisiae* PGAM, as has been suggested (Fothergill-Gilmore and Watson, 1989). The tail clearly interacts both with the 2,3-BPGA substrate and the phosphatase activator 2-phosphoglycollate (through charge interactions between the negatively charged phospho groups of the ligands and the positively charged lysines of the tail), but this first interaction is not essential for enzyme activity. Further studies on the interaction of the tail with active site-bound ligands, and differences between *S. pombe* and *S. cerevisiae* mutases are described in chapter five.

Chapter Five

Inhibitor Studies

5.1 Introduction

The crystal structure of *S.cerevisiae* PGAM shows that the cleft containing the active site is rich in basic residues. Analysis of the enzyme's electrostatic field shows that it is consistent with a role for these residues in the long range attraction of substrates (Warwicker, 1986. The recent 2.3Å strucuture shows that this effect is even greater than the original analysis of the 2.8 Å structure suggested (Rigden *et al.*, 1997). Figure 5.1 shows the solvent-accessible surface highlighting positive and negative electroststic potentials. The concentration of basic residues in the active site cleft is very clear. As would be expected, the enzyme has been shown to be inhibited by a wide range of anionic compounds (Rose, 1980), with K_i values in the micromolar to millimolar range. Among the best inhibitors found were benzene carboxylates and inositol hexakisphosphate.

Some of these compounds have recently been modelled into an unligated structure of *S. cerevisiae* PGAM (Rigden, D.J., unpublished results). The coordinates used for the modelling of the ligand-enzyme complexes were those of Littlechild, J. A., Campbell, J., Rawas, A. & Watson, H. C. (unpublished data). This structure is of 2.0Å resolution and shows some differences at or near the active site, probably due to the absence of the sulphate groups which are bound in the active site of the 2.8Å structure. The implied flexibility was taken into account during the refinement procedure. When this work was being carried out, the 2.3Å structure (Rigden *et al.*, 1997) had not been determined. The compounds modelled were inositol hexakis-phosphate (IHP), benzene hexaphosphate (BHC), benzene-1,2,4,5-tetraphosphate (B1245), benzene-1,2,4-triphosphate (B124), benzene- 1,2,3-triphosphate (B123) and benzene-1,2,4-triphosphate (B124). Favourable structures were found with each of the molecules binding in the active site. Figures 5.2-5.7 show the positions of these molecules in the active site, and possible interactions between the ligands and active site residues. As would be expected, the ligands with a higher number of negatively charged phospho groups look likely to form more hydrogen bonds with the enzyme, and therefore would be expected to have lower K_i values. With the three benzene triphosphates, the different positions of the phospho groups on the molecule mean

Figure 5.1

The solvent-accessible surface of a PGAM subunit with the positive and negative electrostatic potential coloured red and blue respectively. The catalytic site cleft is in the centre of the figure, and the concntration of basic residues is clear. The active site histidines are located in the upper left area of the electrostatically positive area. The small electrostatically negative area at the base of the cleft is due to Glu86.

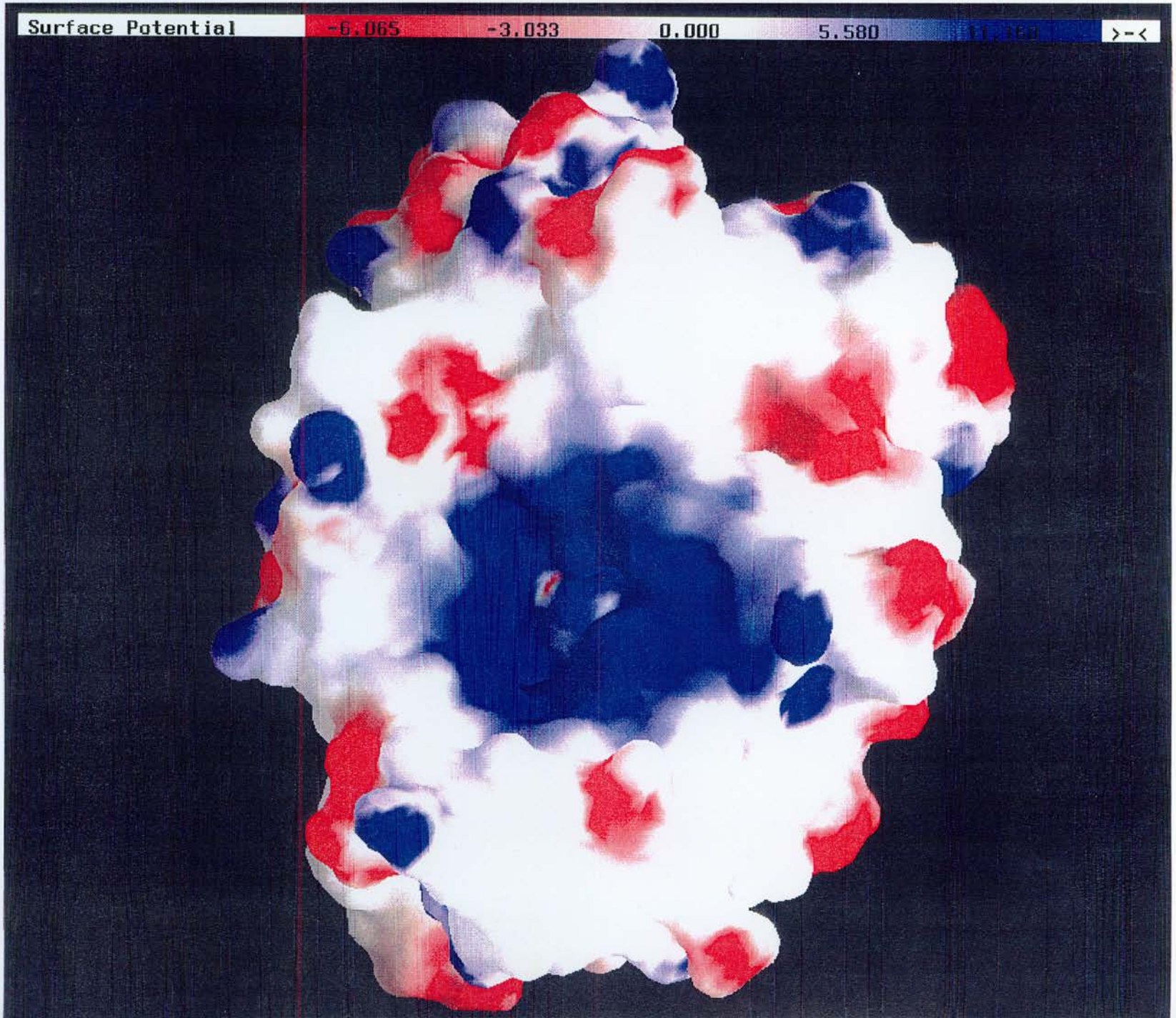
Surface Potential
-6.065
-3.033
0.000
5.580
>-<

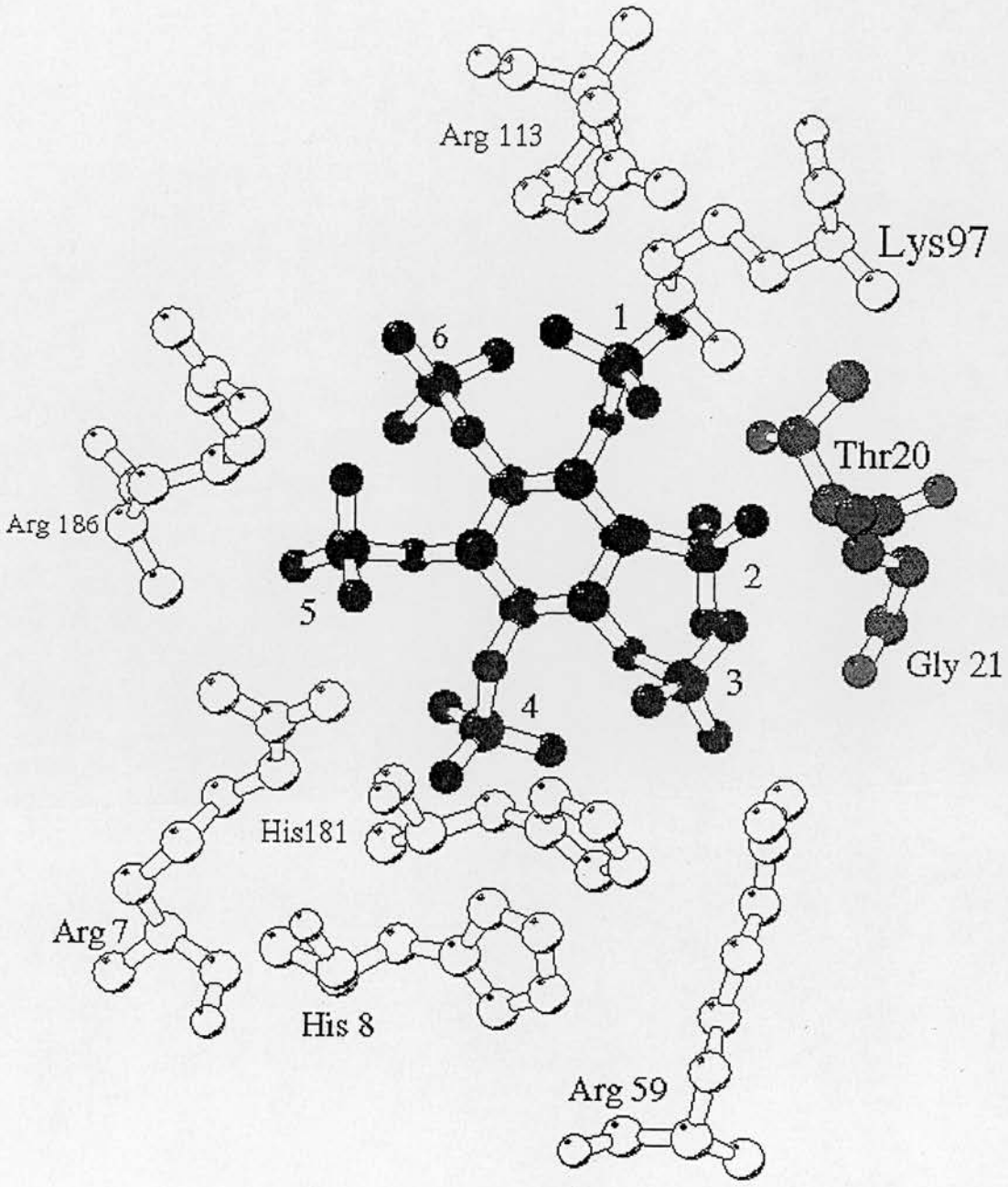

Figure 5.2
A MOLSCRIPT diagram showing inositol hexakisphosphate (IHP) modelled in to the active site of *S.cerevisiae* PGAM. Residues which are not thought to hydrogen bond to IHP have been omitted.
IHP was placed in the active site using manual positioning obtained using the program GRID.

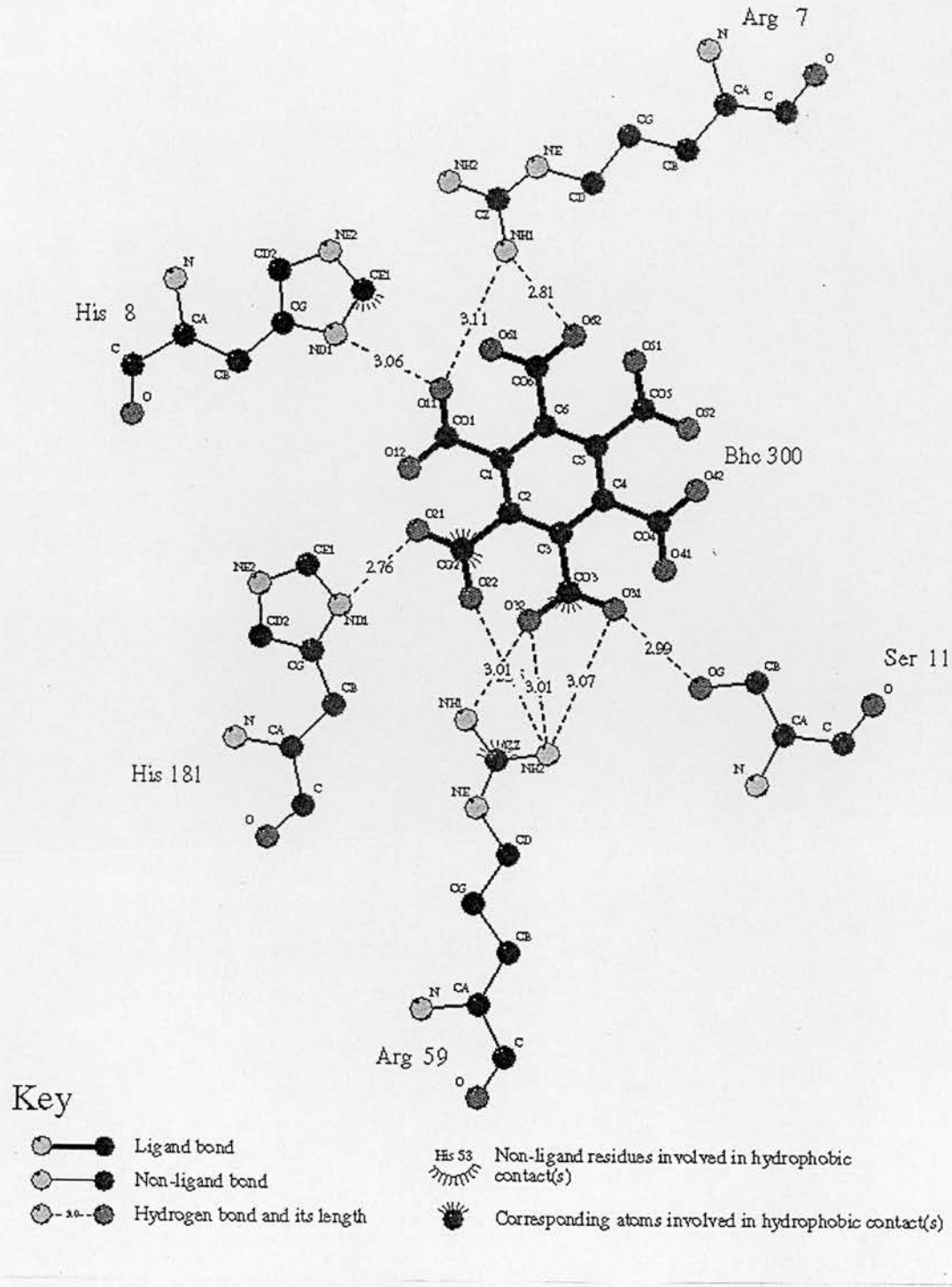

Figure 5.3
A LIGPLOT diagram of benzene hexacarboxylate (BHC) modelled in to the active site of *S.cerevisiae* PGAM, showing possible interactions between the ligand and active site residues.
The benzene carboxylates were placed using the program LIGIN, and the positions refined by a combined energy minimization and molecular dynamics procedure using the program XPLOR.

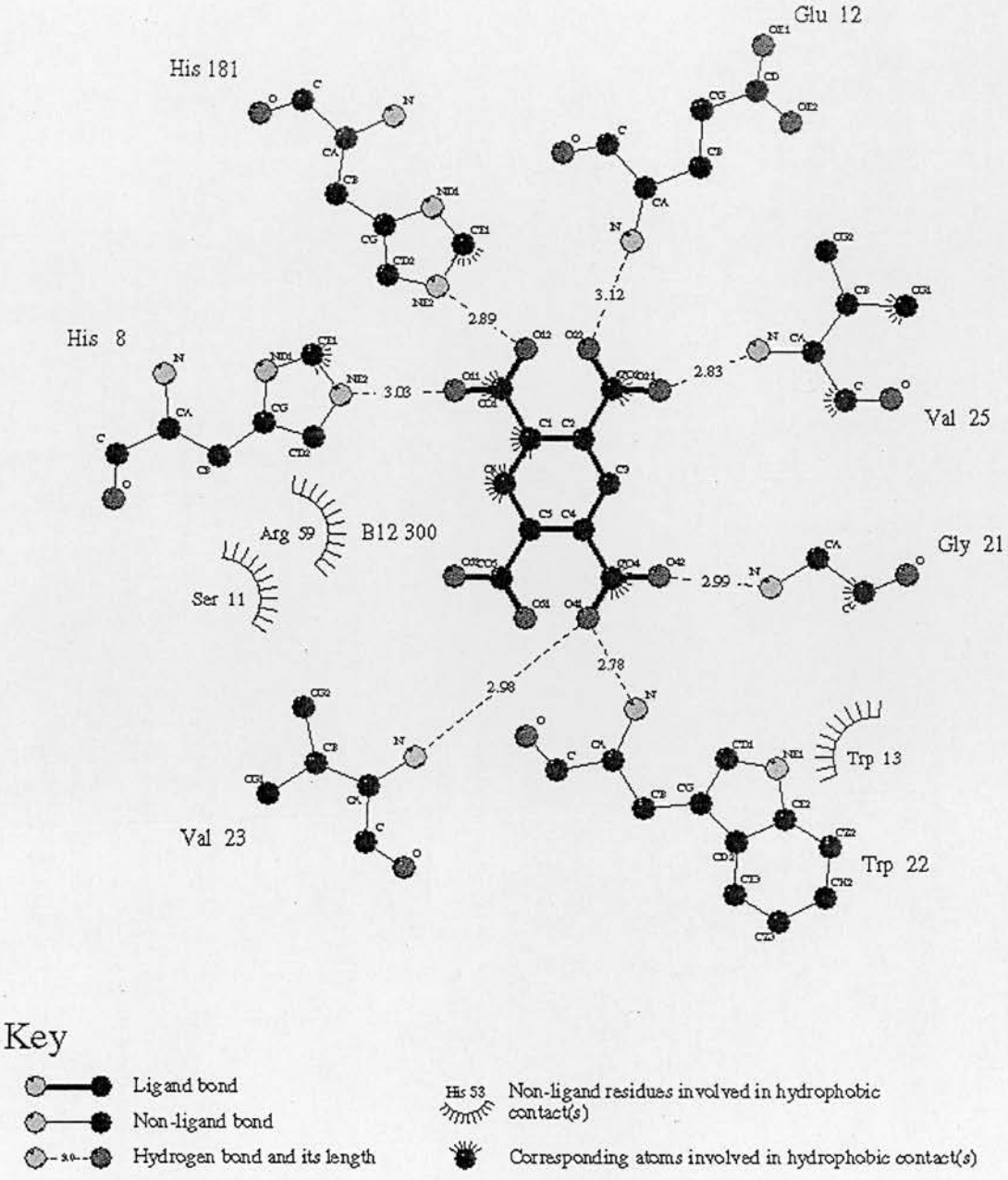

Figure 5.4
Benzene 1,2,4,5-tetracarboxylate (B1245) modelled in to the active site of *S.cerevisiae* PGAM, showing possible interactions between the ligand and active site residues.

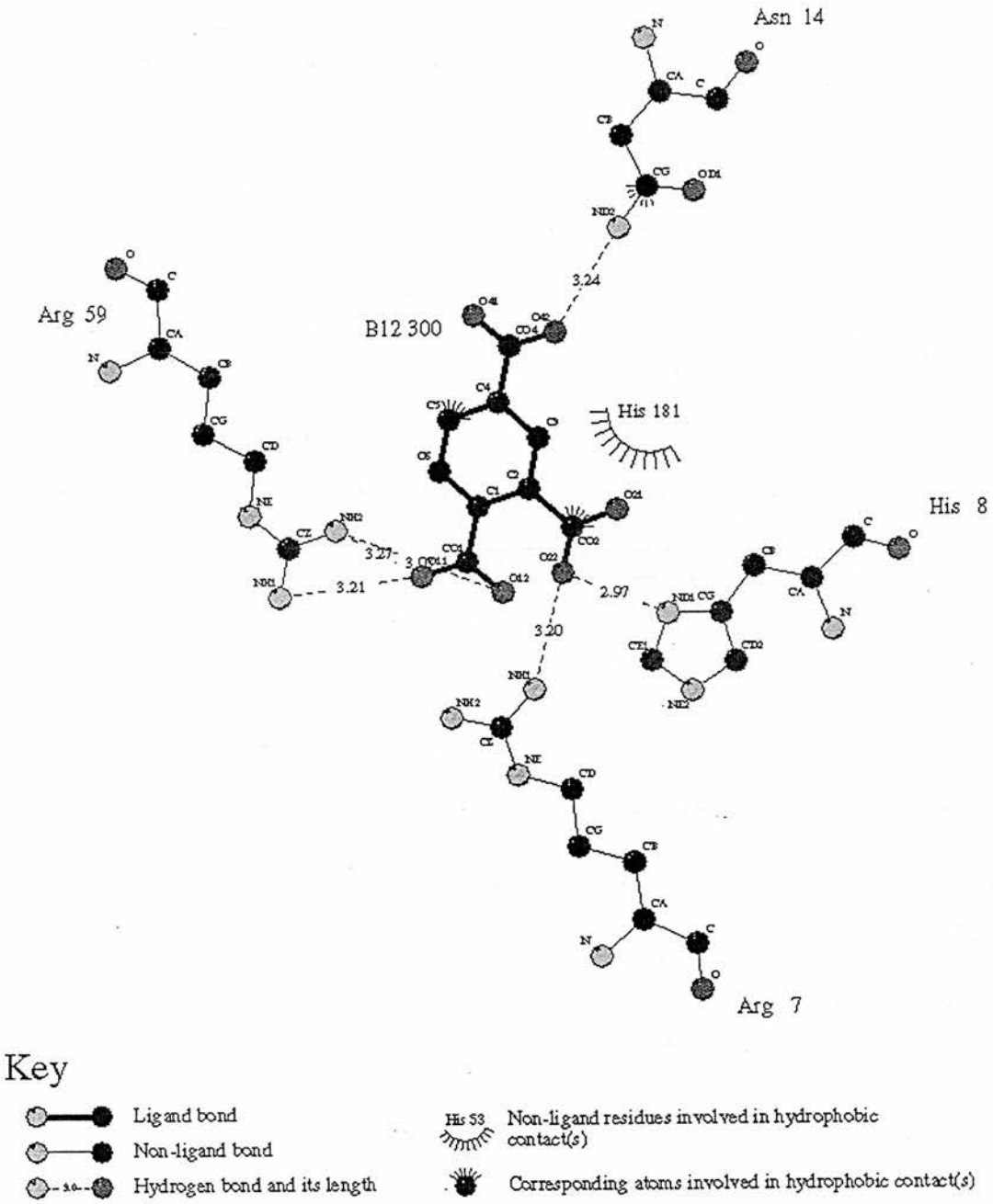

Figure 5.5
Benzene 1,2,4-carboxylate (B124) modelled in to the active site of *S.cerevisiae* PGAM, showing possible interactions between the ligand and active site residues.

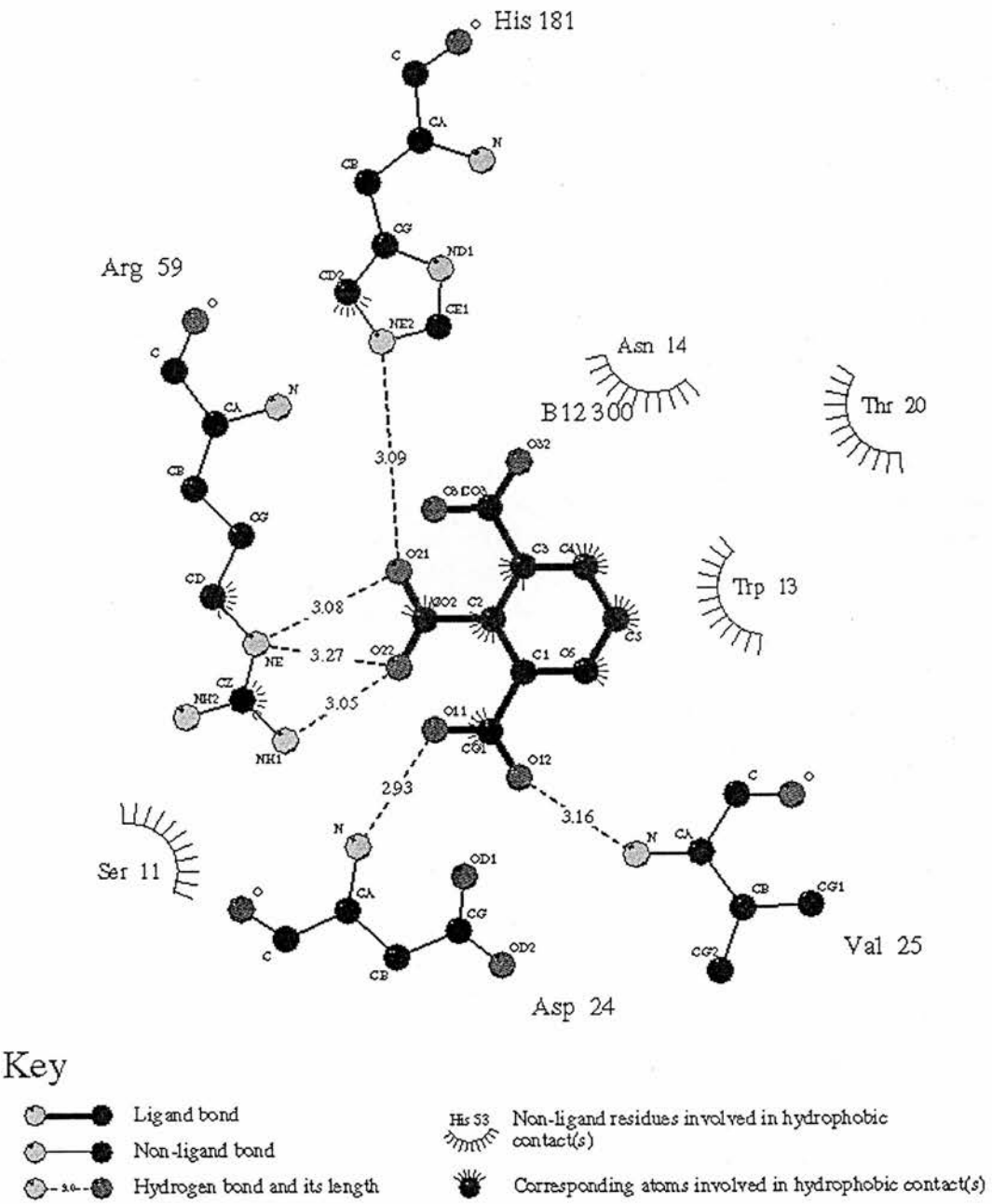

Figure 5.6
Benzene 1,2,3-tricarboxylate (B123) modelled in to the active site of *S.cerevisiae* PGAM, showing possible interactions between the ligand and active site residues.

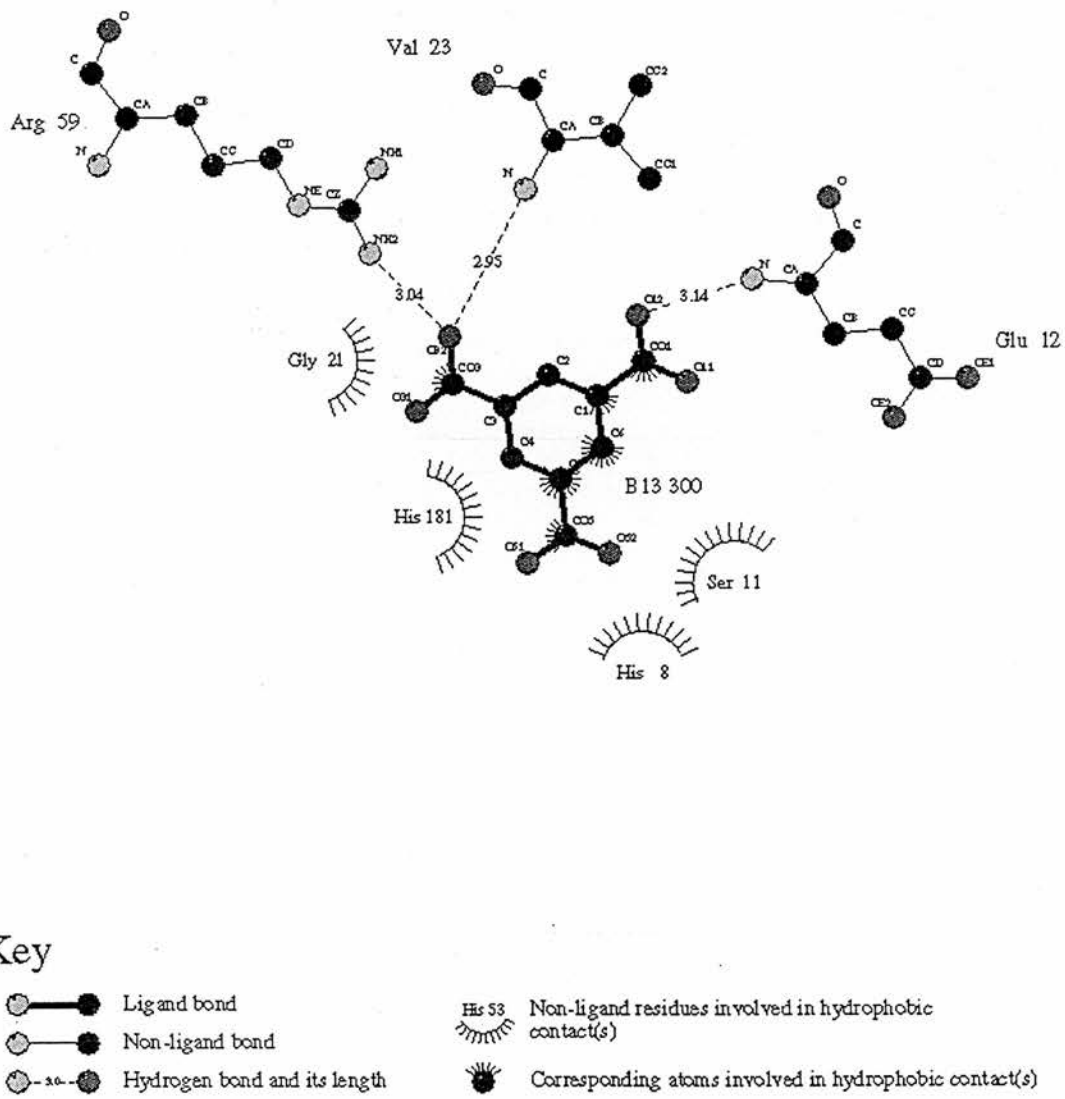

Figure 5.7
Benzene 1,3,5-tricarboxylate (B135) modelled in to the active site of *S.cerevisiae* PGAM, showing possible interactions between the ligand and active site residues.

that different interactions are formed, and we would therefore expect to see differences between the K_i values of these inhibitors. The determination of the K_i values could provide support for the models of inhibitor binding.

It has previously been described how exposure to thermolysin causes a decrease in the *S. cerevisiae* mutase activity (Section 3.2). 60% of the activity is lost in the first twenty minutes of proteolysis, during which time a portion of the tail is removed. Further loss of activity is attributed to more extensive digestion affecting other parts of the enzyme. However, the presence of the substrate 2,3-BPGA provides some protection against limited proteolysis by thermolysin (Section 3.5), which suggests that the tail is interacting with the ligand bound in the active site. 3-PGA does not provide this protection and it was therefore concluded that the presence of at least two phospho groups was necessary to draw the tail into the active site. Benzene hexacarboxylate (BHC) and IHP carry multiple negative charges and therefore could be expected to provide protection against proteolysis if they also bind in a suitable position in the active site. However, the benzene carboxylates are likely to bind deeper in the catalytic pocket than IHP and therefore would be less accessible, and so there may be a difference in the degree of protection afforded by the different inhibitors. The proposed positions of IHP and BHC relative to the pocket mouth are shown in figure 5.8.

The role of the tail in binding these ligands can be further studied using the mutase from *S. pombe*. This enzyme does not have a tail, and the k_{cat} of this enzyme is around one-fifth that of the *S. cerevisiae* mutase (Nairn *et al.* 1994). We would therefore expect the effects of treatment with thermolysin to be different. As there is no tail to lose, we would not expect to see the first sharp loss of activity. There may however be a more gradual loss, with the protein being digested in the same way that the *S. cerevisiae* mutase is further digested on prolonged exposure to the protease. If, as thought, protection against proteolysis is afforded by the bisphosphoglycerate as a result of the negative charges drawing the tail into the active site, there should be no such protection with the *S. pombe* mutase. If the tail is involved in ligand binding, we might also expect to see differences in the binding efficiencies of the two enzymes.

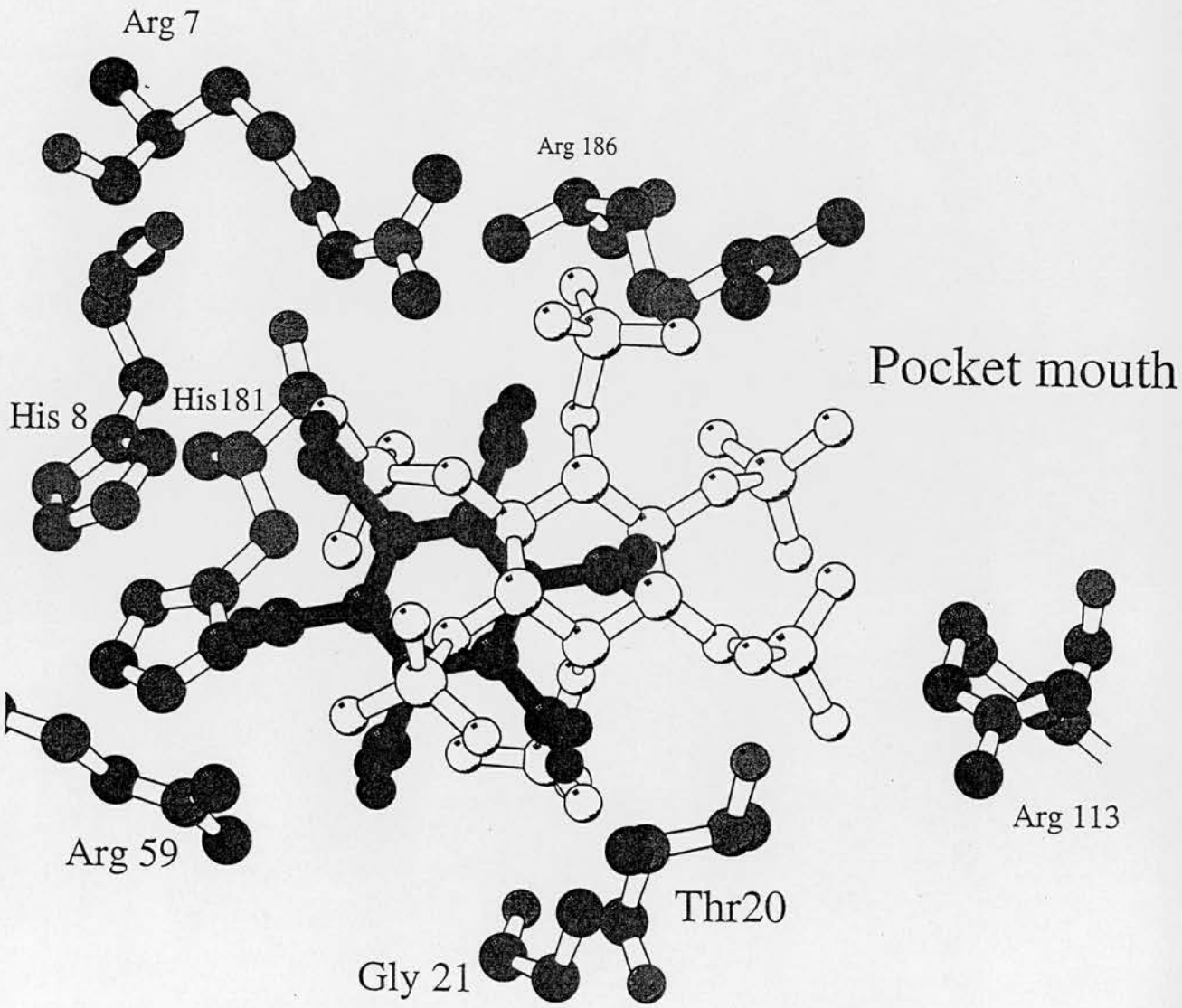

Figure 5.8

A MOLSCRIPT diagram comparing the most favoured position of IHP (in white) and BHC (in black).

A sample of recombinant *S. pombe* PGAM (Nairn *et al.* 1996) was available in a partially purified form (a gift from Dr. J. Nairn) and was purified to homogeneity as described in Section 2.2.6. The kinetic constants and K_M values for each of the substrates were determined as a basis for further study of the effects of the inhibitors.

5.2 Phosphoglycerate mutase from *Schizosaccharomyces pombe*

5.2.1 Preparation of pure enzyme

Recombinant *S.pombe* PGAM was obtained partially purified (after ammonium sulphate fractionation and ion exchange chromatography). It was purified to homogeneity (as indicated by a single band on a Coomassie-stained SDS-PAGE gel) using a single gel filtration step, identical to the final step in the purification of the *S.cerevisiae* enzyme.

5.2.2 S.pombe phosphoglycerate mutase kinetics

The kinetic properties of *S.pombe* PGAM were determined in the same way as for the *S.cerevisiae* enzyme. The Hanes primary plot shows the shape characteric of a ping pong mechanism, with the lines intersecting at the y axis (See figure 5.9). The secondary plot gives the kinetic constants.

$\mathbf{K_M}^{\mathbf{3PGA}}$ - 580μM

$\mathbf{K_M}^{\mathbf{2,3BPGA}}$ - 4.6μM

$\mathbf{V_{max}}$ - 310 EU/mg.

The K_M values for the substrates are very similar to those for the wild type *S.cerevisiae* enzyme (K_M^{3PGA} - 560μM, $K_M^{2,3BPGA}$ - 3.2μM). The V_{max} is approximately one quarter that of *S.cerevisiae* PGAM.

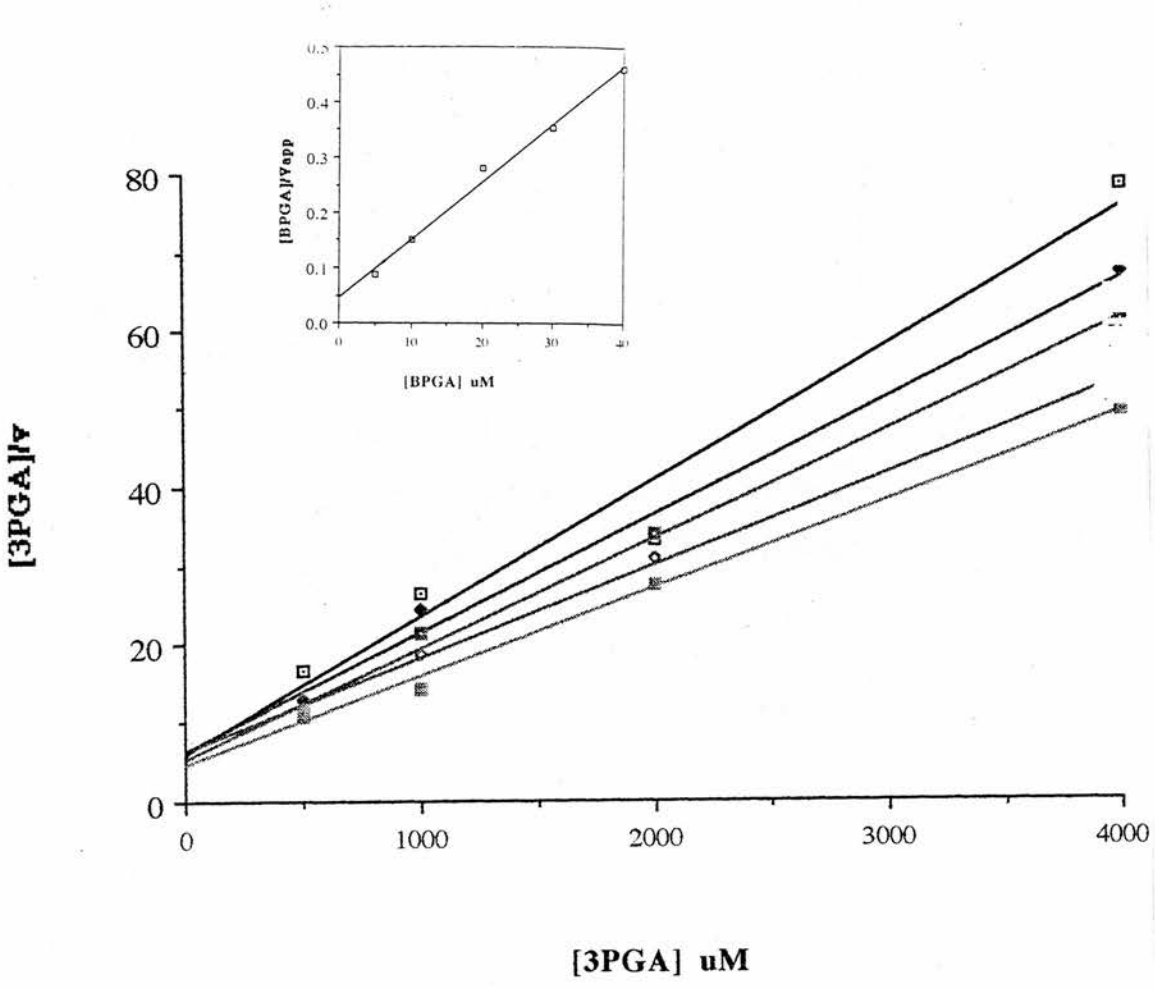

Figure 5.9
Hanes plots showing kinetic data obtained for *S.pombe* PGAM. The pattern seen in the primary plot corresponds to a ping-pong mechanism. The inset graph is the secondary plot required for calculating the kinetic constants. Assays carried out as described in section 2.2.8.

5.3 The effect of inhibitors on coupling enzymes

The mutase activity of PGAM is measured using the coupled assay system described in section 2.2.8. There is a possibility that the inhibitors tested also have an affinity for the coupling enzymes enolase, pyruvate kinase and lactate dehydrogenase, and therefore the coupled assay may not give an accurate measure of the effect on mutase activity only. Coupling enzymes are added in excess to ensure that the overall measured rate is that of the first reaction only. In the mutase assay, the product (2-PGA) is converted to lactate (via PEP and pyruvate) as soon as it is formed, with the concomitant measurable oxidation of NADH.

PGAM is routinely added to the assay in dilutions which give a change in A_{340} of 0.02/min or less, which is equivalent to 0.0032μmol of 2-PGA produced/min. An excss of enolase (0.08 units) is added to the assay mix, allowing the turnover of 0.08μmol of 2-PGA/min. The potential turnover of enolase is therefore 25x that of the maximum allowed mutase turnover.

Pyruvate kinase and lactate dehydrogenase (0.5 units each) are added, allowing a turnover 6x that of the enolase and 150x that of the mutase. As the coupling enzymes are present in such excess, it should be possible to retain sufficient activity to immediately convert the mutase product, even if the inhibitors do have significant affinity for the coupling enzymes.

This was tested by adding low concentrations of 2-PGA to the standard assay mix (without the mutase substrates, 3-PGA and 2,3-BPGA, and PGAM) in the presence and absence of the highest concentration of inhibitor assayed. This was done for each inhibitor studied at different 2-PGA concentrations. At very low concentrations (<2μM) no inhibition was observed. At 5μM 2-PGA (greater than the maximum possible product concentration), a small degree of inhibition (<20%) was observed. This was eliminated when the amount of coupling enzymes in the assay was doubled. It was decided to use this increased enzyme concentration in the inhibitor assays to ensure that any inhibitory effects on the coupling enzymes were insufficient to affect the measured mutase rate. When this increased amount of coupling enzymes was itself doubled, no increase in rate was observed.

5.4 The inhibition of *S.cerevisiae* and *S.pombe* phosphoglycerate mutase activities

Each of the inhibitors was tested with the *S.cerevisiae* and *S.pombe* PGAM, and the results represented on a combination plot (Chan, 1995). The results are shown in figures 5.10-5.13. Each inhibitor gave a horizontal line, indicating that the inhibition was competitive in nature. The value of K_i was given by the reciprocal of the vertical intercept. As the line is horizontal, it is difficult to gauge the goodness of fit, and changing the scale of the vertical axis can give a very different picture. In order to obtain a fair indication of the standard error associated with the value obtained for K_i, the reciprocal of each of the values plotted on the vertical axis was taken. For a perfect straight horizontal line, these values would be equal, and equal to K_i. The standard error for these data was calculated and is given after each value.

In theory, each individual substrate concentration should give the same value for the vertical axis function for any inhibitor concentration. It can be seen from the graphs that there is variation, with points appearing above and below the line of best fit. If higher inhibitor concentrations consistently gave points above the line and lower concentrations points below the line (or *vice versa*), this could indicate a systematic error in the experiment. However, inspection of the data shows that the distribution of points around the line of best fit is random.

The K_i values determined using the combination plots are given below.

	K_i (μM)	
	S.cerevisiae	*S.pombe*
IHP	4 ± 1.0	35 ± 5.5
BHC	6 ± 0.6	22 ± 2.4
B1245	12 ± 1.0	55 ± 3.5
B124	21 ± 2.8	62 ± 5.0
B123	23 ± 1.8	67 ± 2.2
B135	24 ± 3.6	53 ± 3.2

Table 5.1
K_i values for the inhibition of *S. cerevisiae* and *S. pombe* PGAM by IHP and the benzene carboxylates.

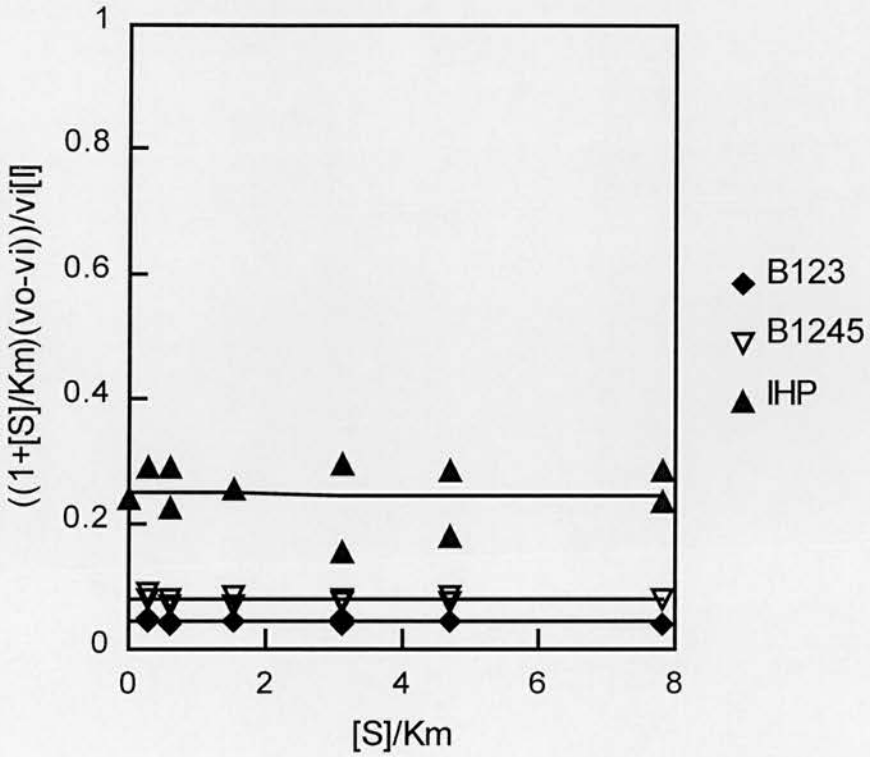

Figure 5.10

Combination plots (Chan, 1995) showing inhibition of *S.cerevisiae* PGAM by IHP, B1245 and B123. Standard kinetic parameters are used, with [I] (concentration of inhibitor), v_o(rate of reaction at a particular substrate concentration in the absence of inhibitor) and v_i (rate of reaction at a particular substrate concentration in the presence of inhibitor). Assays were carried out as described in Section 2.2.10.

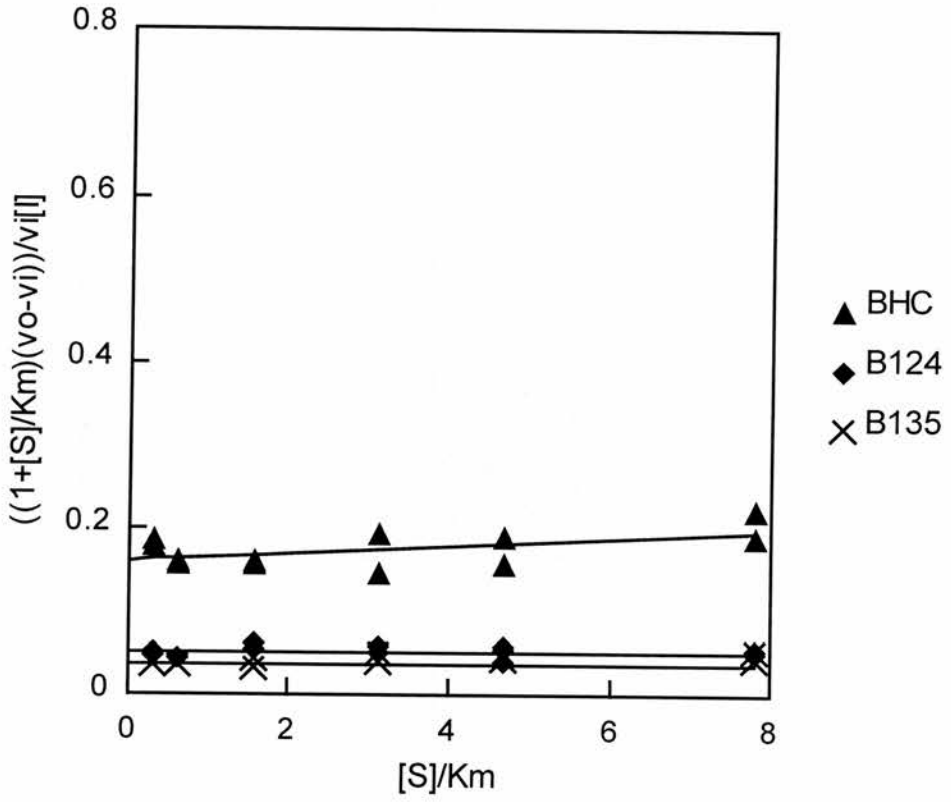

Figure 5.11
Combination plots (Chan, 1995) showing inhibition of *S.cerevisiae* PGAM by BHC, B124 and B135.

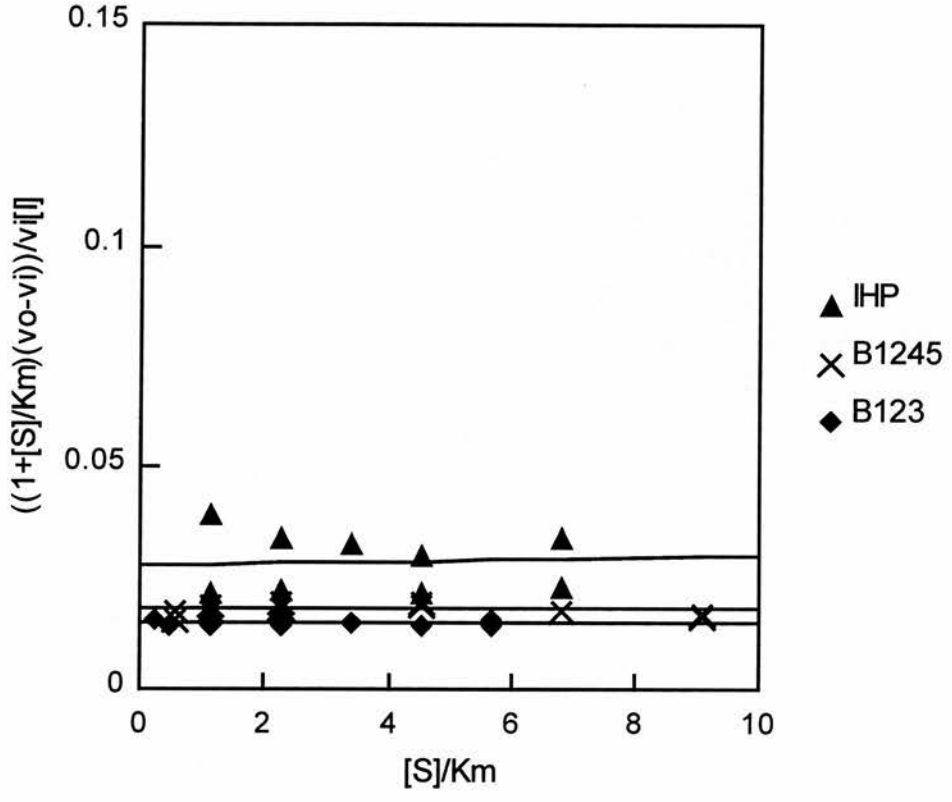

Figure 5.12
Combination plots (Chan, 1995) showing inhibition of *S.pombe* PGAM by IHP, B1245 and B123.

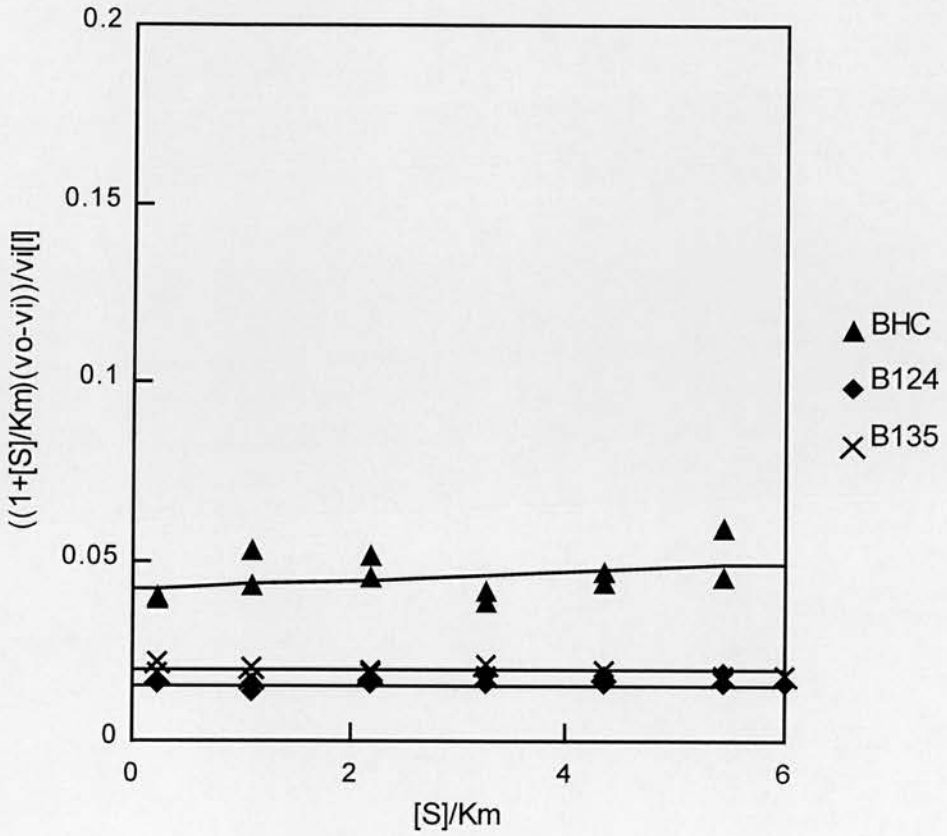

Figure 5.13
Combination plots (Chan, 1995) showing inhibition of *S.pombe* PGAM by BHC, B124 and B135.

With the *S.cerevisiae* enzyme, the tightness of binding of the inhibitors increases with the number of negatively charged groups. Although IHP and BHC are thought to bind in different positions, their K_i values are very similar. There are no significant differences between the K_i values for the benzene tricarboxylates. This is unexpected, as the modelling suggests that the different positions of the negatively charged groups could lead to different interactions and different numbers of interactions being formed (see figures 5.5-5.7), and it was expected that this would be reflected in the binding efficiency.

Differences are seen with the *S.pombe* enzyme which would suggest differences between the two active sites and the interactions formed between active site residues and the inhibitors. The K_i values are significantly higher than for the *S. cerevisiae* mutase. This could be due to the absence of a tail, if it is indeed involved in binding the inhibitors. However, if this were the case, we might also expect the K_M values for the substrates to be higher, and they are very similar. Another possibility is that there are differences in the active site that do not significantly affect the binding of the substrates, but do affect the binding of the more negatively charged inhibitors. Two of the residues thought to be involved in the binding of at least three of the inhibitors (B1245, B124, B123) are Val23 and Val25. In the *S. pombe* PGAM, these residues are a lysine and a proline respectively. The presence of a proline in particular could alter the active site so that the interactions formed with the *S. cerevisiae* enzyme are not possible with that from *S. pombe*. The K_i for B135 is lower than that for the other tricarboxylates, and is similar to that for B1245. Looking at the modelled complexes in Figures 5.4 and 5.7, it is clear that B135 would be likely to form fewer interactions in the *S.cerevisiae* active site than the other inhibitors, but B124 and B123 are thought to interact with the valines that are substituted in the *S. pombe* mutase and this could explain the differences between the two enzymes.

The differences between the *S. pombe* and the *S. cerevisiae* enzyme affect the affinity for IHP more than BHC. The K_i values for these two inhibitors are very similar with the *S. cerevisiae* mutase (4μM and 6μM respectively), but differ quite significantly with *S. pombe* (35μM and 22μM). This may be as a result of a greater interaction of the tail with IHP (see next section), or due to differences in the active

sites. There are two replacements in the vicinity of the proposed IHP binding site. Asn204 in the *S. cerevisiae* enzyme is replaced with a glutamate, and Glu15 is replaced with a lysine. The first change would be expected to reduce the binding efficiency of an anionic molecule, whereas the second would increase affinity. However, BHC is thought to bind near to Glu15 and distant from Asn204, so the overall effect would be different for each molecule, and could give rise to the differences seen in the K_i values.

5.5 Ligand protection against proteolysis

Figure 5.14 shows the effects of thermolysin digestion on *S.cerevisiae* PGAM incubated with saturating (50μM) and non-saturating (5μM) concentrations of BHC. Saturating BHC afforded a similar degree of protection in the initial phase of proteolysis to that provided by 2,3-BPGA, non-saturating rather less. However, the first part of the graph is less steep and as this is the part that is thought to correspond to the removal of the tail, this would suggest at least some protection against its removal.

Figure 5.15 shows the results for saturating and non-saturating IHP, whch appears much more effective than the BHC or 2,3-BPGA. At saturating concentrations (50μM), removal of the tail appeared to be completely stopped, leaving only the slower process involving other parts of the protein. Again, the lower concentration (5μM) was less effective. This is consistent with the idea that inhibition and protection are due to binding at a particular site. These results tie in with the modelling, which shows that BHC binds deeper in the catalytic pocket than IP6. Therefore IP6 would be expected to interact more readily with the tail than BHC and so provide a greater degree of protection.

As detailed in Section 3.2, the loss of activity due to limited proteolysis by thermolysin can be divided into two phases. There is an initial rapid loss of activity due to the removal of a portion of the tail, followed by a gradual decrease due to more extensive proteolytic attacks. As the PGAM from *S.pombe* does not possess a tail region, we would expect to see only the second, more gradual, change in activity.

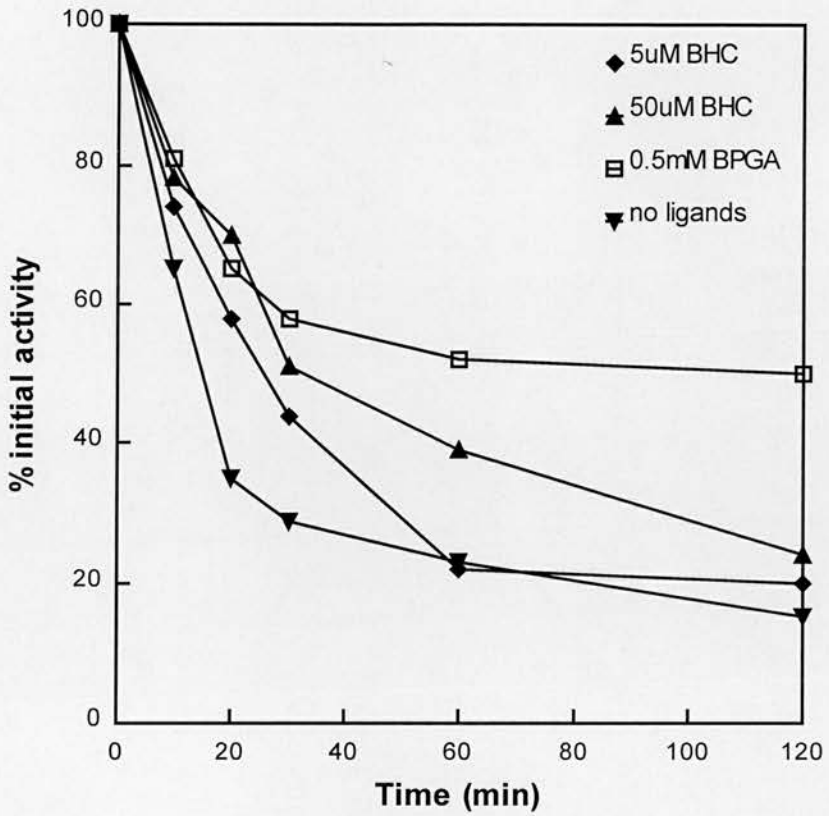

Figure 5.14
Graph showing the loss of activity of *S. cerevisiae* PGAM due to limited proteolysis by thermolysin in the presence and absence of BHC and 2,3-BPGA.
100μg/ml PGAM was incubated with 10μg/ml thermolysin and ligands at 20°C. The concentrations of ligands are given in the key. At the times indicated, samples were removed and EDTA added to 10mM to inactivate the thermolysin. Mutase actvity was determined as described in Section 2.2.8

Figure 5.16 compares the effect of thermolysin on the mutase activity of the PGAMs from *S. pombe* and *S. cerevisiae* in the presence and absence of the substrate 2,3-BPGA. Comparing the two unligated enzymes, the *S. pombe* mutase activity is much less affected than that of the *S. cerevisiae* mutase, only losing 35% of activity in two hours compared with over 80%. The main difference is in the initial stages, which is believed to correspond to the loss of a portion of the tail, which is of course absent in the *S. pombe* mutase. The more extensive proteolysis seen in the later stages of incubation of *S. cerevisiae* mutase with thermolysin probably also occurs with the *S. pombe* enzyme and is responsible for the gradual loss of activity observed. The addition of 2,3-BPGA provides a considerable degree of protection against proteolysis for the *S. cerevisiae* enzyme, but has very little effect on the inactivation of *S. pombe* PGAM. This again provides evidence that the protection afforded by the ligand is due to interaction with the tail region.

Figure 5.17 compares the results of incubating *S. pombe* and *S. cerevisiae* mutases with thermolysin and the inhibitors IHP and BHC. It shows that in the presence of saturating IHP, the degree of inactivation is very similar to that of *S. pombe* mutase in the presence or absence of ligands. This concentration of IHP therefore appears to completely protect the tail from removal by thermolysin.

5.6 Discussion

The biochemical data provide support for the modelling of these polyanionic inhibitors in the catalytic site of *S. cerevisiae* PGAM. The K_i values and the degree of protection afforded against digestion by thermolysin are consistent with the proposed binding sites. The tail of the enzyme clearly interacts with IHP and is thought to be drawn over the active site. It was hoped that the inclusion of this ligand in the mother liquor during crystallization would lead to a conformation of the enzyme with a structured tail. This was attempted during the recent crystallization of *S. cerevisiae* PGAM, but no trace of the inhibitor was found in the resulting structure (Rigden *et al.* 1997). The final determination of the binding sites of these compounds must await further X-ray crystallographic studies (or nuclear magnetic resonance

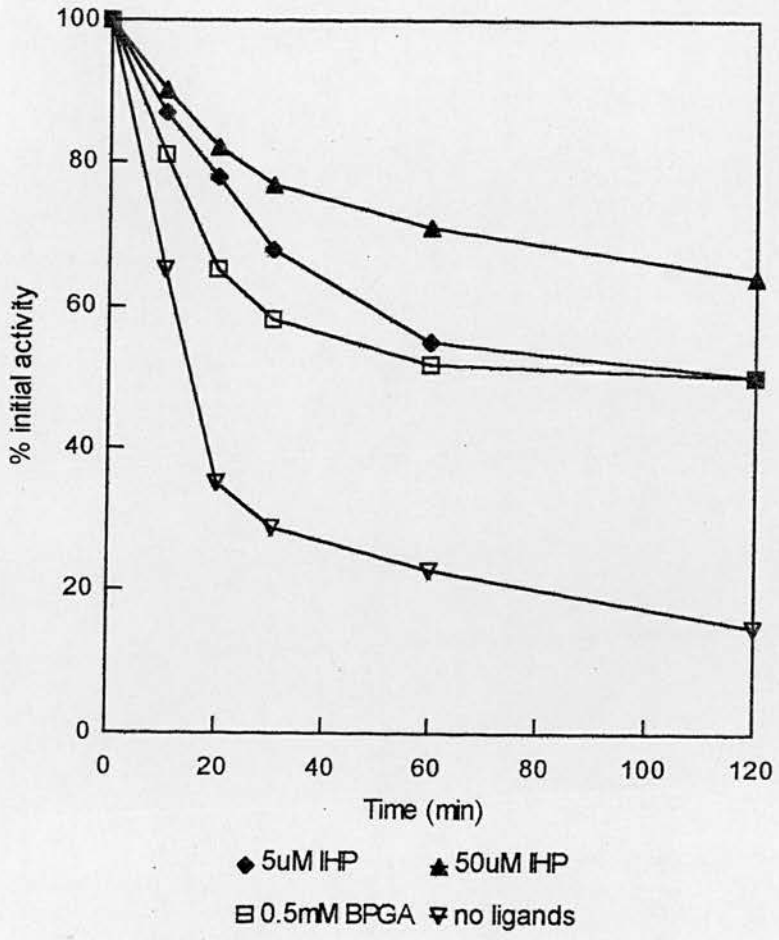

Figure 5.16

Comparison of the effects on limited proteolysis on PGAM from *S. cerevisiae* and *S. pombe* in the presence and absence of 2,3-BPGA.

100μg/ml PGAM was incubated with 10μg/ml thermolysin and ligands at 20°C. The concentrations of ligands are given in the legend. At the times indicated, samples were removed and EDTA added to 10mM to inactivate the thermolysin. Mutase actvity was determined as described in Section 2.2.8.

S.p. - *S. pombe* PGAM

S.c. - *S. cerevisiae* PGAM

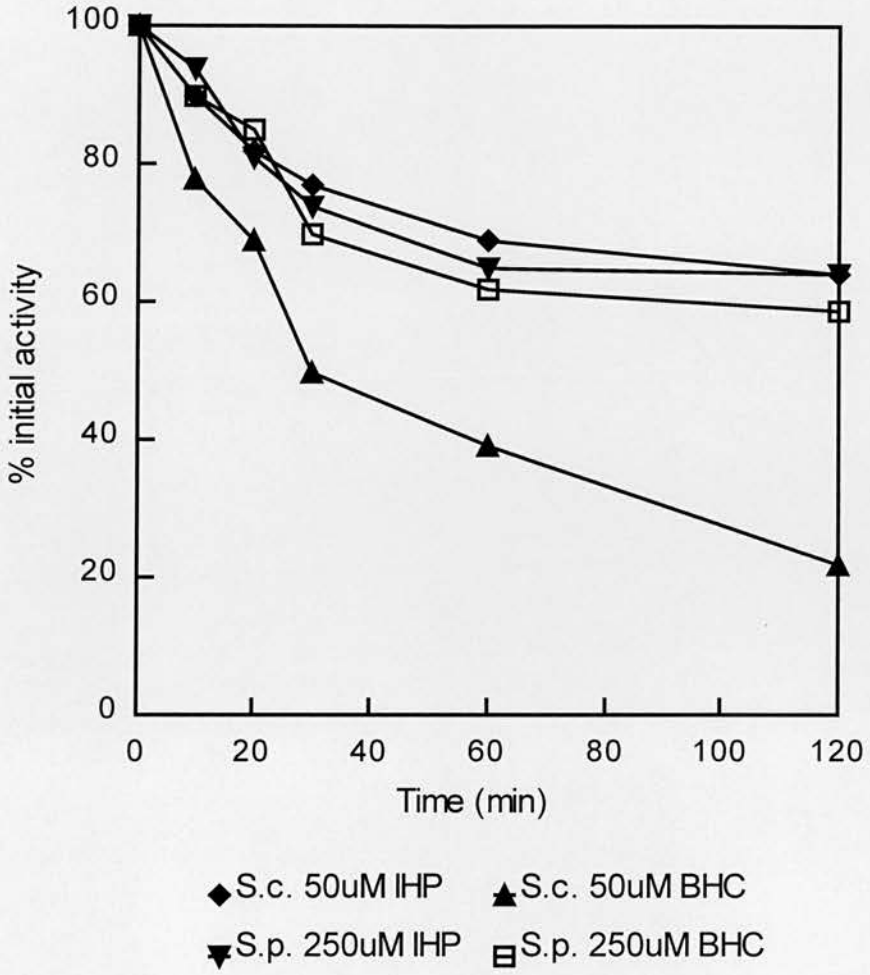

Figure 5.17

Comparison of the effects of BHC and IHP on the limited proteolysis of PGAM from *S. cerevisiae* and *S. pombe*.

100µg/ml PGAM was incubated with 10µg/ml thermolysin and ligands at 20°C. The concentrations of ligands are given in the legend. At the times indicated, samples were removed and EDTA added to 10mM to inactivate the thermolysin. Mutase actvity was determined as described in Section 2.2.8.

S.p. - *S. pombe* PGAM

S.c. - *S. cerevisiae* PGAM

studies for the smaller *S. pombe* PGAM), especially in light of the revised structure recently determined.

The results obtained from the limited proteolysis experiments provide additional support for the work described in chapters three and four. It was shown in chapter three that the initial rapid inactivation of *S. cerevisiae* PGAM incubated with thermolysin was due to the loss of a portion of the flexible tail region, and the addition of 2,3-BPGA provides protection against this inactivation. It was shown in chapter four that a mutant with the two C-terminal lysines replaced with uncharged alanines is not protected against proteolysis by 2,3-BPGA, suggesting that these positively charged lysines interact with the negatively charged groups, drawing the tail over the active site. As would be expected, the highly charged inhibitor molecules also appear to interact with the tail, and also provide protection against proteolysis. The modelling suggests that IHP and BHC bind in different positions, with IHP nearer the mouth of the catalytic pocket, and this is supported by the observation that IHP provides a greater degree of protection. The *S. pombe* enzyme does not have a tail, and the pattern of inactivation and the lack of protection by 2,3-BPGA are consistent with the role of the tail as described.

As described in section 1.13 and chapter 6, the cofactor-dependent monophosphoglycerate mutases such as those from *S. cerevisiae* and *S. pombe* are closely related to the bisphosphoglycerate mutases found in mammalian erythrocytes, with sequence identities in the 40-50% range (see table 1.2). BPGAM is of pharmacological interest as it controls the concentration of 2,3-BPGA in erythrocytes and so influences the affinity of haemoglobin for oxygen. Therefore the results described here may provide a useful starting point for the design of inhibitors for BPGAM.

Chapter Six

The Mutase/Synthase Relationship

6.1 Introduction

The differences between the mono- and bisphosphoglycerate mutases have been described in Section 1.11. One of the key differences in the amino acid sequences of the phosphoglycerate mutases is at residue 11 (using *S. cerevisiae* numbering). This is a serine in all the monophosphoglycerate mutases for which sequences have been determined, but a glycine in bisphosphoglycerate mutases (see Figure 1.4). It has been suggested that this serine residue provides a phospho ligand for the binding of the 2,3-BPGA substrate to the active site of the *S. cerevisiae* enzyme (Fothergill-Gilmore and Watson, 1989). This residue would interact with the phospho group that is transferred to His8. Clearly, the presence of a glycine in this position would reduce the number of phospho ligands available, and facilitate the release of this molecule once formed in the active site of the bisphosphoglycerate mutase, which primarily catalyzes the 2,3-BPGA synthase activity.

Another residue that differs between the mono- and bisphosphoglycerate mutases is residue 60, conserved as an alanine in monophosphoglycerate mutases and as a serine in bisphosphoglycerate mutases. This residue is in the active site, but has not been specifically implicated in ligand binding. Part of the 2.8Å structure (Watson, 1982) showing the positions of key active site residues (including Ser11 and Ala60) are shown in Figure 6.1. On the left side of the diagram (under the heading PGAM) are the residues found in the *S. cerevisiae* enzyme. BPGAM simply has Ser11 to Gly and Ala60 to Ser substitutions. Also shown are the sulphates which were present in the active site, and were thought to bind in the same position as the phospho groups on the 2,3-BPGA substrate. The functional group of Ser11 is clearly directed into the active site, and is close to one of the bound sulphates. This is the sulphate binding near His8, which would represent the phospho group that is transferred to this residue to form the phospho enzyme. When Ala60 is replaced by a serine, the functional group is nearer to the second sulphate.

A mutant in which Ser11 was replaced with glycine was shown to have considerably reduced mutase activity, but was extremely unstable (White, 1989). It was hoped that replacement of the serine with the larger alanine would eliminate this problem. Three

Figure 6.1

PGAM

The active site of phosphoglycerate mutase from *S. cerevisiae* showing residues thought to be involved in the mutase/synthase relationship. Also shown are the sulphates which were bound in the active site when the enzyme was crystallized, and which are presumed to bind in the positions occupied by the phospho groups of 2,3-BPGA when this is bound to the enzyme (Winn et al., 1981).

BPGAM

This shows the same structure, and simply replaces Ser11 and Ala60 with alanine and serine respectively. These are substitutions suggested by the alignment of the amino acid sequences of mono- and bisphosphoglycerate mutases.

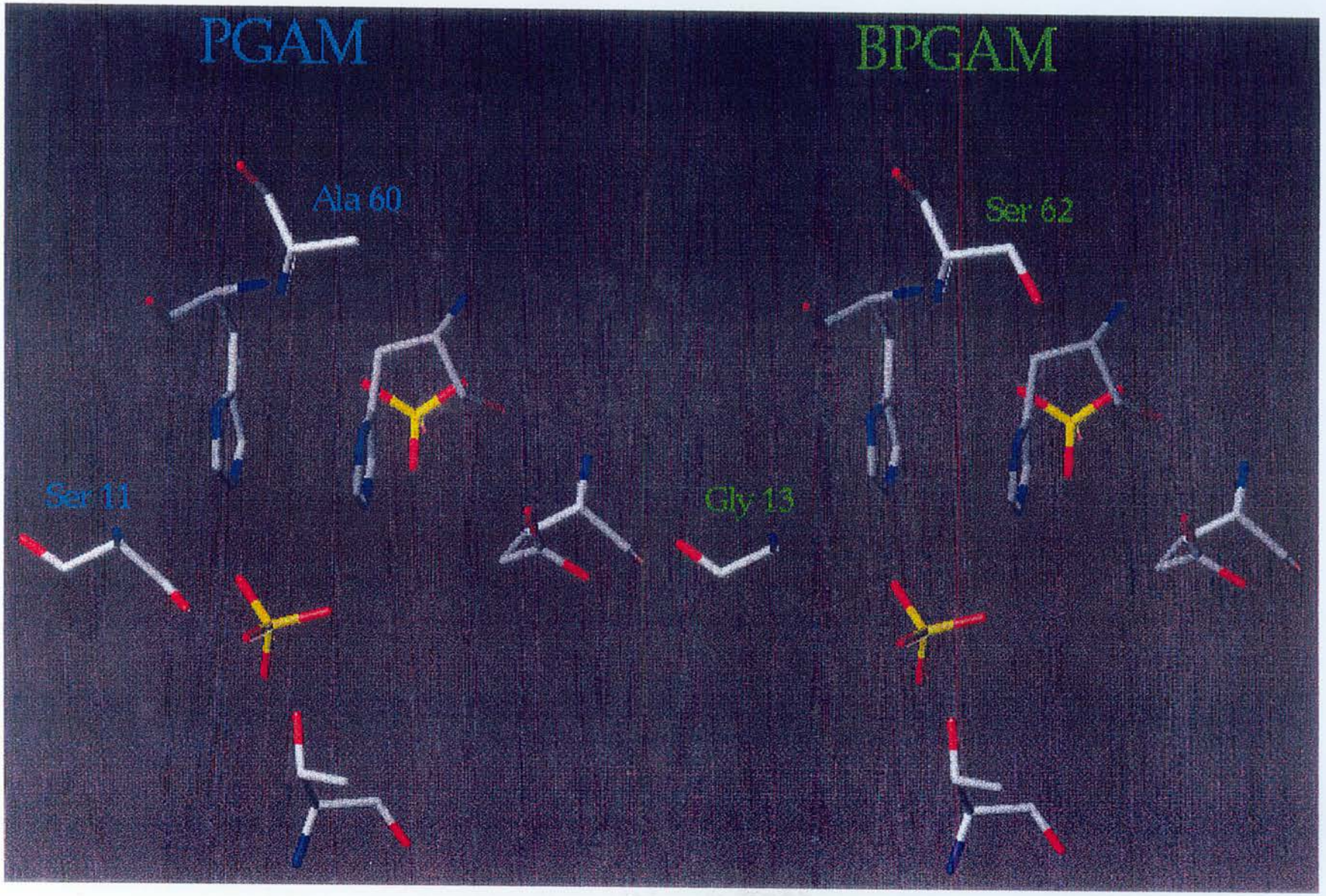
PGAM
BPGAM
Ala 60
Ser 62
Ser 11
Gly 13

mutants designed to study the role of Ser11 and Ala60 were available - S11A, A60S and the double mutant S11A/A60S. These were constructed by Dr. Malcolm White using the mutagenesis and expression system described previously (Section 1.14, White and Fothergill-Gilmore, 1992).

6.2 Expression of mutants

All the mutants grew on YEPD using glucose as a carbon source and so show some mutase activity. The yeast was lysed using glass beads after overnight growth (as described in Section 2.2.4) and the lysate electrophoresed in an SDS-PAGE gel (see figure 6.2). All the mutants are overexpressed to about the same level as the wild type enzyme, around 20-30% of total cell protein (as estimated using SDS-PAGE).

6.3 Growth of mutants

The growth characteristics of the mutants in YEPD were investigated and growth curves are shown in figure 6.3. A60S gives a curve similar in shape to the wild type, but where Ser-11 is replaced with Ala (S11A and S11A/A60S), there is a noticeably slower doubling time in logarithmic phase, so these mutants reach stationary phase later than the wild type and A60S mutant, although they do ultimately reach the same cell density in stationary phase.

6.4 Purification of S11A and A60S

The A60S mutant was purified in the same way as the wild type enzyme, as described in section 2.2.6. The S11A mutant did not bind to the QA52-cellulose ion exchange column under the conditions used in the standard purification procedure (10mM Tris.HCl pH8.0, 4°C). The S11A was collected in the buffer wash and purified to homogeneity on the Superose 12 column.

The behaviour of the S11A mutant on the Superose 12 column was also different to the other PGAMs studied. The wild type and other mutants all elute from the column in the same fraction, but S11A elutes significantly later (figure 6.4). As

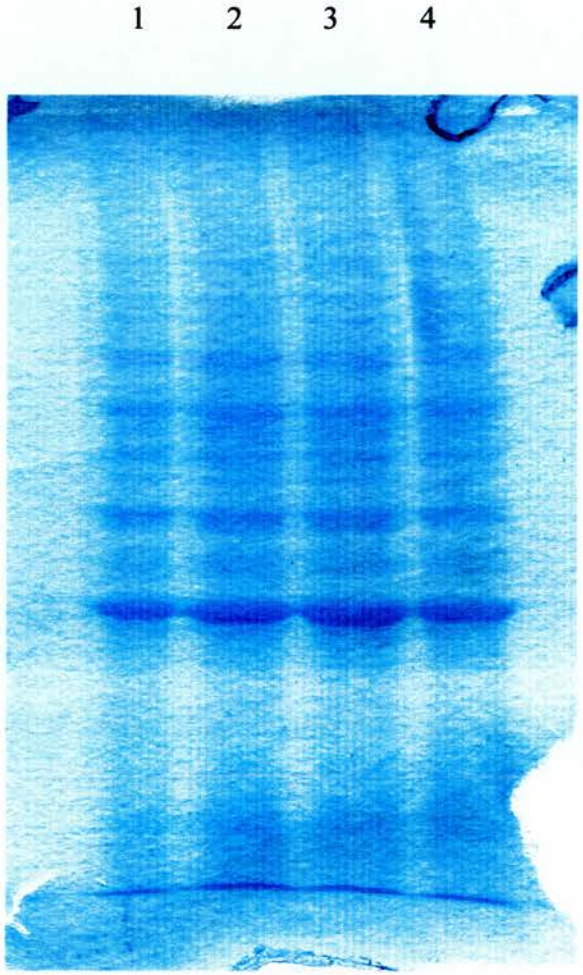

Figure 6.2

Cell lysates from overnight cultures lysed with glass beads and electrophoresed in a 12% SDS-PAGE gel as described in Section 2.2.3.

1. S150-2B GPM::HIS3 + pVT-gpm
2. S150-2B GPM::HIS3 + pVT-A60S
3. S150-2B GPM::HIS3 + pVT-S11A
4. S150-2B GPM::HIS3 + pVT-S11A/A60S

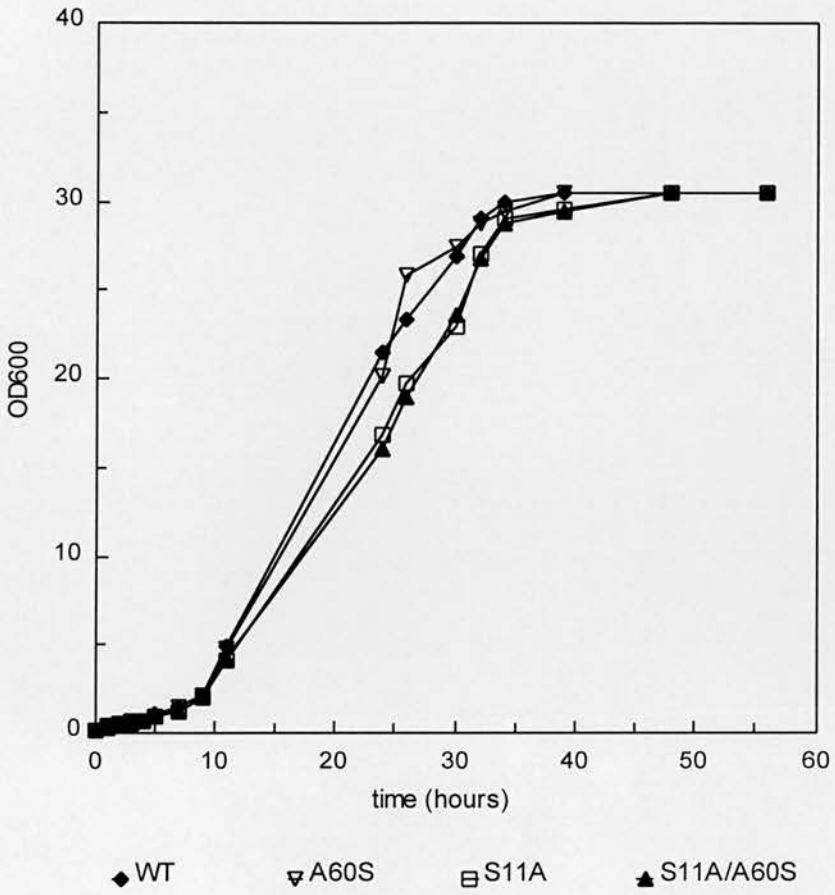

Figure 6.3
Growth curves for S150-2B GPM::HIS3 expressing wild type or mutant PGAM. An overnight culture of each was used to innoculate 500ml YEPD (section 2.2.2.1) to 0.1 OD_{600}. This was then incubated (with shaking) at 30°C, and small samples taken at intervals to determine optical density. Each point represents the mean value obtained from three cultures.

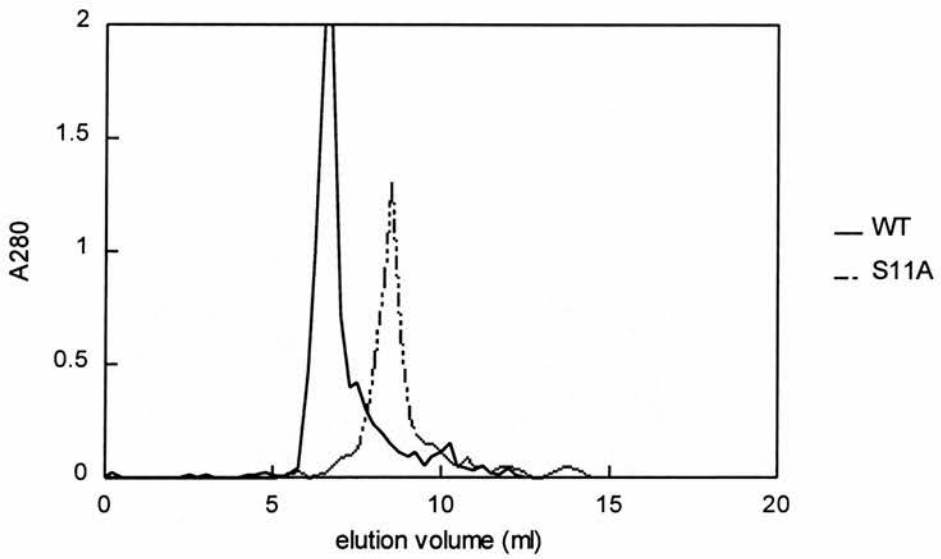

Figure 6.4
Elution profiles of wild type PGAM and S11A from a Superose HR12 gel filtration column. Flow rate 0.3ml/min, chart speed 0.5cm/ml.

Superose 12 is a size exclusion column, this would imply a change in the size or shape of the molecule. This change could be due either to a change in the size of the subunit or a change in the oligomeric structure. It can be seen from the SDS-PAGE of the crude lysates (Figure 6.2) that there is no significant change in the subunit size.

In order to investigate the oligomeric structure, samples of wild type and S11A protein (in the presence and absence of 2,3-BPGA) were cross-linked using glutaraldehyde (see section 2.2.11) and run on a 9% SDS-PAGE gel (figure 6.5). This gel shows clearly that the S11A exists in a tetrameric form like the wild type under these conditions. However, the size of the S11A tetramer appears to be slightly smaller than the wild type tetramer, and this could explain the retardation on the size exclusion column. No change is seen when the enzyme is incubated with the substrate 2,3-BPGA (0.5mM) before cross-linking. The enzyme is still in tetrameric form.

6.5 Specific activities of S11A and A60S

The mutase, synthase and phosphatase activities were measured as described in section 2.2.8, and are shown in the table below.

	mutase	synthase	phosphatase	fold increase with 2-PG
WT	970	0.01	0.02	18
A60S	620	0.01	0.02	3.1
S11A	40	nd	nd	nd

Table 6.1
The specific activities of S11A and A60S PGAM. Activities are expressed as μmol NAD^+produced/min/mg PGAM.
nd - no activity detected.

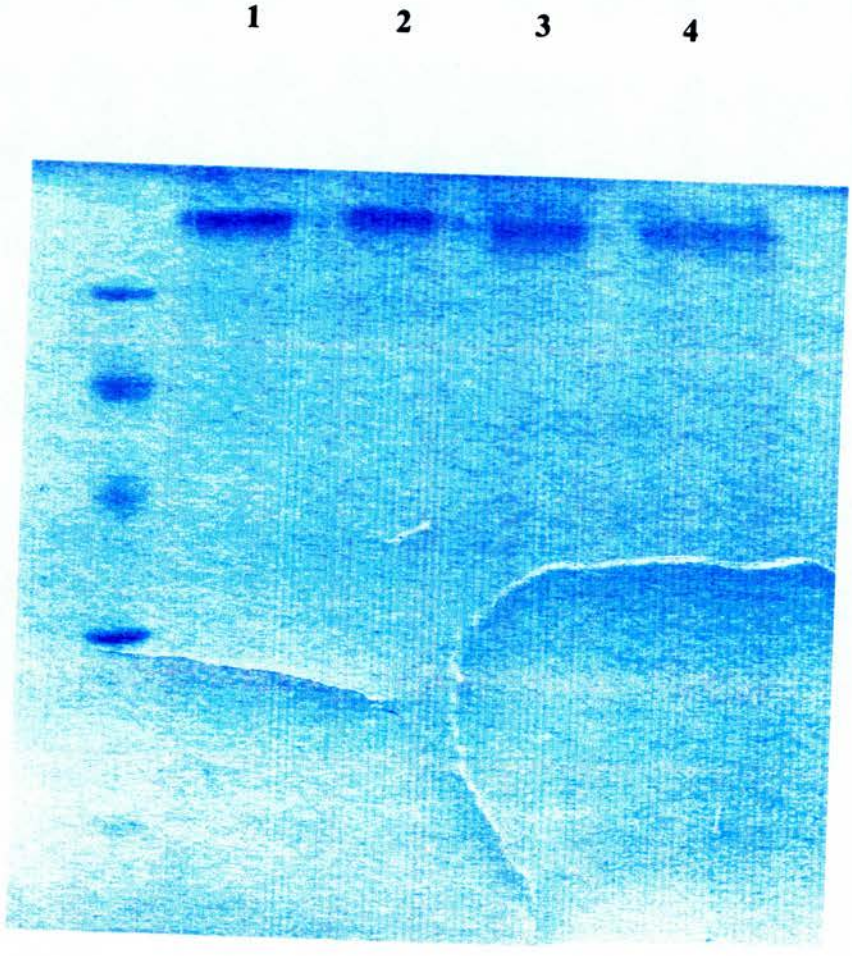

Figure 6.5
SDS-PAGE showing the results of cross-linking wild-type PGAM and S11A. The position of the tetramer is marked.
1. Wild type PGAM
2. Wild type PGAM incubated with 0.5mM 2,3-BPGA
3. S11A
4. S11A incubated with 0.5mM 2,3-BPGA

6.6 Kinetic data for A60S and S11A

The kinetic parameters of the mutase reaction (K_M^{3PGA}, K_M^{BPGA} and k_{cat}) were measured. Figure 6.6 shows Hanes plots for each and these show the characteristic pattern expected for a Ping-Pong mechanism. The table below shows the kinetic data derived from these graphs.

	K_M^{3PGA} μM	K_M^{BPGA} μM	k_{cat} s^{-1}
WT	470	3.2	530
A60S	430	7.2	370
S11A	710	30	20

Table 6.2
Kinetic constants for S11A and A60S.

The kinetic parameters for A60S are similar to those for the wild type. The K_M for 3-PGA is slightly lower, the K_M for 2,3-BPGA is aproximately doubled, and the k_{cat} is slightly decreased. S11A shows more significant differences to the wild type. Both K_M values are increased - for 3-PGA only slightly, but for 2,3-BPGA the difference is 10-fold. The k_{cat} is reduced 25-fold.

6.7 Stability of S11A

Mutant S11A is considerably more labile than the wild type enzyme. Wild type PGAM is stable for at least five days in 50mM Tris.HCl pH8.0 at 4°C (see figure 6.7). For longer term storage, the enzyme is kept in 80% saturated ammonium sulphate at 4°C. Under these conditions it is stable for at least one month. S11A loses activity rapidly under the same conditions. After 5 days at 4°C, 80% of activity is lost, and a doublet is seen on an SDS gel, indicating that some degree of degradation has occurred (figure not shown). In 80% saturated ammonium sulphate, S11A is stable for around 14 days at 4°C, and activity decreases slowly after this. The fractions exhibiting mutase activity that eluted from the QA52-cellulose column were collected and stored in 80% saturated ammonium sulphate. Small aliquots were

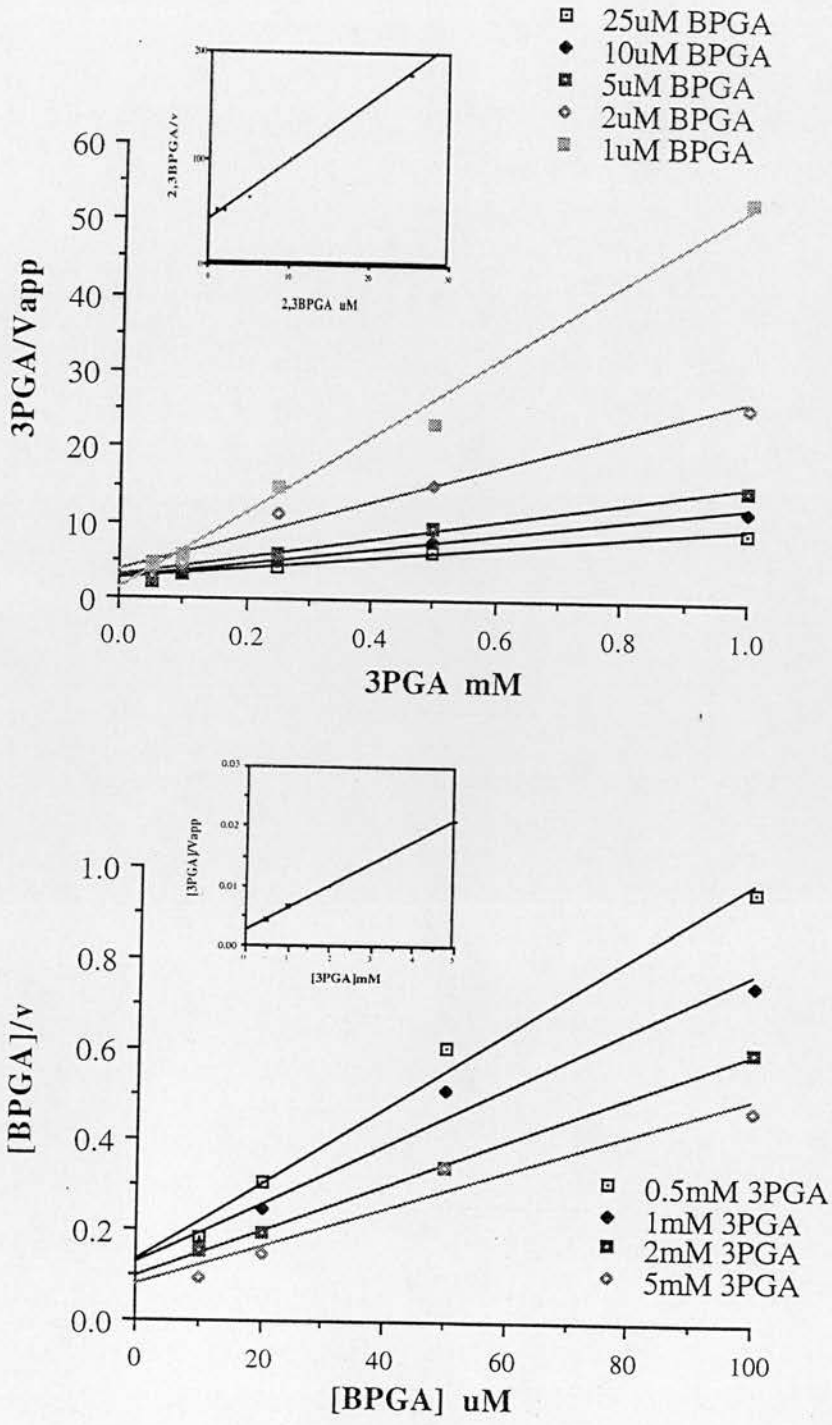

Figure 6.6

Hanes plots showing kinetic data obtained for A60S (A) and S11A (B). The pattern seen in the primary plots correspond to a ping-pong mechanism. The inset graphs are the secondary plots required for calculating the kinetic constants. Assays carried out as described in section 2.2.8.

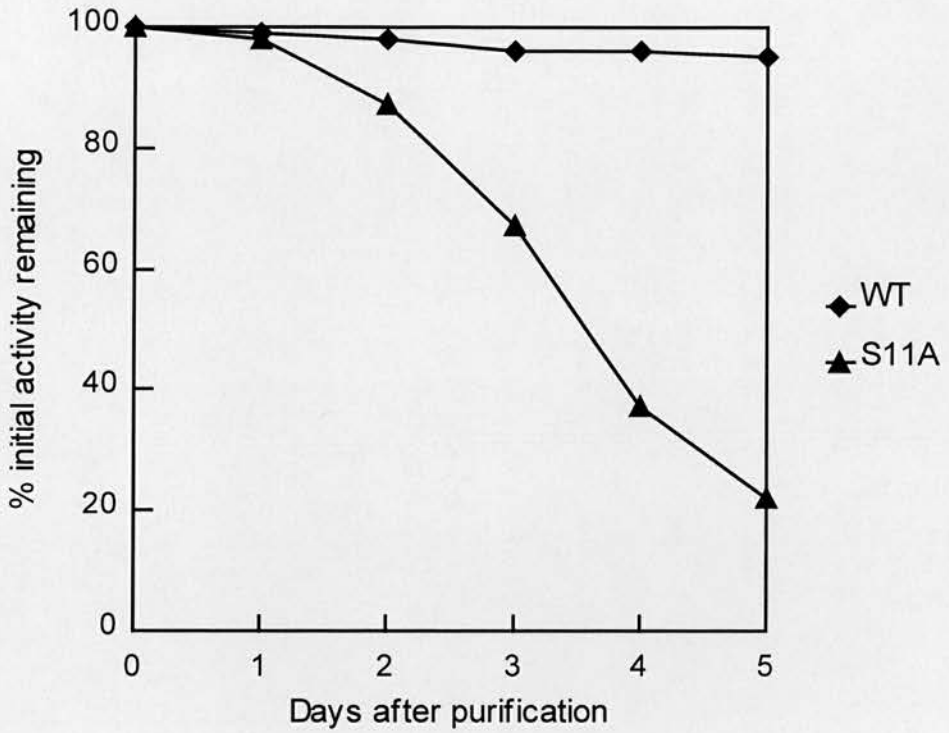

Figure 6.7
Graph showing the stability of wild type PGAM and S11A over time.
Storage conditions: 50mM Tris-HCl pH 8.0, 4°C.
Mutase activity was measured as described in Section 2.2.8, and expressed as a percentage of initial actvity, ie-activity immediately following purification on Day 0.

taken from this stock and further purified on the Superose gel filtration column as required for kinetic analysis.

6.8 Circular dichroism spectra.

The far uv spectra of the wild type and A60S and S11A mutants are shown in figure 6.8, and their near uv spectra in figure 6.9. There are some significant differences, particularly in the spectra of S11A, which imply that both the secondary and tertiary structures of this mutant differ from the wild type. This ties in with the results from the gel filtration column.

It has been demonstrated previously that the addition of 2,3BPGA to the wild type enzyme (which would lead to the phosphorylation of His 8 in the active site) does not have any effect on the far and near uv spectra, and therefore does not significantly affect the structure of the enzyme (White *et al.* 1993). Figures 6.10, 6.11 and 6.12 are the far uv spectra of wild type PGAM, A60S and S11A respectively, alone and incubated with 0.5mM BPGA (the concentration used in the standard mutase and phosphatase actvity assays). The spectra for both the mutants change when the BPGA is added, suggesting that the phosphorylation of the enzymes leads to a change in secondary structure. No such change was observed for the wild type enzyme.

6.9 The S11A/A60S mutant

6.9.1 Purification of S11A/A60S

This mutant was very unstable, and could not be purified to homogeneity using the methods previously described. After the overnight dialysis following the ammonium sulphate fractionation step, there was a considerable amount of precipitation in the dialysis tube. On testing the remaining soluble contents of the tube, it was found that 50% of the total protein content and 100% of mutase activity had been lost. It seems clear that the mutant enzyme denatures during the dialysis and comes out of the solution. The addition of glycerol (25% v/v) to the dialysis buffer

Figure 6.8

Far uv cd spectra of wild type PGAM, A60S and S11A.
Key to colours: Green - wild type PGAM, brown - A60S, blue - S11A.
Protein concentrations and path lengths: WT - 0.36mg/ml, 0.02cm, A60S - 0.47mg/ml, 0.02cm, S11A - 0.59mg/ml, 0.02cm

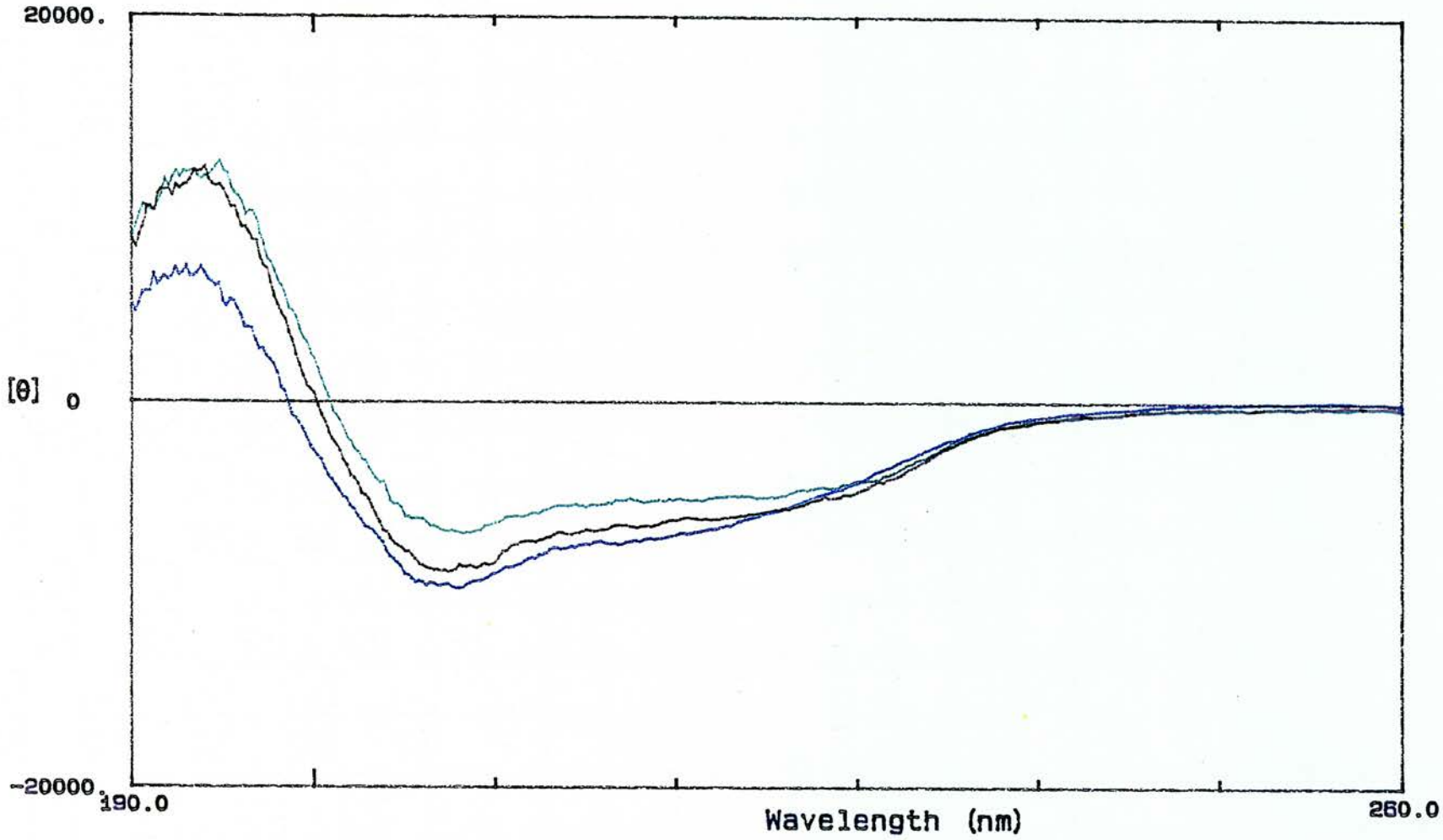
20000.
[θ]
0
-20000.
190.0
260.0
Wavelength (nm)

Figure 6.9
Near uv cd spectra of wild type PGAM, A60S and S11A.
Key to colours: Green - wild type PGAM, black - A60S, blue - S11A.
Protein concentrations and path lengths: WT - 0.36mg/ml, 0.5cm, A60S - 0.47mg/ml, 1cm, S11A - 0.59mg/ml, 1cm

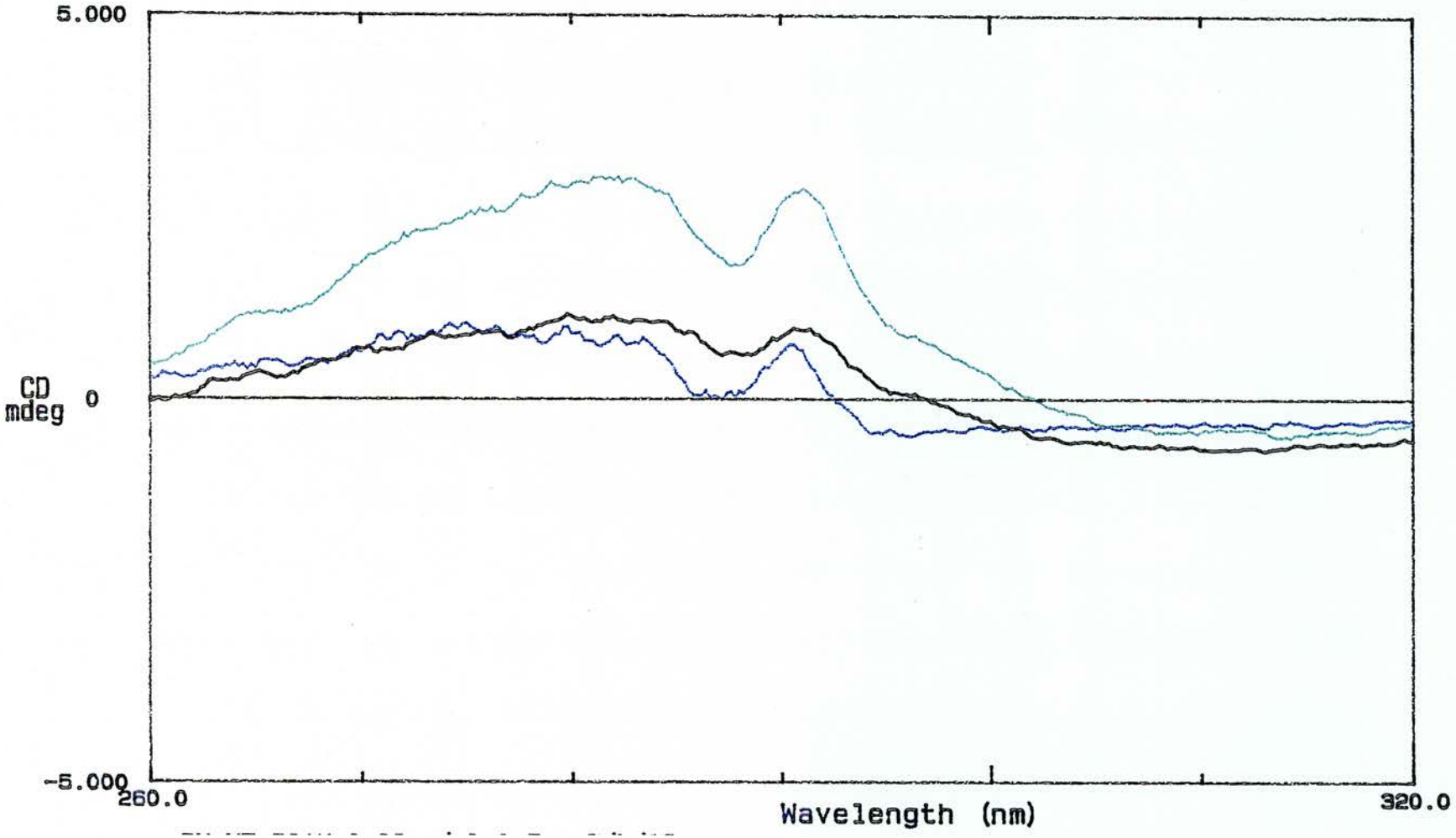
5.000
CD
mdeg
0
-5.000
260.0
320.0
Wavelength (nm)

Figure 6.10
Far uv cd spectrum of wild type PGAM incubated for five minutes with 0.5mM 2,3-BPGA. Protein concentration - 0.36mg/ml, path length - 0.02cm.
Key to colours: Green - without 2,3-BPGA, blue - with 2,3-BPGA

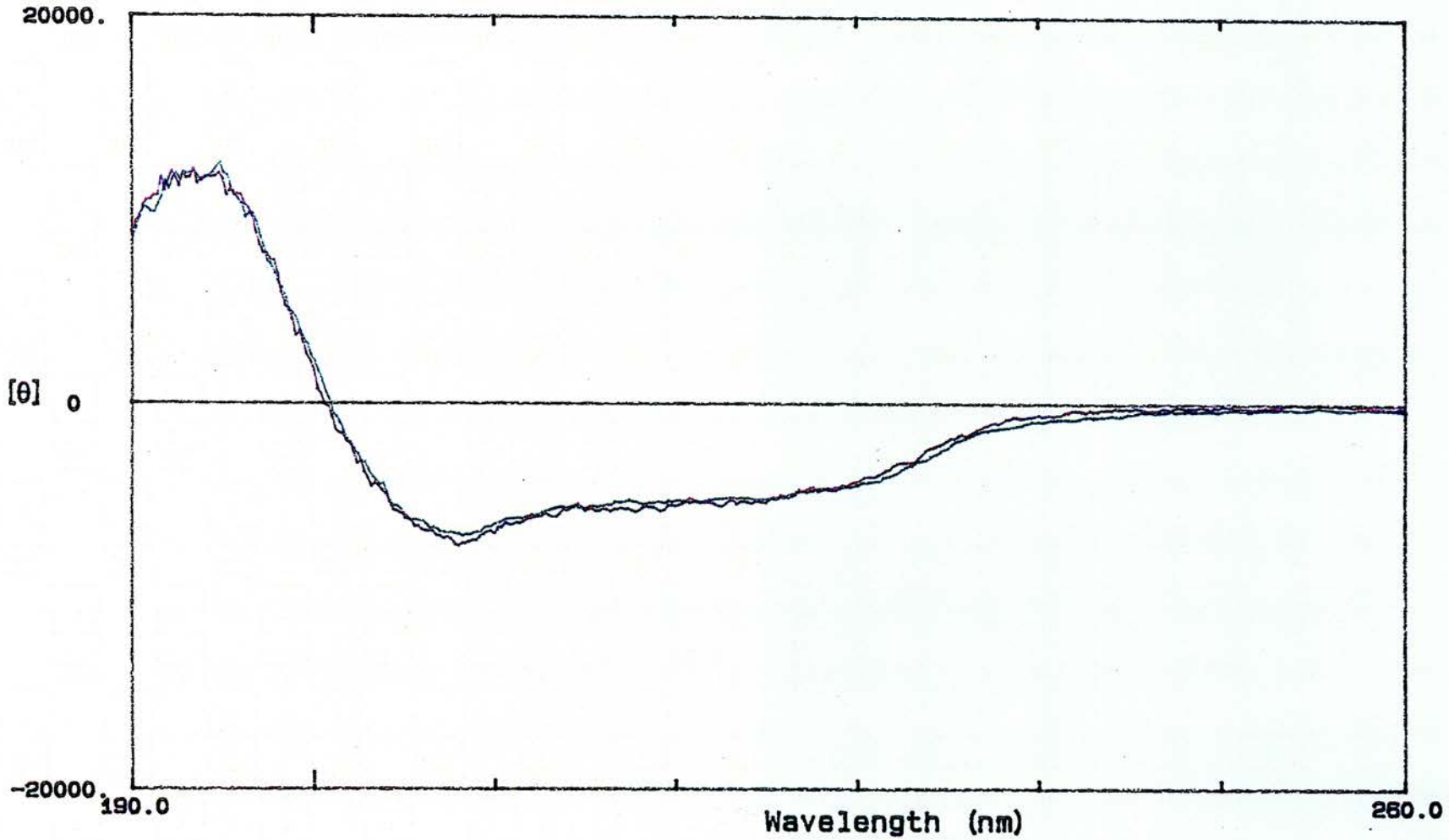
20000.
[θ]
0
-20000.
190.0
260.0
Wavelength (nm)

Figure 6.11
Far uv cd spectrum of A60S incubated for five minutes with 0.5mM 2,3-BPGA. Protein concentration - 0.47mg/ml, path length - 0.02cm.
Key to colours: Brown - without 2,3-BPGA, black - with 2,3-BPGA

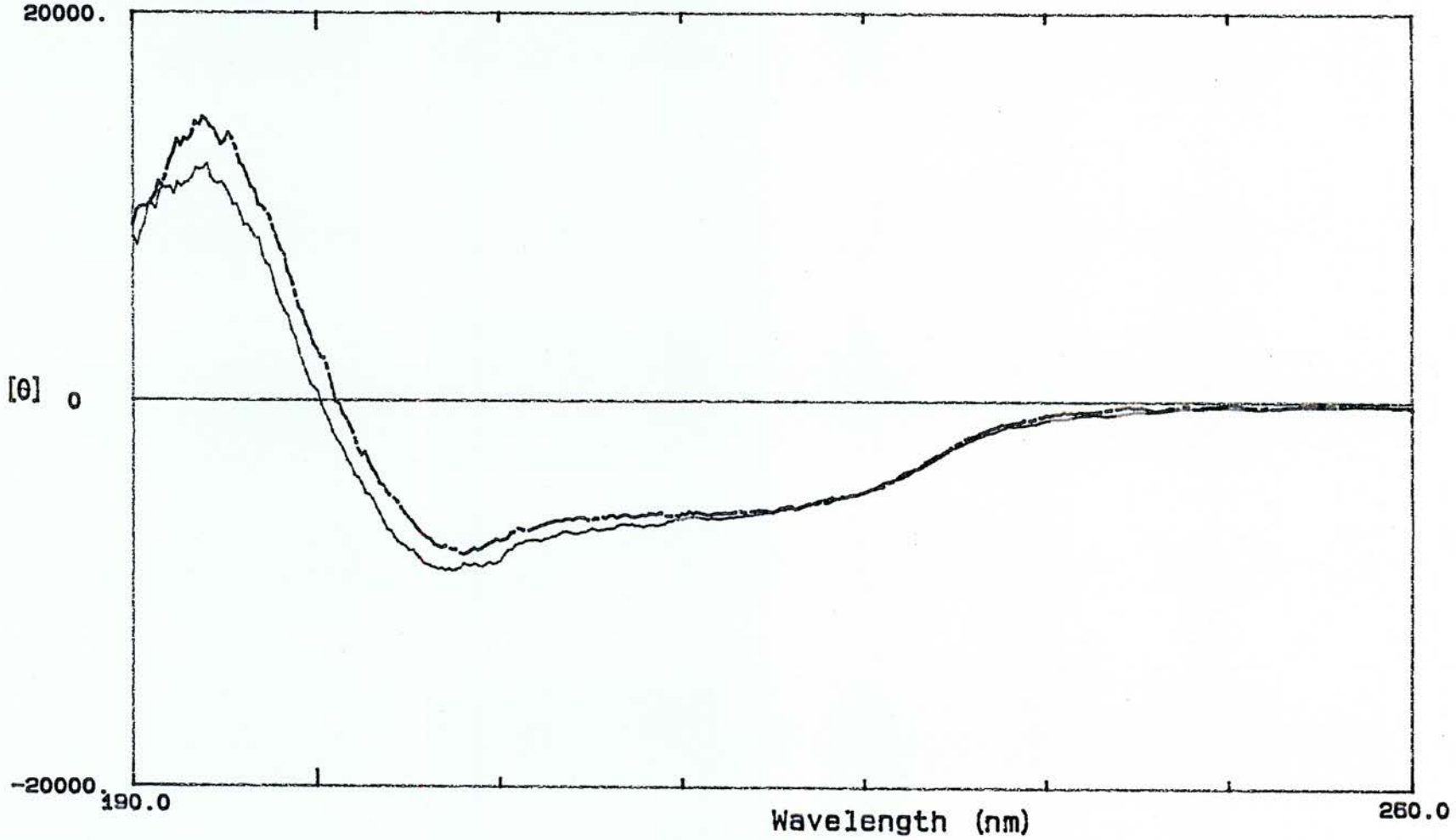
20000.
[θ]
0
-20000.
190.0
Wavelength (nm)
260.0

Figure 6.12
Far uv cd spectrum of S11A incubated for five minutes with 0.5mM 2,3-BPGA. Protein concentration - 0.59 mg/ml, path length - 0.02cm.
Key to colours: Blue - without 2,3-BPGA, orange - with 2,3-BPGA

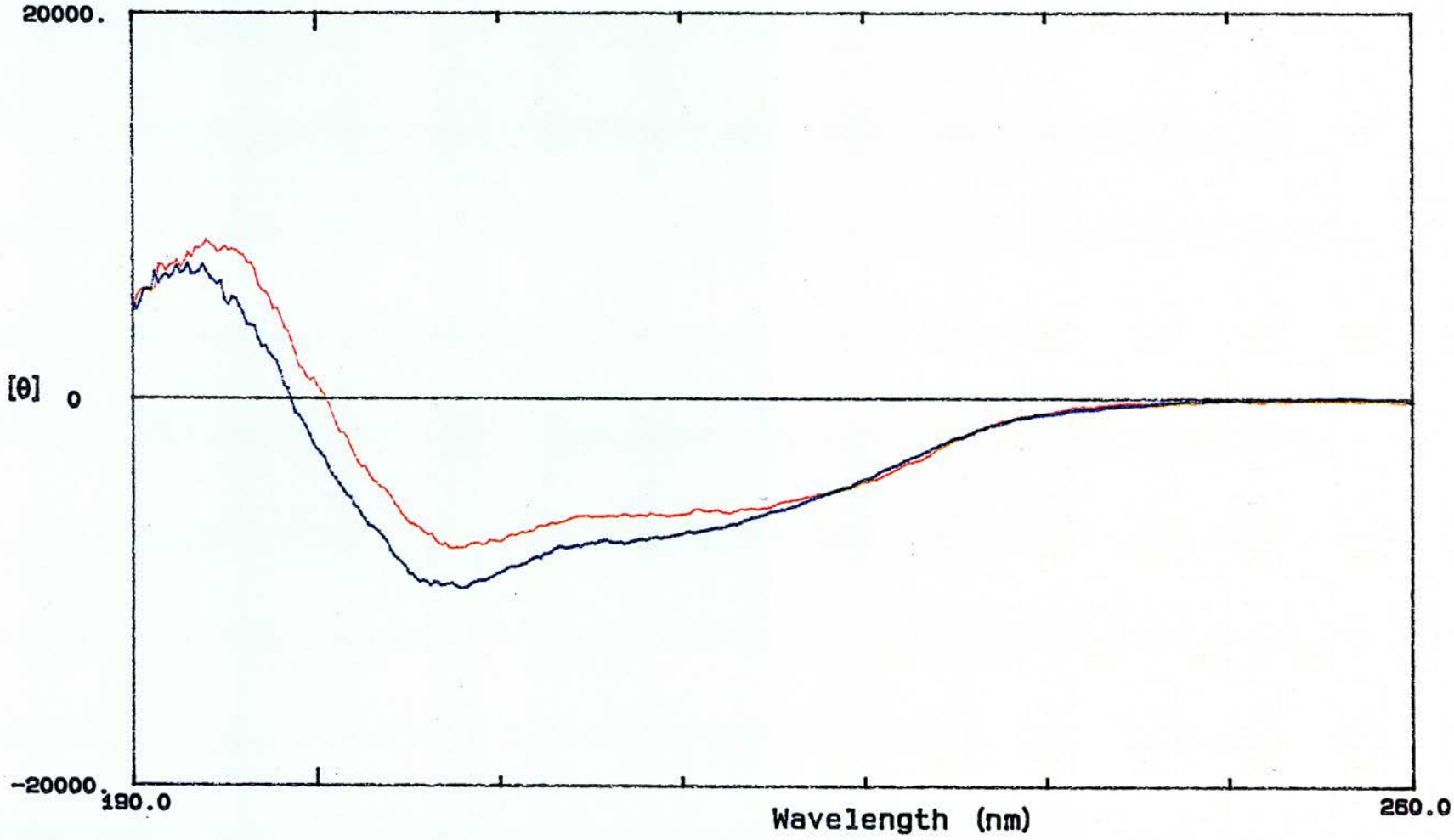
20000.
[θ]
0
-20000.
190.0
260.0
Wavelength (nm)

did not stop this denaturation. Shorter dialysis times were also tried, but the enzyme was found to denature within four hours. Polyethyleneimine (PEI) has been used to remove cell debris, lipids and nucleic acid from lysates of *S. cerevisiae* (Millburn et al., 1990). The lysate must first be clarified, either centrifugally or by the addition of borax. Addition of PEI at low concentrations (0.075% v/v) followed by centrifugation to remove the flocculated material gives a supernatant that is almost free of DNA, RNA and lipids. Millburn *et al.* also found that up to 30% of protein is removed, although the two soluble enzymes monitored in their trials were unaffected. Using PEI flocculation as the first stage in purification would remove the need for prolonged dialysis as the supernatant could be loaded directly onto the QA52-cellulose column. In the work described, 1.5% NaCl was added, although it was noted that this was probably not necessary due to the concentration of salt present in yeast homogenates. This could of course be a problem if the supernatant was loaded directly onto the ion exchange column, as it may affect the binding of the proteins to the matrix. However, the S11A mutant does not bind the matrix, and so we would not expect the double mutant to bind. The problem would be increased contamination from other proteins not binding.

The yeast expressing the double mutant was grown and lysed in the usual way, although the lysis buffer used was 30mM Tris-HCl pH8.0 containing 25% glycerol. The lysate was clarified by centrifugation (20 minutes, 2000g). An equal volume of 0.2% polyethyleneimine and 25% glycerol (pH adjusted to 8.0) was added and the mixture stirred for 30 minutes at 4°C. This gave final concentrations of 0.1% PEI and 15mM Tris-HCl. The flocculant was removed by centrifugation (20 minutes, 2000g), and the supernatant was loaded onto the QA52-cellulose column (equilibrated with 15mM Tris-HCl, 25% glycerol, pH 8.0 at 4°C), at a flow rate of 0.1ml/min. As expected, the protein with associated mutase activity did not bind to the column under these conditions, however a significant degree of purification is evident (figure 6.13). From SDS-PAGE, it is estimated that at least 80% of the protein that does not bind to the ion exchange column is the S11A/A60S mutant. However, the mutant was extremely unstable, and denatured within hours, even at

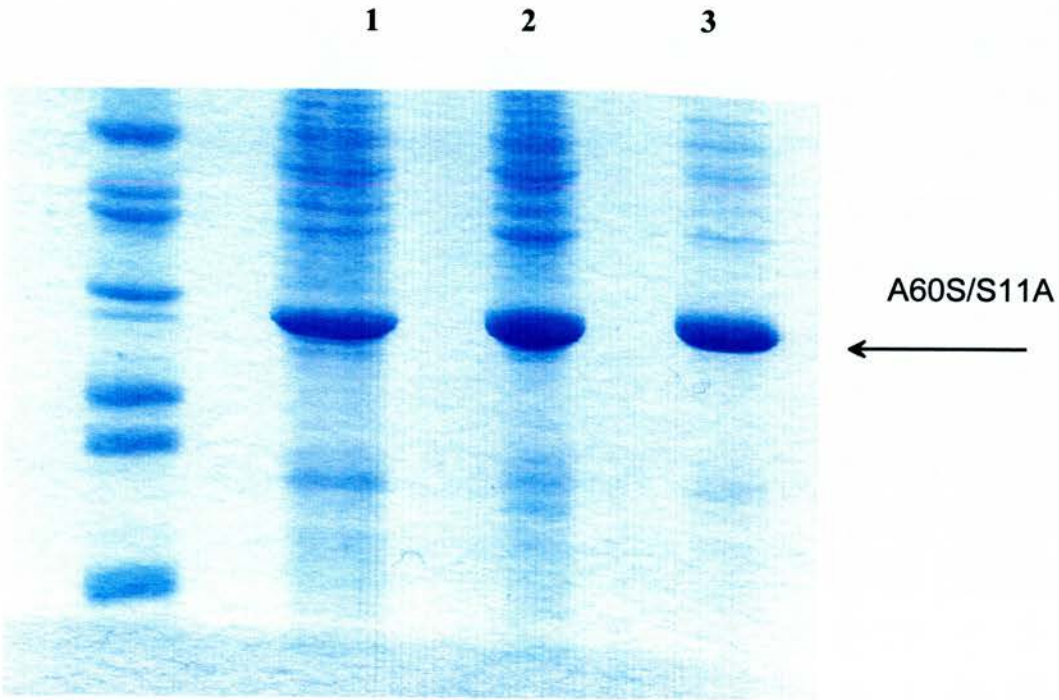

Figure 6.13
SDS-PAGE showing the partial purification of S11A/A60S.
1. Crude lysate of S150-2B GPM::HIS3 + pVT-S11A/A60S
2. Lysate after treatment with PEI
3.Partially purified S11A/A60S following ion exchange chromatography on the QA52- cellulose column.
The position of the S11AA60S subunit is shown.

4°C. Therefore it was not possible to further purify the mutant using the Superose 12 column, as the FPLC system operates at room temperature. The partially purified enzyme was used to give an indication of the level of the three activities exhibited by this mutant, but it was clear that it was too unstable to give further useful information.

6.9.2 Activities of S11A/A60S.

The mutase, synthase and phosphatase activities of the partially purified double mutant were measured as described in section 2.2.8. The protein concentration was determined using the dye-binding assay of Sedmak and Grossberg (1977). The generally more accurate spectrophotometric method (Edelhoch *et al.*, 1957) could not be used due to the presence of contaminating proteins. The specific activities were calculated, and modified to take into account the other proteins present which did not contribute to the activities. It was estimated that 80% of protein present was the S11A/A60S mutant, and so 80% of the measured protein concentration was used to calculate the modified specific activities. Both are given in the table below. The activities are expressed as μmol NADH oxidized min^{-1} mg^{-1}, and the modified values are given in brackets.

mutase	20 (23)
synthase	nd
phosphatase	nd

6.10 Discussion

The replacement of Ala60 with a serine residue reduced the mutase activity by approximately one-third, but had no noticeable effect on synthase or phosphatase activities. This mutation effectively adds another potential phospho ligand to the active site. Figure 6.1 shows that this would be situated close to one of the sulphates that is found bound in the active site of the 2.8Å structure (Winn et al., 1981). It is not in a position that would affect the phospho group bound to His8 in the phosphoenzyme, but it could be in a position to form an interaction with the phospho

group of a monophosphoglycerate, or the second phospho group of 2,3-BPGA. However, the K_M values for 3-PGA and 2,3-BPGA are not significantly affected by the substitution. K_M^{3PGA} is very slightly decreased, and K_M^{BPGA} is about twice the value for the wild type. The k_{cat} for the mutase reaction is reduced by about two thirds. The decreased binding efficiency of 2,3-BPGA could be responsible for the decreased catalytic efficiency. Alternatively, the 2.8Å structure (see section 1.8.2) shows that there is an intricate web of hydrogen bonds surrounding the two active site histidines which are likely to be responsible in maintaining these crucial residues in the correct orientation (Rigden *et al.*, 1997), and the introduction of another group into the active site may upset this. Part of the active site of this structure is shown in figure 6.15, showing the revised positions of Ser11 and Ala60. From the position of Ala60, the second explanation appears more likely to be correct.

The Ser11 to alanine mutation has a more profound effect. The K_M for 2,3-BPGA in particular is increased 10-fold, and the k_{cat} is reduced 25-fold. The K_M for 3-PGA is less affected, only 1.5-fold higher than that of the wild type enzyme. These are the results that would be expected due to the position of Ser11 in the active site. It is thought to provide a ligand for the phopsho group that is transferred to His8 to form the phospho enzyme, and so would affect the binding of the bisphosphoglycerate substrate more than the monophosphoglycerates, the phospho groups of which would be in the other phospho group binding postition (interacting with the helix dipole, see section 1.9.2). The results obtained with the S11A mutant are in agreement with the corresponding mutant of human bisphosphoglycerate mutase, G13S (Garel et al., 1994). This mutant shows an increased mutase activity and a decreased K_M for 2,3-BPGA, while the synthase activity and the K_M for 3-PGA are not significantly altered by the substitution.

The position of Ser11 also suggests a role in the stabilization of the phospho enzyme. It has been suggested that the low level of phosphatase activity is due to the non-productive transfer of the phospho group from the phospho enzyme to water. This activity is enhanced by the addition of the substrate analogue 2-phosphoglycollate. This is thought to stimulate the phosphatase activity by binding in the active site and mimicking the monophosphoglycerate substrate which accepts

the phospho group in the mutase reaction. 2-phosphoglycollate cannot accept the group, but facilitates its transfer to water. The phosphorylated form of bisphosphoglycerate mutase is more unstable than that of monophosphoglycerate mutases (Rose, 1980), which would correspond to the lack of this extra phospho ligand in the former. The G13S mutant of human red cell bisphosphoglycerate mutase has a decreased phosphatase activity, which would be the expected result of adding this phospho ligand. However, in the S11A mutant the phosphatase activity is completely abolished. The enhanced phosphatase activity in the presence of 2-phosphoglycollate is also absent in this mutant. It is considerably reduced in the A60S mutant (from 18-fold in the wild type to 3-fold), and so this residue is implicated in the binding of this acceptor analogue.

It is possible that the differences in activity and binding efficiency between the wild type and mutant enzymes are not due to a single residue substitution. When the circular dichroism (cd) spectra of the wild type and mutants are compared (both near and far uv), it is clear that there are some differences, particularly with S11A, which correspond to differences in the secondary and tertiary structure of the proteins. A change in the structure of this mutant is also suggested by its failure to bind to the ion exchange column. Ser11 is implicated in the intricate web of hydrogen bonds that are found around the two active site histidines, and it is possible that the replacement of this residue leads to the loss of stablizing contacts. It has been shown in previous site-directed mutagenesis studies that the replacement of one of the active site histidines (His181) led to the destabilization of the enzyme (White *et al.*, 1993). With this mutant (H181A), the binding of 2,3-BPGA and subsequent phosphorylation of the enzyme led to changes in the conformation of the protein, and dissociation of the tetramer. With S11A, the tetramer remains intact, as shown by the cross-linking studies described in Section 6.4 (see figure 6.5), but there are changes to the protein conformation, as shown by cd spectra (figures 6.10-6.12). The conformation of the wild type enzyme is unaffected by phosphorylation.

These results underline the need for caution in interpreting the results of site-directed mutagenesis studies. It is very tempting to attribute differences in activity and binding efficiency to the addition or removal of a functional group from

the enzyme. It is important however to ensure that this is indeed the only change to take place when an amino acid substitution is made. Groups that are involved in the binding of substrates or in some other way involved with the reaction mechanism may also be involved in structurally important contacts in the native enzyme. If this is the case, the replacement of these residues may affect the binding of substrates and turnover of the enzyme in more ways than by, for example, the loss of a single ligand.

Chapter Seven

The Role of Glu86

7.1 Introduction

The residue Glu327 is conserved in the cofactor-dependent phosphoglycerate mutases and the C-terminal phosphatase domain of the bifunctional enzyme 6-phosphofructo-2-kinase/fructose-2,6-bisphosphatase (Fru-2,6-BPase), see Figures 1.4 and 1.13. Site-directed mutagenesis studies have suggested a role for this residue in catalysis. One of the key features of the active site of the histidine phosphatase family of enzymes, which includes the cofactor-dependent phosphoglycerate mutases, rat prostatic acid phosphatase (RPAP) and Fru-2,6-BPase is a pair of histidine residues. In the the 2.8 Å structure of PGAM from *S. cerevisiae* (where they are numbered His8 and His181, they appeared to adopt a parallel or "clapping hands" formation, about 4Å apart. In the new higher resolution structure (Rigden *et al.*, 1997), they are no longer parallel, but in a conformation closer to that seen in the related enzymes RPAP and Fru-2,6-P_2ase, which could be related to the different crystallization conditions.

Only His8 (and the corresponding His residue in other mutases) has been shown to be phosphorylated (Fothergill and Harkins, 1982, Haggarty and Fothergill, 1980, Han and Rose, 1979, Hass *et al.*, 1980). A role for the second His in phospho transfer has been proposed by Rose (1980), who suggested that this residue donates a proton to the leaving group. In the unligated enzyme therefore, His181 would be in the positively charged, protonated state. The phosphorylation of the Fru-2,6-P_2ase domain of rat liver 6-phosphofructo-2-kinase/ fructose-2,6-bisphosphatase is thought to proceed in a similar fashion, with the nucleophilic attack of one active site His (His258) at the phospho group of the substrate leading to the formation of the phosphoenzyme, with proton donation from the other His (His392) to the leaving group. Site-directed mutagenesis studies on this enzyme have suggested a role in catalysis for another active site residue, Glu327, which is conserved in the cofactor-dependent phosphoglycerate mutases (Lin *et al.*, 1992).

The replacement of this residue with an alanine or a glutamine reduced the phosphatase activity to 4% and 2% of the wild type activity respectively. When aspartate was introduced in place of glutamate, activity was reduced by 20%. The

rate of formation of the phosphoenzyme intermediate was drastically decreased in each of the mutants, by a factor of at least 1000. The K_M values for the substrate fructose-2,6-bisphosphate were not significantly affected. These results suggest that Glu327 plays a crucial role in the catalysis of the phosphatase reaction due to involvement in the formation of the phosphoenzyme. It is proposed that the negatively charged carboxylate group of the residue maintains the protonated state of His392. The small effect on the K_M of the substrate implies that the major role of this residue is in catalysis, and not in the binding of the substrate and/or product. It is also implicated in the hydrolysis of the phosphoenzyme. The rate constants for the hydrolysis for Glu to Ala and Glu to Gln mutants are 2.7% and 1.3%, respectively, of the wild type, while that for the Glu to Asp mutant is 60% of the wild type. Glu327 may act as a base catalyst by forming an OH^- ion from a water molecule, which then breaks down the phosphoenzyme by nucleophilic attack (Lee *et al.*, 1996). The Asp residue also has a carboxylate group, but this is shorter and is in a different orientation. It appears that the correct orientation of the carboxylate is more important in the formation of the phosphoenzyme (i.e. in the protonation of His392) than its hydrolysis.

This Glu residue is also conserved in the cofactor-dependent PGAMs (in *S. cerevisiae* PGAM the corresponding residue is Glu86), and it is possible that it plays an analogous role in the formation of the phosphoenzyme in the mutase reaction. The replacement of the glutamate with a glutamine should not significantly affect the structure of the enzyme, as a glutamate and a glutamine would be expected to occupy a similar space, and glutamine is able to form hydrogen bonds in a similar manner to glutamate. Therefore the only change should be the removal of the negatively charged carboxyl group.

The vector pVT-E86Q was constructed as part of an Honours project by four students (Eve Laird, Elizabeth Lovejoy, Kim Midwood and Sue Webber) using the Kunkel method as described in Section 2.2.16. The mutant enzyme has subsequently been expressed in the gpm-deleted strain of *S. cerevisiae,* purified to homogeneity and the kinetic parameters determined.

7.2 Expression of E86Q

The vector pVT-E86Q was used to transform S150-2B GPM::HIS3 using the method described in Section 2.2.3. The gpm-deleted strain must be grown using a non-fermentable carbon source (in this case glycerol and ethanol), as the glycolytic pathway cannot function due to the absence of PGAM. This does create a difficulty for transformation, as yeast grows only very slowly in this medium (S150-2B growing in YEPD, with glucose as the carbon source has a doubling time of around five hours, whereas the doubling time of S150-2B GPM::HIS3 growing in YEPGE, with glycerol and ethanol as carbon sources is around fourteen hours). It therefore takes a considerable time for the yeast to reach the required optical density. Using standard methods, no transformants were obtained. The addition of carrier DNA (sonicated herring sperm DNA) did not improve the yield. A modified version of the method of Geitz *et al.* (1992) was found to give an improved transformation efficiency. This method eliminates the incubation of cells with lithium acetate solution prior to the addition of DNA, and also involves a considerably extended heat shock, at 15 minutes rather than the usual two. The transformed cells were then grown in 3 ml of the non-selective YEPGE overnight, before being plated out and incubated at 30°C. The usual medium for plating out the cells was YOD ura$^-$ (see Section 2.2.2) which is doubly selective: the absence of uracil selects for the presence of the URA3 gene on the phagemid, and the use of glucose as a carbon source selects for the presence of the GPM gene. However, the mutase activity of the E86Q mutant was expected to be much reduced and may be absent altogether, so half of each overnight culture was plated out onto YOD ura$^-$, and half onto YOGE ura$^-$, which still selects for the phagemid but does not require an active mutase. Colonies appeared after 14 days on the YOD ura$^-$ plates, and after 21 days on the YOGE ura$^-$ plates. This shows that at least some mutase activity is retained by the E86Q mutant. SDS-PAGE shows that, similar to the other mutants, E86Q is expressed at a high level, and constitutes around 30% of the total cell protein (see Figure 7.1).

The growth curves for wild type and E86Q PGAM in YEPD are shown in Figure 7.2. The logarithmic phase of growth is considerably slower in the mutant,

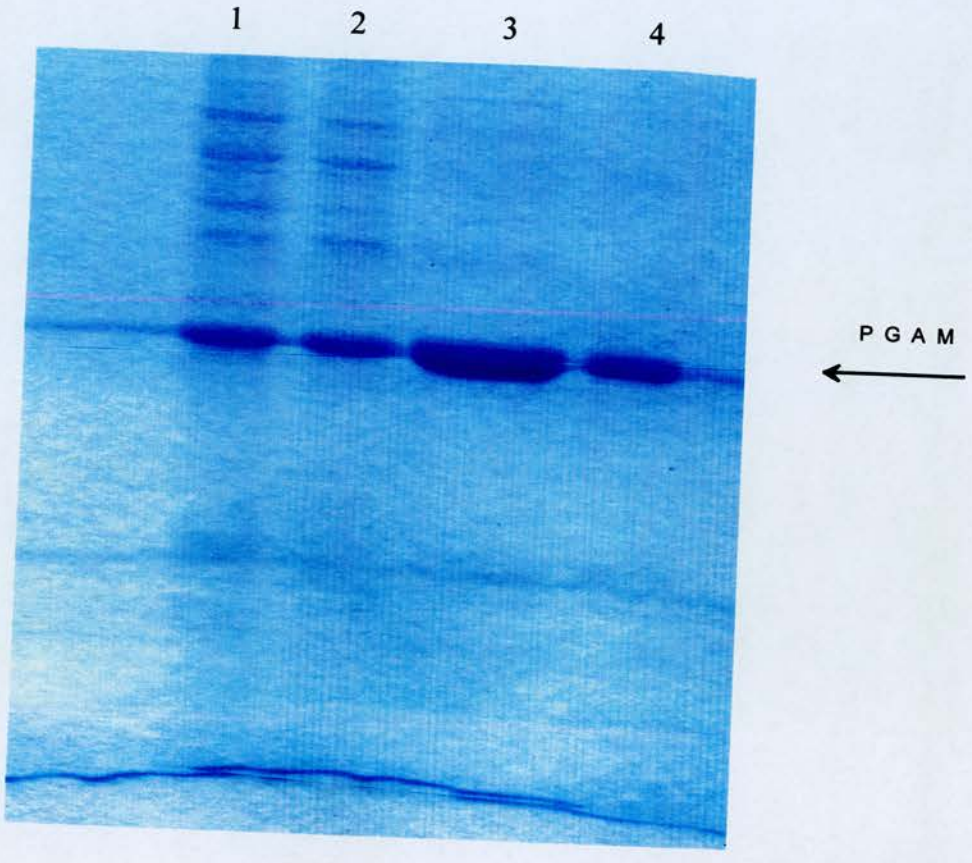

Figure 7.1

SDS-PAGE showing the purification of E86Q. The position of the PGAM subunit is indicated.

Lane	1	Crude cell lysate
	2	After ammonium sulphate fractionation.
	3	After ion exchange chromatography (QA52-cellulose)
	4	After gel filtration (Superose 12)

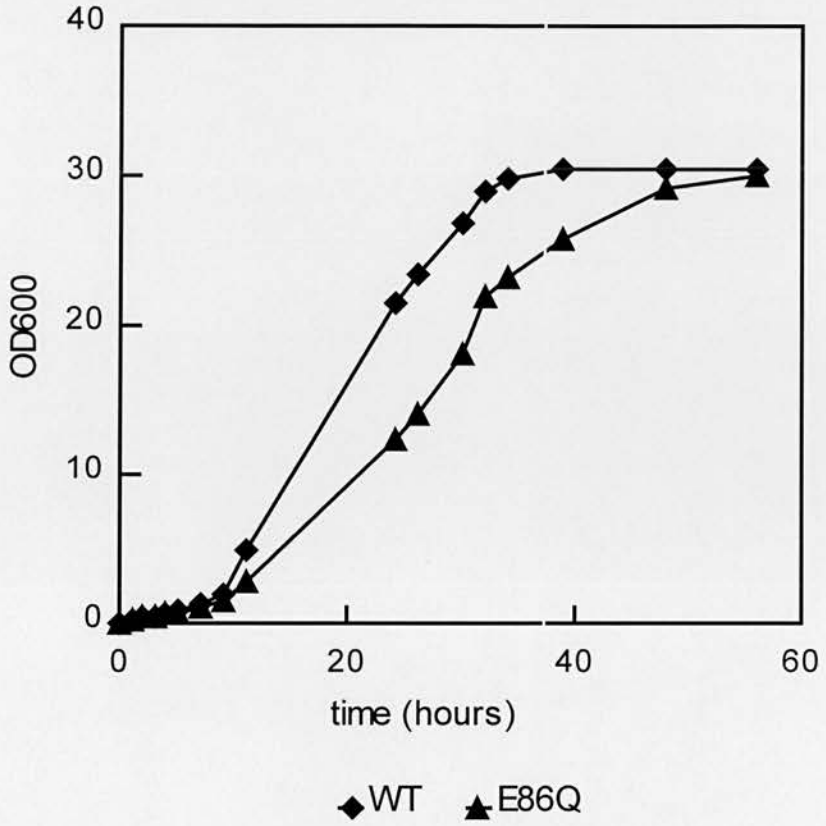

Figure 7.2
Growth curves for S150-2B GPM::HIS3 expressing wild type or E86Q PGAM.
An overnight culture of each was used to innoculate 500ml YEPD (section 2.2.2.1) to 0.1 OD_{600}. This was then incubated (with shaking) at 30°C, and small samples taken at intervals to determine optical density. Each point represents the mean value obtained from three cultures.

which has a doubling time of about ten hours. The mutase activity present in a crude lysate of S150-2B (the parental strain expressing the single chromosomal copy of the GPM gene) is about 10 EU/mg (where one EU is defined as 1μmol NADH oxidized /min/mg of protein). This is increased to around 350 EU/mg with S150-2B GPM::HIS3 transformed with pVT-gpm and expressing the wild type mutase. However, the cells expressing the E86Q mutant show a mutase activity of less than 2 EU/mg. This is only one-fifth of the activity found in "normal" cells, i.e. those expressing a single gene copy, and could lead to a decrease in glycolytic flux, with a build up of metabolites at phosphoglycerate mutase, and therefore a decreased growth rate.

7.3 Purification of E86Q

The E86Q mutant was purified to homogeneity using the method described in Section 2.2.5, and no modifications to the standard procedure were required. The mutant protein displayed similar behaviour to the wild type enzyme on the QA52-cellulose ion exchange column, and eluted in the same fraction from the Superose 12 size exclusion column. This mutation is therefore unlikely to have caused the same disruption to the structure as the replacement of another active site residue, Ser11 (Chapter Six). The SDS-PAGE characterization of fractions from the purification of E86Q is shown in Figure 7.1.

7.4 Specific Activities

The mutase, synthase and phosphatase activities of the E86Q mutant PGAM were assayed as described in Section 2.2.8. The results are shown in the table below, with the specific activities of the wild type enzyme for comparison.

	E86Q	WT
mutase	6.1	970
synthase	0.01	0.01
phosphatase	nd	0.02
phosphatase +0.2mM 2-PG	nd	0.35

Table 7.1
Specific activities of wild type and E86Q PGAM. All values are determined from three different experiments and given as means with less than 5% standard error. Results are expressed as enzyme units (EU), where one EU represents 1μmol NADH oxidized / min / mg of enzyme, and nd means not detectable under the assay conditions.

7.5 Kinetic Data

The K_m values for 3-PGA and 2,3-BPGA in the mutase reaction were determined for the mutant. The Hanes plot is shown in Figures 7.3. It shows ping-pong kinetics as described for the wild type. The kinetic data are shown in the table below, with those of the wild type enzyme for comparison.

	K_M^{3PGA} (μM)	K_M^{BPGA} (μM)	k_{cat} (s^{-1})
E86Q	1,110	8.1	4.7
WT	470	3.2	530

Table 7.2
The kinetic constants for wild type and E86Q PGAM.

7.6 Discussion

The results obtained with the E86Q mutant are consistent with a role for this residue analogous to that suggested for the corresponding residue in the bisphosphatase domain of the bifunctional enzyme 6-phosphofructo-2-kinase/ fructose-2,6-bisphosphatase (Fru-2,6-P2ase). The mutase activity of the enzyme is

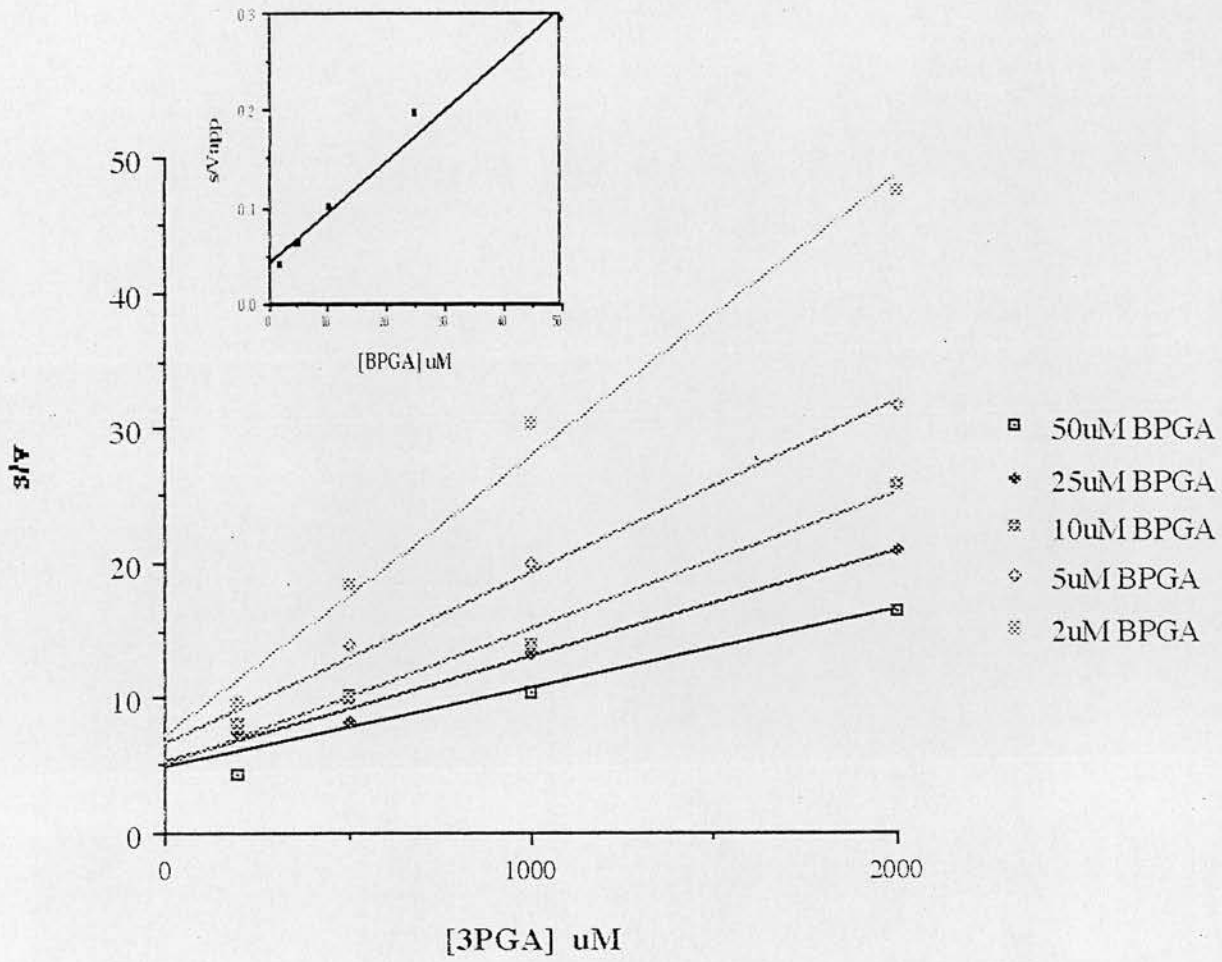

Figure 7.3
Hanes plot showing kinetic data obtained for E86Q PGAM. The pattern seen in the primary plot corresponds to a ping-pong mechanism. The inset graph is the secondary plot required for calculating the kinetic constants. Assays carried out as described in section 2.2.9.

considerably reduced (over 150-fold), and the phosphatase activity is abolished. The binding of the substrates, reflected in the K_M values, is considerably less affected than the turnover or catalytic efficiency - the k_{cat} is reduced over 100-fold, while the K_M values for each substrate are increased only two-fold. It appears therefore that this residue affects mutase and phosphatase activity by affecting catalysis, rather than by involvement in the binding of the substrates.

In the higher resolution structure of *S. cerevisiae* PGAM determined recently (Rigden *et al.*, 1997), Glu86 is 4.5Å from the ND1 atom of His181. This distance would be too far to exert influence over the protonation state of this residue. However, the enzyme was crystallized at pH8.65, and His 181 is very unlikely to be protonated at this high pH. At the pH optimum of 7.0, the pH at which mutase activity is assayed, the residue may be protonated, and this may induce the glutamate to move closer. The position of key active site residues in the 2.3Å structure is shown in figure 7.4.

The synthase activity aapears to be much less affected by the replacement of the glutamate than the mutase or phosphatase activities (although as described previously, the low levels of phosphatase and synthase activities does present difficulties in accurate analysis of changes). This is also consistent with the role suggested for the residue in phospho transfer. As described in Section 7.1, the first step of both the mutase and phosphatase activities is the binding of 2,3-BPGA to the active site, and the transfer of a phospho group to His8. Efficient phospho transfer requires a proton to be donated, probably from His181, which would therefore need to be in the protonated state in the unbound enzyme. The first step in the synthase reaction, on the other hand, involves the binding of 1,3-BPGA, and the transfer of an acyl phosphate. This does not require the donation of a proton, and is therefore not dependent on the protonation state of His181. It is likely therefore that the replacement of a residue which affects the protonation state of His181 would have a greater effect on the mutase and phosphatase activties than the synthase activity, and this is seen. The residue is conserved in the bisphosphoglycerate mutases (see figure 1.4), as would be expected in view of their significant levels of mutase and phosphatase activities. However, it is not conserved in the third member of the

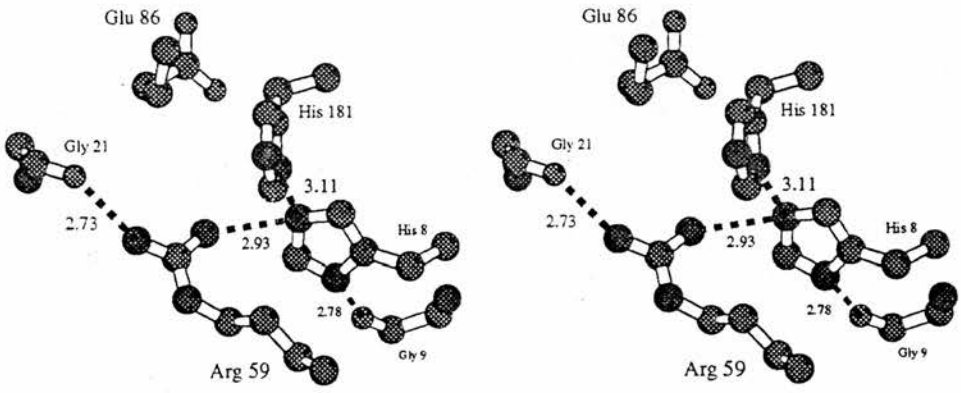

Figure 7.4

Stereo diagram of the active site of *S. cerevisiae* PGAM (from the recent high resolution structure, Rigden *et al.*, 1997) showing residues thought to be involved in the reaction mechanism.

histidine phosphatase family previously described - the acid phosphatases. Only three out of the five known acid phosphatases have the corresponding residue conserved. However, recent studies on this enzyme suggest a mechanism that differs from that of the phosphoglycerate mutases and F-2,6BPase. It is suggested by Lindqvist *et al.* (1994) that the proton for phospho transfer is donated not by the second active site histidine but by an aspartic acid, based both on the proximity and orientation of the residues and the low pH optimum of the acid phosphatases. The histidine is implicated in phosphate binding.

References

Bartrons, R. & Carreras, J., (1982) *Biochim. Biophys. Acta.* **708**, 167-177.

Bazan, F., Fletterick, R. & Pilkis, S.J., (1989) *Proc. Nat. Acad. Sci.* **86**, 9642-9646.

Benesch, R., Benesch, R.E. & Yu, C.I., (1968). *Proc. Nat. Acad. Sci.* **59**, 526-532.

Bordo, D. & Argos, P. , (1991) **217**, 721-729.

Botha, F.C. & Dennis, D.T., (1986) *Arch. Biochem. Biophys.* **245**, 96-103.

Breathnach, R. & Knowles, J.R., (1977) *Biochemistry* **16**, 3054-3060.

Brewer, G.J. & Eaton, J.W., (1971). *Science*. **171**, 1205-1211.

Britton, H.G., Carreras, J. & Grisolia, S., (1972*a*) *Biochemistry*. **11**, 3008-3014.

Britton, H.G., Carreras, J. & Grisolia, S., (1972*b*) *Biochim. Biophys. Acta* **289,** 311-322.

Britton, H.G. & Clarke, J.B. (1972) *Biochem. J.* **130,** 397-410.

Budgen, N. & Danson, M.J. (1986)

Campbell, J. W., Watson, H. C. & Hodgson, G. I. (1974) *Nature*, **250**, 301-303.

Carreras, J. & Bartrons, R. (1980) *Biochem. Biophys. Res. Commun.*, **96**, 1267-1273.

Carreras, J., Climent, F., Bartrons, R and Pons, G. (1982) *Biochim. Biophys. Acta*, **705**, 238-242.

Carreras, J., Mezquita, J., Bosch, J., Bartrons, R. & Pons, G. (1982). *Comp. Biochem. Physiol.* **7113**, 591-597.

Cascales, M. & Grisolia, S. (1966) *Biochemistry.* **5**, 3116-3122.

Castella-Escola, J., Montoliu, L., Pons, G., Puigdomenech, P., Cohen-Solal, M., Carreras, J., Rigau, J. and Climent, F. (1989) *Biochem. Biophys. Res. Commun.*, **165**, 1345-1351.

Castella-Escola, J., Urena, J., Alterio, J., Carreras, J., Martelly, I. and Climent, F. (1990). *FEBS Lett.* **268**, 24-26.

Chan, W.W.-C. (1995) *Biochem. J.* **311**, 981-985.

Cherfils, J., Rosa, R., Garel, M.C., Calvin, M.C., Rosa, J. & Janin, J. (1991) *J. Mol. Biol.* **218**, 269-270.

Chiba, H., Ikura, K., Sasaki, R., Sugimoto, E. & Saimoyoji, H. (1974) *J. Biochem.* **76,** 91-97.

Chiba, H., Sugimoto, E., Sasaki, R. & Hirose, M. (1970) *Agric. Biol. Chem.* **34**, 498-505.

Cornish-Bowden, A. Fundamentals of Enzyme Kinetics. Butterworth & Co. (Publishers) Ltd.

Cowgill, R.W. & Pizer, L.I. (1956) *J. Biol. Chem.* **223,** 885-895.

D'Alessio, G., & Josse, J. (1971) *J. Biol.Chem.* **246,** 4319-4325.

De Rosa, M., Gambacorta, A., Nicolaus, B., Giardina, P., Poerio, E. & Buonocorte, V. (1984) *Biochem J.* **224**, 407-414.

Edelhoch, H., Rodwell, V.W. and Grisolia, S. (1957). *J. Biol.Chem.* **228**, 891-903.

Fothergill, L.A. & Harkins, R.N. (1982) *Proc. R. Soc. Lond.* B **215**, 19-44.

Fothergill-Gilmore, L.A. & Michels, P.A.M. (1993) *Prog. Biophys. molec. Biol.* **59**, 105-235.

Fothergill-Gilmore, L.A. & Watson, H.C. (1989) *Adv. Enzymol.* **62**, 227-313.

Fundele, R., Bucher, T., Gropp, A., & Winkling, H. (1981) *Dev. Genet.*, **2**, 291-303.

Garel, M.-C., Arous, N., Calvin, M.-C., Craescu, C. T., Rosa, J. & Rosa, R. (1994). *Proc. Natl. Acad. Sci. USA,* **91**, 3593-3597.

Garel, M.-C., Joulin, V., LeBoulch, P., Calvin, M.-C., Prehu, M.-O., Arous, N., Longin, R, Rosa, R., Rosa, J. & Cohen-Solal, M. (1989). *J. Biol. Chem.* **264**, 18966-18972.

Garel, M.-C., LeMarchandel, V., Calvin, M.-C., Arous, N., Craescu, C. T., Prehu, M.-O., Rosa, J. & Rosa, R. (1993) *Eur. J. Biochem..* **213,** 493-500.

Geitz, D., St. Jean, A., Woods, R.A.& Shiestl, R.H. (1992) *Nuc. Ac. Res.* **20**, 1425.

Girg, R., Rudolph, R. & Jaenicke, R. (1981) *Eur. J. Biochem.* **119**, 301-305.

Grana, X., Delecea, L., Elmaghrabi, M.R., Urena, J.M., Caellas, C., Carreras, J., Puigdomenech, P., Pilkis, S.J. & Climent, F. (1992). *J. Biol. Chem.* **267**, 12797-12803.

Grisolia, S. and Cleland, W.W. (1968) *Biochemistry,* **7**, 1115-1121.

Grisolia, S. & Joyce, B. K. (1959) *J. Biol. Chem.* **234**, 1335-1337.

Haggarty, N.W., Dunbar, B & Fothergill, L.A. (1983) *EMBO. J.* **2**, 1213-1230.

Haggarty, N.W. & Fothergill, L.A. (1980) *FEBS Lett.* **109**, 18-20.

Han, C.H. & Rose, Z.B. (1979) *J. Biol. Chem.* **254**, 8836-8840.

Harkness, D. R., Ponce, J. & Grayson, V. (1969) *Comp. Biochem. Physiol.*, **28**, 129-138.

Hass, L.F., Place, A.R., Miller, K.B. & Powers, D.A. (1980) *Biochem. Biophys. Res. Comm.* **95**, 1570-1576.

Hill, B. & Attwood, M.M. (1976) *J. Gen. Microbiol.* **96**, 185-193.

Hsaio, K. (1991) *Nuc.Ac.Res.*, **19**, 2787.

Huang, Y., Blakeley, S.D., McAleese, S.M., Fothergill-Gilmore, L.A. & Dennis, D.T. (1993) *Plant Mol.Biol.* **23**, 1039-1052.

Huang, Y. & Dennis, D.T. (1995) *Eur. J. Biochem.* **229**, 395-402.

Ikura, K., Sasaki, R., Narita, H., Sugimoto, E. & Chiba, H. (1976) *Eur. J. Biochem.* **66**, 515-522.

Jaenicke, R. & Rudolph, R. (1986) *Methods Enzymol.* **131**, 218-250.

Johnson, C. M. & Price, N. C. (1988) *Biochem. J.*, **252**, 111-117.

Joulin, V., Peduzzi, J., Romeo, P.H., Rosa, R., Valentin, C., Dubart, A., Lapeyre, B., Blouquit, Y., Garel, M-C & Goossens, M., Rosa, J. & Cohen-Solal, M. (1986) *EMBO J.*, **5**, 2275-2283.

Junien, C., Despoisse, S., Turleau, C., Grouchy, J., Bucher, T. & Fundele, R. (1982) *Ann. Genet.* **25**, 25-27.

Kuhn, N.J, Setlow, B. & Setlow, P. (1993) *Arch. Biochem. Biophys.* **306,** 342-349.

Kunkel, T.A., Roberts, J.D. & Zakour, R.A. (1987) *Methods Enzymol.* **154**, 367.

Laforet, M.T., Butterfield, J.B. & Alpers, J.B. (1974) *Arch. Biochem. Biophys.* **165**, 179-187.

Leadley, P. F., Breathnach, R., Gatehouse, J. A., Johnson, P. E. & Knowles, J. R. (1977) *Biochemistry*, **16**, 3050-3053.

LeBoulch, P., Joulin, V., Garel, M.C., Rosa, J. & Cohen-Solal, M. (1988) *Biochem. Biophys. Res. Commun.* **156**, 874-881.

Lee, Y-H., Ogata, C., Pflugrath, J.W., Levitt, D.G., Sarma, R., Banaszak, L.J. & Pilkis, S.J. (1996) *Biochemistry*, **35**, 6010-6019.

Lin, K., Li, L., Correia, J.J. & Pilkis, S.J. (1992) *J. Biol. Chem.* **267**, 6556-6562.

Lindqvist, Y., Schneider, G. & Vihko, P. (1994) *Eur. J. Biochem.* **221**, 139-142.

Liu, S., Gresser, M J. & Tracey, A. S. (1992) *Biochemistry*, **31**, 2677-2685.

Lively, M. O., El-Maghrabi, M. R., Pilkis, J., D'Angelo, G., Colosia, A. D., Ciavola, J.-A., Fraser, B. A. & Pilkis, S. J. (1988) *J. Biol. Chem.* **263**, 839-849.

Magill, N.G., Cowan, A.E., Koppel, D.E. & Setlow, P. *J.Bacteriol.* **176**, 2252-2258.

Mezquita, J., Bartrons, R., Pons, G. & Carreras, J. (1981) *Comp. Biochem. Physiol.* **70B**, 247-255.

Mezquita, J. & Carreras, J. (1981) *Comp. Biochem. Physiol.* **70B**, 237-245.

Milburn, P., Bonnerjea, J., Hoare, M & Dunnill, P. (1990) *Enzyme Microb. Technol.*, **12**, 527-532.

Morris, V.L., Jackson, D.P., Grattan, M., Ainsworth, T.& Cuppels, D.A. (1995) *J.Bacteriol.* **177**, 1727-1733.

Nairn, J., Price, N.C., Fothergill-Gilmore, L.A., Walker, G.E., Fothergill, J.E. & Dunbar, B. (1994) *Biochem. J.* **297**, 603-608.

Nairn, J., Price, N.C., Kelly, S.M., Rigden, D., Fothergill-Gilmore, L.A. & Krell, T. (1996) *Biochim. Biophys. Acta* **1296**, 69-75.

Ohlsson, I., Nordstrom, B. & Branden, C.-I. (1974) *J. molec. Biol.* **89**, 339-354.

Ostanin, K., Harms E.H., Stevis, P.E., Kuciel, R., Zhou, M-M & Van Etten R.L. (1992) *J. Biol. Chem.* **267**, 22830-22836.

Pawluk, A., Scopes R.K. & Griffiths-Smith, K. (1986) *Biochem. J.* **238**, 275-281.

Pizer, L.I. and Ballou, C.E. (1959) *J.Biol.Chem.* **234**, 1138-1142.

Pons, G., Bartrons, R. & Carreras, J. (1985) *Biochem. Biophys. Res. Commun.* **129**, 658-663.

Prehu, M-O., Prehu, C., Calvin, M-C. & Rosa, R. (1988) *Comp. Biochem. Physiol.* **89B**, 257-262.

Price, N.C., Duncan, D. & McAlister, J.W. (1985) *Biochem. J.* **229**, 167-171.

Price, N.C., Duncan, D. & Ogg, D.J. (1985) *Int .J. Biochem.* **17**, 843-846.

Price, N.C., Stevens, E. & Rogers, P.M. (1983) *FEMS Microbiol. Lett.* **19**, 257-259.

Rapoport, S. & Luebering, J. (1950) *J. Biol. Chem.* **183**, 507-516.

Ravel, P., Arous, N., Croisille, L., Craescu, C. T., Rosa, J., Rosa, R. & Garel, M.-C. (1996) *Br. J. Haem.*, **93**, Abstract 717.

Rigden, D. J., Phillips, S., Alexeev, D. & Fothergill-Gilmore, L. A. (1997) Manuscript submitted.

Roiko, K., Janne, O.A. & Vihko P. (1990) *Gene* **89**, 223-229.

Rosa, R., Blouquit, Y., Calvin, M.-C., Prome, D., Prome, J.-C. & Rosa, J. (1989). *J. Biol. Chem.*, **264**, 7837-7843.

Rosa, R., Gaillardon, J. & Rosa, J. (1973) *Biochem. Biophys. Res. Comm.* **51**, 536-542.

Rosa, R., Audit, I. & Rosa, J. (1975) *Biochimie.* **57**, 1059-1063.

Rose, Z.B. (1968) *J. Biol. Chem.* **243**, 4810-4820.

Rose, Z.B. (1970) *Arch. Biochem. Biophys.* **140**, 508-513.

Rose, Z.B. (1971) *Arch. Biochem. Biophys.* **146**, 359-360.

Rose, Z.B. (1980) *Adv. Enzymol. Relat. Areas Mol. Biol.* **51**, 211-253.

Rose, Z.B. & Dube, S. (1976) *J. Biol. Chem.* **251**, 4871-4822.

Rose, Z.B. & Liebowitz, J. (1970) *J. Biol. Chem.* **245**, 3232-3241.

Rose, Z.B. & Salon, J. (1979) *Biochem. Biophys. Res. Commun.* **87**, 869-875.

Sakoda, S., Shankse, S., DiMauro, S. and Schon, E.A. (1988).

Sambrook, J., Fritsch, E.F. & Maniatis, T. (1989) Molecular Cloning - A Laboratory Manual (Second Edition). Cold Spring Harbour Laboratory Press.

Sasaki, R., Hirose, M. & Chiba, H. (1966). *Archs Biochem. Biophys.* **115**, 53-61.

Sasaki, R., Hirose, M. Sugimoto, E. & Chiba, H. (1971) *Biochim. Biophys. Acta.* **227**, 595-607.

Sasaki, R., Ikura, K., Narita, H., Yanagawa, S. & Chiba, H. (1982) *TIBS* **7**, 140-142.

Sasaki, R., Ikura, K., Sugimoto, E. & Chiba, H. (1975) *Eur. J. Biochem.* **50**, 581-593.

Schneider, G., Lindqvist, Y. & Vihko, P. (1993) *EMBO J.*, **12**, 2609-2615.

Sedmak, J.J. and Grossberg, S.E. (1977). *Anal. Biochem.* **79**, 544-552.

Shankse, S., Sakoda, S., Hermodson, M.A., DiMauro, S. and Schon, E.A. (1987) *J. Biol. Chem,* **262**, 14612-14617.

Shulman, M.D. & Valentino, D. (1981) *Mol. Biochem. Parasitol.* **5**, 321-332.

Singh, R.P. and Setlow, P. (1979) *J.Bacteriol.* **137**, 1024-1027.

Stankiewicz, P. J., Gresser, M. J., Tracey, A. S. & Hass, L. F. (1987) *Biochemistry*, **26**, 1264-1269.

Sutherland, E.W., Posternak, T.Z. & Cori, C.F. (1949) *J. Biol. Chem.*, **179**, 501-502.

Urena, J.M., Grana, X., de Lecea, L., Ruiz, P., Castella, J., Carreras, J., Pons, G. & Climent, F. (1992) . *Gene*, **113**, 281-282.

Van Etten, R.L. (1982) *Ann. NY Acad. Sci.* **390**, 27-51.

Wallace, A. C., Laskowski, R. A. & Thornton, J. M. (1995) *Prot. Eng.* **8**, 127-134.

Warwicker, J. (1986) *J. Theor. Biol.* **121**, 199-210.

Watanabe, K. and Freese, E. (1979) *J.Bacteriol.* **137**, 773-778.

Watson, H. C. (1982) Protein Data Bank Entry: Phosphoglycerate mutase (yeast) [3PGM], Brookhaven, New York.

White, M. F. (1989). PhD Thesis. University of Edinburgh.

White,M.F. and Fothergill-Gilmore, L.A. (1988) *FEBS Lett.*, **229**, 383-387.

White,M.F. and Fothergill-Gilmore, L.A. (1992) *Eur. J. Biochem.*, **207**, 709-714.

White,M.F., Fothergill-Gilmore, L.A., Kelly, S. M. & Price, N. C. (1993a) *Biochem. J.*, **291**, 479-483.

White,M.F., Fothergill-Gilmore, L.A., Kelly, S. M. & Price, N. C. (1993b) *Biochem. J.*, **295**, 743-748.

White, P.J., Nairn, J., Price, N.C., Nimmo, H.G., Coggins, J.R. and Hunter, I.S. (1992) *J. Bacteriol,* **174**, 434-440.

Willets, A. (1980) *Biochim. Biophys. Acta.* **632**, 454-462.

Winn, S.I., Watson, H.C., Harkins, R.N. & Fothergill, L.A. (1977) *Biochem. Soc. Trans.* **5**, 657-659.

Winn, S.I., Watson, H.C., Harkins, R.N. & Fothergill, L.A. (1981) *Phil. Trans. R. Soc. Lond.* B **293**, 121-130.
Yanagawa, S., Hitomi, K., Sasaki, R. & Chiba, H. (1986)

Yomano, L.P., Scopes, R.K.& Ingram, L.O. (1993) *J. Bacteriol.* **175,** 3926-3933.

FEBS Letters 359 (1995) 192–194 FEBS 15116

The use of mass spectrometry to examine the formation and hydrolysis of the phosphorylated form of phosphoglycerate mutase

Jacqueline Nairn[a], Tino Krell[b], John R. Coggins[b], Andrew R. Pitt[c], Linda A. Fothergill-Gilmore[d], Rebecca Walter[d], Nicholas C. Price[a,*]

[a]*Department of Biological and Molecular Sciences, University of Stirling, Stirling, Scotand, FK9 4LA, UK*
[b]*Division of Biochemistry and Molecular Biology, Institute of Biomedical and Life Sciences, Unversity of Glasgow, Glasgow, Scotland, G12 8QQ, UK*
[c]*Department of Pure and Applied Chemistry, University of Strathclyde, 295 Cathedral Street, Glasgow, Scotland, G1 1XL, UK*
[d]*Department of Biochemistry, University of Edinburgh, George Square, Edinburgh, Scotland, EH8 9XD, UK*

Received 5 January 1995

Abstract Electrospray mass spectrometry has been used to study the formation and hydrolysis of the phopshorylated forms of two phosphoglycerate mutases. The half-life of the enzyme from *Saccharomyces cerevisiae* was 35 min at 20°C in 10 mM ammonium bicarbonate, pH 8.0. Addition of 1 mM 2-phosphoglycollate reduced this value by at least 100-fold. The phosphorylated form of the enzyme from *Schizosaccharomyces pombe* was much less stable with a half-life of less than 1 min. The results are discussed in terms of the kinetic properties of the enzymes. Mass spectrometry would appear to be a powerful method to study the formation and breakdown of phosphorylated proteins, processes which are of widespread significance in regulatory mechanisms.

Key words: Electrospray mass spectrometry; Protein phosphorylation; Phosphoglycerate mutase

1. Introduction

The advent of electrospray mass spectrometry with its ability to measure molecular masses with a precision of ±0.01% has made it much easier to detect and characterise both post-translational and chemical modifications of proteins [1–3]. The introduction of the phospho group ($-OPO_3^{2-}$) in place of -H would lead to a mass increase of 78 units and thus be readily detectable. This approach has been used, for instance, in the delineation of the sites of phosphorylation in glycogen synthase [4] after separation of the modified peptides. However, examination of an intact phosphorylated protein by mass spectrometry does not appear to have been widely studied. In this paper we describe the use of electrospray mass spectrometry to monitor the formation of the phosphorylated forms of two phosphoglycerate mutases (PGAMs) and to examine the stability of these phosphorylated enzymes towards hydrolysis.

The catalytic cycle of phosphoglycerate mutase is thought to proceed via an enzyme-substitution pathway involving the enzyme phosphorylated on a histidine side chain (His-8 in the case of *S. cerevisiae* PGAM) [5]. The phosphorylated PGAM is slightly unstable towards hydroysis leading to a low level of phosphatase activity (approx. 0.002% that of the mutase activity in the case of the *S. cerevisiae* enzyme). It has been suggested [5] that the flexible C-terminal segment (14 amino acids) of this enzyme may be important in preventing access of water to the active site and thus maintain a high level of mutase to phosphatase activity. Recently the monomeric PGAM from the fission yeast *Schizosaccharomyces pombe* has been shown to lack this flexible C-terminal tail sequence [6]. The kinetic properties of the *S. pombe* enzyme have not yet been explored in detail.

*Corresponding author. Fax: (44) (1786) 464 994.
E-mail: ncp1@stirling.ac.uk

Abbreviations: PGAM, phosphoglycerate mutase; BPG, 2,3-bisphosphoglycerate.

2. Experimental

PGAM from an overexpressing strain of *S. cerevisiae* was isolated as described previously [7], with the addition of a final FPLC Superose-12 gel-filtration step. The concentration of the enzyme was determined spectrophotometrically assuming a value of 1.45 for the A_{280} of a 1 mg/ml solution [8].

PGAM from *S. pombe* was produced using the PGK-based vector pMA91 [9] for the high level expression of recombinant GPM^{sp} in a transformed null mutant strain of *S. cerevisiae* (*S150-gpm::HIS3*) [7]. The overexpressed *S. pombe* PGAM was purified in a similar manner to overexpressed *S. cerevisiae* PGAM [7]; routinely 10–15 mg of enzyme of at least 95% purity on SDS-PAGE [10] could be obtained per litre of cells. Full details of the expression system and enzyme purification will be published elsewhere (Nairn, Fothergill-Gilmore and Price, in preparation).

The concentrations of the *S. pombe* enzyme were determined by a Coomassie blue binding method [11] using bovine serum albumin as a standard, or spectrophotometrically using a value for the A_{280} (1.40 for a 1 mg/ml solution) calculated from the aromatic amino acid content of the enzyme [6,12]; the values agreed to within 5%.

The assays of mutase, phosphatase and synthase activities were performed as described previously [7].

The phosphorylated forms of the PGAMs from *S. cerevisiae* and *S. pombe* were prepared by mixing the enzymes with 2,3-bisphosphoglycerate (BPG) in 10 mM Tris/HCl, pH 8.0, followed by rapid gel-filtration on NAP 5 columns (Pharmacia) equilibrated with 10 mM ammonium bicarbonate, pH 8.0, to remove free mono- and bisphosphoglycerates. This procedure allowed samples to be studied by mass spectrometry within 3 min of the mixing.

Mass spectrometry was performed on a VG Platform quadrupole mass spectrometer (2–3000 amu range) fitted with a pneumatically assisted electrospray (ionspray) source and controlled via the VG MassLynx software (VG Biotech. Ltd, Altrincham, Cheshire, UK). Carrier solvent (1:1 (v:v) acetonitrile/water) infusion was controlled at 10 μl/min using a Harvard syringe pump (Harvard Apparatus, South Natic, MA, USA). Capillary voltages were between 2.8 and 3.2 kV, extraction cone voltages 20–30 V, and the focussing cone voltage offset by +10 V. The source temperature was set at 65°C, the nebulising gas flow at 10 l/h, and the drying gas flow at 250 l/h. Lens stack voltages were adjusted to give maximum ion currents. The M_r range 700–1500, which contained >95% of the signal intensity for both unmodified and phosphorylated forms of PGAM, was scanned with a sweep time of 5 s. The instrument was calibrated over this M_r range immediately before use with horse heart myoglobin (Sigma). Samples for analysis were

SSDI 0014-5793(95)00044-5

diluted with an equal volume of 4% (v:v) formic acid in acetonitrile and 10–20 μl aliquots injected directly into the carrier stream. The MaxEnt deconvolution procedure [13] was applied for quantitative analysis of the raw data using 1.0 Da peak width and 1 Da/channel resolution.

3. Results and discussion

3.1. S. cerevisiae *PGAM*

The specific activities of the *S. cerevisiae* enzyme in the mutase and the phosphatase assays (970 and 0.020 μmol/min/mg, respectively) and the effect of 1 mM substrate analogue 2-phosphoglycollate on the latter activity (18-fold stimulation) were very similar to those described previously [7].

The mass spectrum of the *S. cerevisiae* enzyme shows a single peak of M_r 27478.9 ± 1.0 consistent with the subunit M_r (27,477) calculated from the cDNA-derived sequence of the enzyme [14]. After addition of 0.8 molar equivalents (expressed per active site) of BPG, followed by rapid gel-filtration, the mass spectrum clearly shows the formation of the (mono)phosphorylated enzyme, with a mass increase of 79 amu (Fig. 1a). Under these conditions, 60% of the total enzyme was present in the phosphorylated form. There was little or no (≤0.05 molar equivalents per active site) BPG or monophosphoglycerates either free or enzyme bound after the gel-filtration. By increasing the molar ratio of BPG to 10-fold, more than 95% of the enzyme could be isolated in the phosphorylated form (data not shown). When the enzyme which had been prepared by reaction with the sub-stoichiometric amount of BPG and then gel-filtered was subsequently incubated at 20°C, there was a slow loss of the phospho group from the enzyme. Fig. 1b shows the mass spectrum of the sample taken after 18.5 min incubation. The data from three independent experiments expressed as a semi-logarithmic plot are shown in Fig. 1c; in each case the proportion of the enzyme in the phosphorylated form is expressed relative to the initial proportion as 100%. From the semi-logarithmic plot the rate constant for the hydrolysis of the phosphorylated enzyme is 0.02 min^{-1}, corresponding to a half-life of approximately 35 min. This direct estimate half-life of the phosphorylated form of *S. cerevisiae* PGAM is rather longer than the value (1–2 min) quoted by Britton et al. [15] on the basis of unpublished work. It is, however, clear from preliminary work that the measured phosphatase activity is markedly influenced by factors such as ionic strength and the presence of phosphorylated substrates and analogues, and this may well account for at least some of the observed differences in stability of the phosphorylated enzyme, i.e. the phosphorylated enzyme would appear to be much less stable when the enzyme is turning over.

When the mass spectrometry experiment was repeated with 1 mM 2-phosphoglycollate added to the phosphorylated enzyme immediately after gel-filtration, it was found that within 1 min, less than 5% of the enzyme remained in the phosphorylated form (data not shown). This result indicates that in the presence of 2-phosphoglycollate the half-life of the phosphorylated enzyme is less than 20 s (i.e. the rate of the dephosphorylation reaction is accelerated at least 100-fold in the presence of this substrate analogue; a somewhat greater effect than the 18-fold stimulation of phosphatase activity).

In the presence of acetonitrile (50% (v:v)), the phosphorylated enzyme showed no detectable breakdown after 70 min incubation (data not shown). Since this concentration of acetonitrile leads to a considerable loss of secondary structure (as shown by far UV CD measurements), it can be concluded that the denatured phosphorylated enzyme is considerably more stable towards hydrolysis than is the native phosphorylated enzyme. This conclusion would be consistent with earlier work in which negligible breakdown had been shown to occur over 120 min in the presence of 1.5% (w/v) SDS [16].

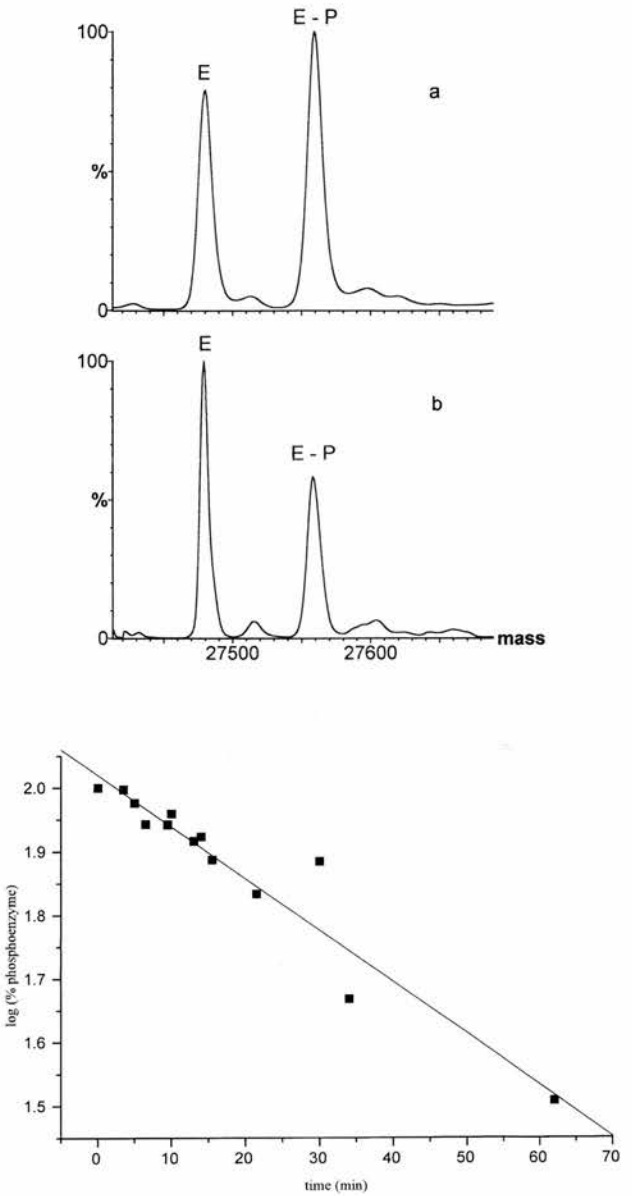

Fig. 1. Formation and hydrolysis of the phosphorylated form of *S. cerevisiae* PGAM monitored by mass spectrometry. The spectra over the M_r range shown (27,420–27,680) were obtained by applying the MaxEnt deconvolution procedure to the raw data. In each case the size of the major peak is set as 100%. The peaks labelled E and E-P represent the dephosphorylated and phosphorylated forms of the enzyme, respectively. (a) Mass spectrum of the sample immediately after gel-filtration. (b) Mass spectrum recorded after a further 18.5 min incubation. (c) Semi-logarithmic plot to show the conversion of the phosphorylated form to the dephosphorylated form of the enzyme. Data from three independent experiments are plotted; in each case the initial proportion of phosphoenzyme (immediately after gel-filtration) is scaled to 100%.

3.2. S. pombe *PGAM*

In the mutase assays, the specific activity of *S. pombe* PGAM (215 μmol/min/mg) is about 20% of that of the *S. cerevisiae* enzyme, whereas in the phosphatase assay it is some 2.5-fold higher (0.06 μmol/min/mg). Thus the ratio of the phosphatase/mutase assays is 12-fold higher for the *S. pombe* enzyme. The degree of stimulation of the phosphatase activity by 2-phosphoglycollate is considerably lower in the case of the *S. pombe* enzyme (4.2-fold).

The mass spectrum of *S. pombe* PGAM shows a peak with an M_r of 23679.4 ± 1.5, corresponding to that calculated from the published sequence [6], assuming that the initiating Met has been removed and the N-terminal threonine acetylated. On addition of 0.8 molar equivalents of BPG followed by gel-filtration (a process lasting 3 min), less than 5% of the enzyme was present in the phosphorylated form (data not shown). This was not due to an inability to form the phosphorylated enzyme since the mixture prior to gel-filtration showed that 60% of the enzyme was present in the phosphorylated form. From these results it could be concluded that the half-life of the phosphorylated form of *S. pombe* PGAM was less than 1 min (at least 35-fold shorter than that of the *S. cerevisiae* enzyme). This greater instability of the phosphorylated form of the *S. pombe* enzyme is in qualitative agreement with the higher ratio of phosphatase to mutase activities for this enzyme.

In conclusion, mass spectrometry should prove to be a very useful technique for monitoring the phosphorylation and dephosphorylation of a number of enzymes and proteins, a process which has been recognised to be a key regulatory mechanism for a large number of crucial biological processes [17]. The mass spectrometric technique avoids the necessity of using radioactive isotopes. Further refinements would include increasing the time resolution, allowing the rates of faster processes to be monitored accurately.

Acknowledgements: We wish to thank the Wellcome Trust and the BBSRC for financial support and for the provision of a studentship (R.W.). We are grateful to Dr. M.F. White for preparing the *S150- gpm:: HIS3* strain of *S. cerevisiae* and to Dr. S.M. Kingsman for supplying the plasmid pMA91.

References

[1] Feng, R. and Konishi, Y. (1992) Anal. Chem. 64, 2090–2095.
[2] Meyer, H.E., Eisermann, B., Heber, M., Hoffmann-Posorske, E., Korte, H., Weigt, C., Wegner, A., Hutton, T., Donella-Deana, A. and Perich, J.W. (1993) FASEB J. 7, 776–782.
[3] Akashi, S., Niitsu, U., Yuji, R., Ide, H. and Hirayama, K. (1993) Biol. Mass Spectrom. 22, 124–132.
[4] Gibson, B.W. and Cohen, P. (1990) Methods Enzymol. 193, 480–501.
[5] Fothergill-Gilmore, L.A. and Watson, H.C. (1989) Adv. Enzymol. Relat. Areas Mol. Biol. 62, 227–313.
[6] Nairn, J., Price, N.C., Fothergill-Gilmore, L.A., Walker, G.E., Fothergill, J.E. and Dunbar, B. (1994) Biochem. J. 297, 603–608.
[7] White, M.F. and Fothergill-Gilmore, L.A. (1992) Eur. J. Biochem. 207, 709–714.
[8] Edelhoch, H., Rodwell, V.W. and Grisolia, S. (1957) J. Biol. Chem. 228, 891–903.
[9] Mellor, J., Dobson, M.J., Roberts, N.A., Tuite, M.F., Emtage, J.S., White, S., Lowe, P.A., Patel, T., Kingsman, A.J. and Kingsman, S.M. (1983) Gene 24, 1–14.
[10] Laemmli, U.K. (1970) Nature 227, 680–685.
[11] Sedmak, J.J. and Grossberg, S.E. (1977) Anal. Biochem. 79, 544–552.
[12] Gill, S.C. and von Hippel, P.H. (1989) Anal. Biochem. 182, 319–326.
[13] Ferridge, A.G., Seddon, M.J., Green, B.N., Jarvis, S.A. and Skilling, J. (1992) Rapid Commun. Mass Spectrom. 6, 707–711.
[14] White, M.F. and Fothergill-Gilmore, L.A. (1988) FEBS Lett. 229, 383–387.
[15] Britton, H.G., Carreras, J. and Grisolia, S. (1972) Biochemistry 11, 3008–3014.
[16] Han, C.-H. and Rose, Z.B. (1979) J. Biol. Chem. 254, 8836–8840.
[17] Hardie, D.G. (1993) Protein Phosphorylation: A Practical Approach, IRL Press, Oxford.